MONTAN
UNIVERSITÄT
LEOBEN

Chair of Energy Network Technology

Master's Thesis

Energy Optimization of an Upstream Plant using Pinch Analysis

Roberta Cvetkovska

March 2020

MONTANUNIVERSITÄT LEOBEN
www.unileoben.ac.at

EIDESSTATTLICHE ERKLÄRUNG

Ich erkläre an Eides statt, dass ich diese Arbeit selbständig verfasst, andere als die angegebenen Quellen und Hilfsmittel nicht benutzt, und mich auch sonst keiner unerlaubten Hilfsmittel bedient habe.

Ich erkläre, dass ich die Richtlinien des Senats der Montanuniversität Leoben zu "Gute wissenschaftliche Praxis" gelesen, verstanden und befolgt habe.

Weiters erkläre ich, dass die elektronische und gedruckte Version der eingereichten wissenschaftlichen Abschlussarbeit formal und inhaltlich identisch sind.

Datum 04.03.2020

Unterschrift Verfasser/in
Roberta, Cvetkovska

KURZFASSUNG

Wärmerückgewinnung durch Wärmeintegration ist eine der effektivsten Strategien, die in vielen Branchen zur Steigerung der Energieeffizienz von Prozessen durch gleichzeitige Optimierung der Investitionskosten und des Energieverbrauchs umgesetzt wird.

Eines der am häufigsten verwendeten Instrumente zur Wärmeintegration in Raffinerien und petrochemischen Anlagen ist die Pinch-Analyse. In den letzten Jahren wurde die Pinch-Analyse aufgrund der Komplexität der vorgelagerten Anlagen zum Schlüssel für deren technoökonomische Bewertung in der Entwurfsphase.

Ziel dieser Arbeit ist die Entwicklung einer praktisch einfach anwendbaren Methodik zur Wärmeintegration mittels Pinch-Analyse, die in den fortgeschrittenen Entwurfsprozess jeder komplexen vorgelagerten Anlage integriert werden kann. Zu diesem Zweck wurde eine Pinch-Analyse an einer realen Fallstudie durchgeführt, die von einer bestehenden Anlage zur Herstellung von Gas und stabilisiertem Kondensat dargestellt wurde. Nach der Analyse der Wärmedaten aller Gasaufbereitungsanlagen wurden die Sauergas- bzw. die Dehydrierungsanlage als Hauptwärmequellen und die Kondensatstabilisierungseinheit als Wärmesenke der Anlage identifiziert. Die Berechnungen wurden mit Pinch Spreadsheet durchgeführt, das von Gabriel Norwood vom Institute of Chemical Engineers entwickelt wurde.

Die Ergebnisse zeigen, dass die Pinch-Analyse auch für technisch hochoptimierte Anlagen eine schrittweise Optimierung bieten kann. Die Retrofit-Design-Lösungen beinhalten die Nutzung der von den Amin- und Glykol-Regenerationseinheiten zur Verfügung gestellten Wärme, um den Heißölverbrauch in der Kondensatstabilisierungseinheit zu reduzieren. Die Integration wurde durch den Entwurf und die Optimierung eines Wärmetauscher Netzwerks realisiert, ohne den bereits bestehenden Prozess zu verändern.

Eine Validierung der vorgeschlagenen Methodik und eine mögliche Integration als Kompromiss zwischen der betrieblichen Unabhängigkeit der Einheiten und den thermoökonomischen Verbesserungen der gesamten Anlage ist Gegenstand zukünftiger Überlegungen.

ABSTRACT

Heat recovery via heat integration is one of the most effective strategies implemented in many industries for increasing the energy efficiency of processes through simultaneous optimization of the investment cost and the energy consumption.

One of the most used tools for heat integration in refineries and petrochemical plants is the pinch analysis. In the last years, due to the complexity of the upstream facilities, pinch analysis starts to be key for their techno-economic evaluation in the designing phase.

The scope of this thesis is to develop a practical methodology for heat integration via pinch analysis, which can be integrated in the advanced design process of any complex upstream plant. For that purpose, pinch analysis was used on a real case study represented by an existing plant for gas and stabilized condensate production. After analyzing the thermal data of all the gas processing facilities, the gas-sweetening unit and the gas-dehydration unit were identified as the main ‘heat sources’ while the condensate stabilization unit as a ‘heat sink’ of the plant. The calculations have been done using Pinch Spreadsheet developed by Gabriel Norwood from the Institute of Chemical Engineers.

The results show that the pinch analysis can offer step-forward optimization even for high-level engineered plants. The retrofit design solutions include the use of the heat available from the amine and the glycol regeneration units in order to reduce the hot oil duty in the condensate stabilization unit. The integration was realized by designing and optimization of a heat exchangers network without changing the already existing process.

A validation of the proposed methodology and a feasible integration as a trade-off between the operational independence of the units and the thermo-economic improvements of the whole plant is a subject for future consideration.

FOREWORD

This thesis is the final work of my Master studies of the program Industrial Energy Technology at the Montanuniversitaet in Leoben, Austria. It was carried out in cooperation with ILF Consulting Engineers GmbH located in Vienna.

From this point, I would like to express my sincere gratitude to the people who have supported me during my studies and in creating this work. A big appreciation to Univ.-Prof. Dipl.-Ing. Dr.techn. Thomas Kienberger for the proficient support and evaluation of the work. As well as, for drawing my attention in the right direction by setting and resolving numerous problems. I would also like to thank Dipl.-Ing. Dr.mont. Andreas Hammer for his help and shared knowledge in the process of performing the calculations.

Gratitude to the ILF-Consulting Engineers Company for the resourceful support with special thanks to M.Sc. Bogdan Buzatoiu for providing the necessary literature and documentation. His guidance and various discussions have had big contribution in understanding the problematic and developing the methodology.

Last but not least, an important thank you to my family, my fiancé and my closest friends who have been cherished support all along the way.

CONTENTS

NOMENCLATURE

ANSI	American National Standard Institute
BPD	Barrel Oil per Day
CC	Composite Curve
CHP	Combined Heat and Power
CPF	Central Processing Facility
CPI	Center for Process Integration
CSU	Condensate Stabilization Unit
DEG	Dyethylene Glycol
DHR	Direct Heat Recovery
E&P	Exploration and Production
EG	Ethylene Glycol
EPCC	Engineering, Procurement, Construction and Commissioning
ETD	Energy Transfer Diagramm
FGCU	Flash Gas Compressor Unit
GCC	Grand Composite Curve
GDU	Gas Dehydration Unit
GHG	Greenhouse Gases
GSU	Gas Sweetening Unit
H&MB	Heat and Material Balance
HART	Highway Addressable Remote Transducer
HCDPCU	Hydrocarbon Dew Point Control Unit
HEN	Heat Exchangers Network
HI	Heat Integration
HP	High Pressure

HRAT	Heat Recovery Approach Temperature
HRL	Heat Recovery Loop
HSDT	Heat Surplus Deficit Table
IEA	International Energy Agency
IHR	Indirect Heat Recovery
IL/HS	Intermediate Loop and Heat Storage
ISSP	Indirect Source Sink Profile
KOD	Knock Out Drum
LMTD	Logarithmic Mean Temperature Difference
LP	Low Pressure
LTS	Low Temperature Separation
MDEA	Methildiethanolamine
MEA	Monoethanolamine
MER	Maximum Energy Recovery
METD	Modified Energy Transfer Diagramm
MILP	Mixed Integer Linear Programming
MMSCFD	Million Standard Cubic Feet per Day
MP	Mathematical Programming
NLP	Non-Linear Programming
PA	Pinch Analysis
PDM	Pinch Design Method
PFD	Process Flow Diagram
PI	Process Integration
PWS	Produced Water System
RTGD	Retrofit Tracing Grid Diagramm

SCF	Standard Cubic Foot
SSSP	Site Source Sink Profile
TAC	Total Annual Cost
TAM	Time Average Model
TEG	Triethylene Glycol
TSA	Total Site Analysis
TSHI	Total Site Heat Integration
UFD	Utilities Flow Diagram
UMIST	University of Manchester Institute of Science and Technology
WTHP	Well Tube Head Pressure

INDICES

U	Internal energy $[J]$
u	Specific internal energy $[J/kg]$
Q	Thermal energy (Heat) $[J]$
$\dot{Q}$	Heat flow $[kW]$
q	Specific heat $[J/g]$
W	Work $[J]$
H	Enthalpy $[J]$
h	Specific enthalpy $[J/kg]$
p	Pressure $[Pa]$
V	Volume $[m^3]$
v	Specific volume $[m^3/kg]$
T	Temperature $[K;\ °\mathrm{C}]$
S	Enthropy $[J/K]$

C	Heat capacity $[J/K]$
c	Specific heat capacity $[J/g \cdot K]$
c_{mol}	Molar heat capacity $[J/mol \cdot K]$
c_v	Specific heat capacity at constant volume $[J/g \cdot K]$
c_p	Specific heat capacity at constant pressure $[J/g \cdot K]$
$\bar{c}_p$	Average specific heat capacity $[J/g \cdot K]$
CP	Heat Capacity Flowrate $[kW/K]$
m	Mass $[g]$
$\dot{m}$	Mass flow $[g/s]$
t	Time $[s]$
A	Heat transfer surface area in $[m^2]$
k	Heat transfer coefficient in $[W/m^2 \cdot K]$
ΔT_{LM}	Logarithmic mean temperature difference $[K]$
α	Convective heat transfer coefficient $[W/m^2 \cdot K]$
λ	thermal conductivity $[W/m^2 \cdot K]$
γ_g	Specific gravity of gas
ρ	density $[kg/m^3]$
γ_{hc}	Specific gravity of hydrocarbon fluid

LIST OF FIGURES

LIST OF TABLES

1 INTRODUCTION

Process Integration (PI) has evolved from a heat recovery methodology in the 80's to a major strategic design and planning technology in the 90's. Process integration is a powerful approach that allows engineers to systematically analyze an industrial process and the interactions between its units in order to achieve improvements such as productivity enhancement, conservation in mass and energy resources and reductions in the operating and capital costs [1].

Heat integration (HI) via heat recovery refers to methods and techniques used in order to improve the energy efficiency of one process. It also refers to the arrangement and efficiency of the equipment, and the surroundings in case of district heating or district cooling [2]. HI is applied in many industries assessing the heat recovery potential of processes, independent units or complex industrial sites.

Pinch Analysis (PA) as one of the most used tools for heat integration, initiated the development of process integration and still remains its main part. It is based on the change in thermodynamic state of the process streams in order to design maximal energy recovery (MER) heat exchangers network (HEN). It offers a graphical as well as an algebraic technique for energy targeting and HEN design. The basic idea behind the Pinch methodology is cumulative representation of the heating and cooling requirements in a temperature-enthalpy diagram. That results in clearly defined utility requirements for achieving the MER [2].

In the last years, many industries use PA in the designing phase to achieve the MER with the corresponding minimum heating and cooling utilities. This is the so called “Grassroot” design. On the other hand, there is retrofit design, which considers the PA as a tool to optimize already existing processes by achieving maximum heat recovery while minimizing the demand for external utilities.

The improvements achieved in energy efficiency by using Energy Pinch are based on the mass flow rate of the process stream and the change in temperature as a driving force. Besides the energy pinch used as a main tool for heat integration, the pinch methodology has developed in extensions such as Mass Pinch including Water and Hydrogen Pinch. Mass Pinch Analysis manages material resources, such as water and hydrogen to minimize the make-up and the discharge, while maximizing their reuse [2].

The integration of PA in the industries can achieve savings up to 35% in energy consumption, between 25% and 40% in water consumption, and up to 20% in hydrogen consumption [3]. However, this thesis focuses only on Energy Pinch Analysis.

1.1 Research scope

The oil and gas sector is identified as one of the major energy user and supplier in which pinch analysis methods have been developed and integrated [4]. The downstream sector, due to the complexity of the refineries and petrochemical plants have been using the PA methodology from the very beginning. The upstream processes don't have the same complexity, so the standard procedure as for downstream, has been implemented on complex Upstream plants only when requested.

The motivation of this work is to develop Pinch Analysis methodology adapted for Upstream plants which can be implemented in retrofit projects, as well as in the designing phase of future projects.

This thesis focuses on optimizing heat recovery within a real upstream plant for gas and stabilized condensate production. The aim is to identify possibilities for energy recovery through retrofit improvements for heat exchange between different units. This includes implementing new heat exchangers without considering the ones that already exist. For that purpose, the following **research questions** were elaborated:

- Why is the Pinch Analysis eligible for a heat integration in an Upstream plant?
- Which are the key units in such a plant in which PA can be implemented?
- Can the energy efficiency be increased using heat recovery without changing the existing HEN?
- Does the PA offer an advanced optimization of an already well-designed and optimized complex Upstream plant?
- Can the developed methodology for HI via PA between different units of the plant lead to Total Site Analysis (TSA)?

The research scope includes theoretical background of the PA methodology, brief description of the process units, development of a calculation model and evaluation and optimization of the new heat exchangers network.

The theoretical basics of a PA methodology include definitions, methods and guidelines for selecting the corresponding stream flows and obtaining the energy targets. Further on, the plant description gives a brief overview of the basic system configuration, including the equipment, facilities and the processes encountered in the gas processing and condensate stabilization units. It was created according to the “Basis of Design documentation” of the project, detailed process flow diagrams (PFD) and heat and material balance (H&MB) sheet. These sources will be referred to as [5] according to the confidentiality agreement with the company ILF Consulting Engineers, GmbH, in Vienna.

Analyzing the PFDs and the thermal data provided, the key areas for possible improvements were chosen, such as the gas sweetening unit, the gas dehydration unit and the condensate stabilization unit. Afterwards, the adequate process flow streams were selected and the necessary data extracted and calculated so that the methods for PA can be properly implemented.

The Pinch Analysis calculation was done in a Pinch Spreadsheet, developed by Gabriel Norwood as a winning entry in a competition run by the Institution of Chemical Engineers in the United Kingdom. This tool performs calculation of the energy targets and the feasible cascade, as well as plotting of the composite curves, grid diagram and the grand composite curve. According to the outcomes of the performed PA, a new heat exchangers were implemented satisfying the utility requirements defined by the energy targets. The designed HEN was optimized by resolving a closed-loop heat transfer across the pinch point.

This work delivers the following **key-results:**

As **1st key result**, a structured methodology adapted for implementing the Pinch Analysis in a retrofit design of a complex Upstream plant. Therefore, highlighting the key areas and units of such a plant, which need to be considered for heat integration.

As **2nd key result**, the retrofit design optimization suggested in this work includes the use of the heat available from the amine and the glycol regeneration units and reducing of the hot oil duty in the condensate stabilization unit.

2 HEAT INTEGRATION

Heat integration, as defined by the International Energy Agency (IEA) first in 1993, includes systematic and general methods for designing integrated production systems ranging from individual processes to total sites, with special emphasis on the efficient use of energy and reducing environmental effects [6].

The citation above is often used in the literature to define Process Integration (PI), which contributes to the confusion that heat integration is the same as process integration. This confusion exists probably because heat recovery studies inspired by pinch analysis initiated the development of process integration and remains its main part. Structurally, HI and PI can be differentiated as follows:

Heat Integration (HI) is a specific concept of process integration applied in the industry in order to assess the heat recovery potential of processes, process units or complex industrial sites [7].

On the other hand, process integration (PI) is a methodology that was developed as a response to the oil crisis back in the 1970s, which caused fuel to become rare and expensive [2]. It allows industries to develop cost-effective and sustainable solution strategies in order to increase the energy efficiency of the processes on one side; decrease water and raw materials consumption and reduce greenhouse gas (GHG) emissions on the other side. It provides a set of generally applicable tools and enables the engineer to see “the big picture first, and the details later”. This approach provides not only identification of the optimal process development strategy, but also of the most cost-effective way to accomplish the task [1].

The design of process integration has evolved through four generations. Originally, process design started with testing pilot plants before plant construction based on experiments in laboratories, which defines the first generation of process design. The second generation used the concept of unit operation, which acted as a building block for the engineers in the design process. The integration between the units was considered in the third generation; for example, heat recovery between related process streams to save energy. The fourth generation represents the tendency to make improvements between units, not only within units. By allowing more than one phenomenon (reaction, heat transfer, mass transfer, etc.) to take place within the same piece of equipment, significant savings in investment and operating cost have been noticed [1].

The growth and development of process and power generating industries has contributed to the fact that the process integration is now a standard curriculum for process engineers in both chemical and mechanical engineering at the most universities in the world. Researches at UMIST (University of Manchester Institute for Science and Technology) have been supported by a large number of industrial companies through a Consortium that was established in 1984. As part of the IEA project on Process Integration, 35 other universities around the world are involved. The PI concepts include heuristic, thermodynamics and optimization techniques. They have been applied in various domains such as [1], [2]:

- Heat Integration – heat exchange network
- Total Site Integration (TSI)
- Mass integration and resource conservation
- Waste water minimization
- Cogeneration and total site targeting
- Batch process targeting and optimization
- Emission targeting (GHG emission reduction)
- Hydrogen management in refineries
- Pollution prevention [8]
- Supply-chain management [9]

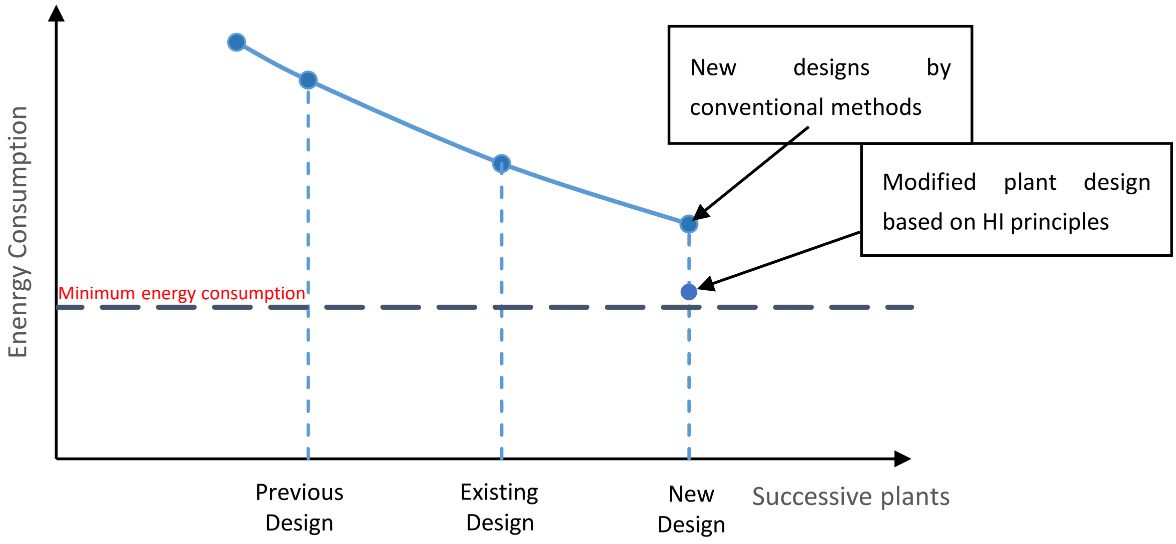

Figure 2-1: Energy consumption depending on the design according to [1]

The implementation of process and heat integration principles has a big contribution in decreasing the energy consumption of processes as shown in Figure 2-1. The dotted black line shows the minimum energy requirement for industry, and the curve presents the energy consumption of different designs with traditional methods. As we can see the gap between the old design and the minimum energy requirement decreases with the implementation of new designs respectively to the conventional methods. If process integration or heat integration is used, better designs can be achieved where the energy consumption gets nearer to the minimum [1].

2.1 Fundamental concepts of heat integration

Heat is form of energy, which can be converted to and from other forms of energy. It is transferred between substances or systems due to a temperature difference between them. The amount of heat transferred by a substance depends on the speed and number of atoms or molecules in motion. Greater heat transfer is, among others, a result of higher temperature, which means increased movement of particles [10]. Temperature, as defined by the American Heritage Dictionary, is “a measure of the average kinetic energy of the particles in a sample of matter, expressed in terms of units or degrees designated on a standard scale" [11].

The fundamentals of thermodynamic are described through four laws, from which the first and the second law are of interest for this thesis.

2.1.1 First law of thermodynamic

The first law of thermodynamic, also known as a principle for conservation of energy, states that energy can be neither created nor destroyed; it can only change forms [12]. Another formulation of the first law declares that the internal energy of a closed system is constant.

The first law of thermodynamic for a closed system, without exchange of mass, can be expressed with equation (2-1): The change in the internal energy of the system (dU) depends on the change of the thermal energy (dQ) and the work (dW) done to or by the system [13].

$$dU = dQ + dW \tag{2-1}$$

When implementing the formula, it must be considered that the signs before the thermal energy (heat) and the work depend on the fact in which direction the heat and/or work transfer flows.

Closely related to the internal energy of a system is the enthalpy, which defines the change of the internal energy plus the product of volume and pressure, equation (2-2). It represents the heat brought to the system at constant pressure [14].

$$H = U + pV \qquad [J] \tag{2-2}$$

If we consider the enthalpy relative to 1 kg mass, then we get the specific enthalpy:

$$h = u + pv \qquad [J/kg] \tag{2-3}$$

While the internal energy is the sum of all the energy forms of the molecules in the system, the enthalpy is the totality of the forms of energy that have contributed to reach a particular state of the system [13].

Interest of this case study are process streams represented by fluid flowing through a pipe, where only heat will be supplied or removed. Their volume and mass flow do not change, whereas the heat absorbed at one temperature level, will be removed at another temperature level. These are characteristics of steady flow processes which internal energy does not change. Such a system is shown in Figure 2-2.

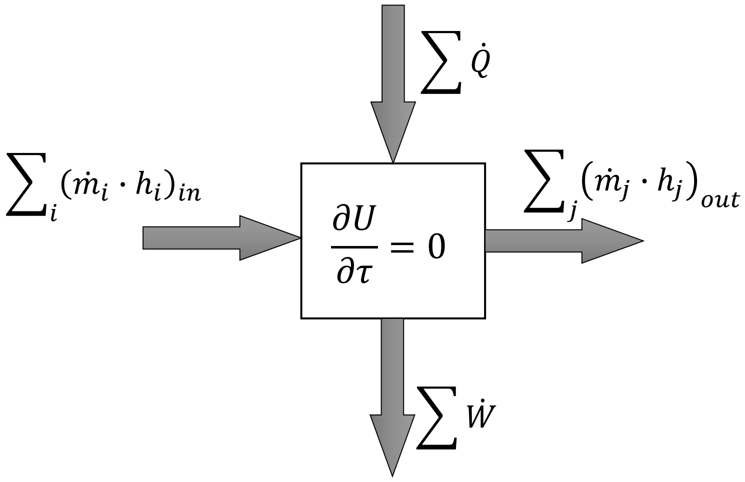

Figure 2-2: Energy balance of steady flow process [15]

The first law of thermodynamics for a steady flow process is expressed with the following equation [15]:

$$\sum \dot{Q} + \sum \dot{W} = \sum_i (\dot{m}_i \cdot h_i)_{in} + \sum_j (\dot{m}_j \cdot h_j)_{out} \tag{2-4}$$

The mass flow doesn't change, meaning $\dot{m}_i = \dot{m}_j$. The volume of the system is constant which means no work is done, $dW = pdv = 0$. This leads to the following equation:

$$\Delta \dot{Q} = \dot{m} \cdot \Delta h \tag{2-5}$$

Heat supply to the process stream flows under isobaric conditions, results in changes in the temperature and increasing the enthalpy of the fluid, equation (2-6).

$$\Delta \dot{Q} = \dot{m} \cdot (h_2 - h_1) = c_p \cdot \dot{m} \cdot (t_2 - t_1) \tag{2-6}$$

2.1.2 Second law of thermodynamic

The first formulation of the second law of thermodynamic was introduced by Clausius, in 1850, stating that heat can never be transferred from a system at a lower temperature to a system at a higher temperature [16], without applying external work to it.

It expresses the three important characteristics of irreversible processes [16]:

- They run spontaneously only in one direction;
- They cause energy dissipation;
- It is possible to reverse them, only if external work is done on the system.

For a mathematical assessment of the second law of thermodynamics, the entropy, as a new extensive property was introduced and expressed as a ratio between the quantity of heat added to a system and the system temperature T:

$$dS = \frac{dQ}{T} \qquad [J/K] \tag{2-7}$$

It is a vivid representation of the “disorder” in the system as a result of the heat and dissipation energy changes that occur in it [10]. A disordered system has a greater number of possible microstates than does an ordered system, so it has a higher entropy [17]. The second law of thermodynamic can be expressed through the entropy: “Entropy in a closed system can never decrease, it can at least stay the same” [15].

$$dS \geq \frac{dQ}{T} \qquad [J/K] \tag{2-8}$$

From equation (2-7) we can see that the heat is proportional to the temperature of the object, as well as to the entropy:

$$dQ = T \cdot dS \qquad [J] \tag{2-9}$$

As the temperature increases, the kinetic energy of the particles also increases, which means bigger disorder and more heat can be transferred.

2.1.3 Specific heat capacity

Different substances behave differently when heat is transferred to them. In order to measure and compare their behavior, the term heat capacity is used.

Heat capacity is the amount of heat that needs to be supplied to a body in order to increase its temperature by a given amount. In the International System of Units, heat capacity is measured in joules per kelvin (J/K) .

$$C = \frac{dQ}{dT} \qquad \left[\frac{J}{K}\right] \tag{2-10}$$

The heat capacity is, according to (2-10), an extensive property, which means it depends on the specific amount of substance to be heated up. If the heat is applied to a generic unit of mass of a substance, the heat capacity is being introduced as an intensive property (independent of the size of the sample) through the molar heat capacity, equation ***(2-11)***, and the specific (gravimetric) heat capacity, equation (2-12***)*** [18]:

$$c_{mol} = \frac{dq}{dT} \qquad \left[\frac{J}{mol \cdot K}\right] \tag{2-11}$$

$$c = \frac{dq}{dT} \qquad \left[\frac{J}{g \cdot K}\right] \tag{2-12}$$

This means that $1J$ of energy increases the temperature of 1g of substance or of 1 mol of substance by one degree (°C or K)[1].

The specific heat capacity can be expressed either in joules per gram per degree ($J/g \cdot ℃\ or\ J/g \cdot K$) or in calories per gram per degree ($cal/g \cdot ℃\ or\ cal/g \cdot K$). In this work it will be expressed in kilojoules per kilogram per Celsius degrees ($kJ/kg \cdot ℃$), considering the big amounts of fluids needed for the calculation and the fact that the temperatures are given in ℃.

The connection between the molar and the specific heat capacity can be presented with help of the molar weight $M\ [g/mol]$ of a substance:

$$c = \frac{c_{mol}}{M} \qquad \left[\frac{J}{g \cdot K}\right] \tag{2-13}$$

The specific heat is a function of the structure of the substance, meaning it depends on the number of particles in a sample (not to its mass) [10], and number of degrees of freedom that the relevant particles have [18]. Increasing the temperature of a certain substance means changing the kinetic energy of its particles (atoms). 1 kg of one substance has different number of atoms then 1 kg of another substance. As one simple example: steel has a specific heat capacity of 510 $J/(kg \cdot ℃)$, water on the other hand has a capacity of 4186 $J/(kg \cdot ℃)$. This

---

[1] A temperature change of 1K is the same as temperature change of 1°C because the Kelvin scale uses the same increment as the Celsius scale.

means that round eight times more heat is needed to increase the temperature of 1 kg water for 1 °C, then for 1 kg steel.

Generally, solids have heat capacities from a few hundred $J/(kg \cdot °\mathrm{C})$, whereas liquids – few thousand $J/(kg \cdot °\mathrm{C})$. For gasses, the specific heat capacity depends on the type of state of change being considered, meaning, if it occurs under constant pressure (isobaric state of change) or constant volume (isochoric state of change). The change of the internal energy with the temperature at a constant volume ($dv = 0$) is defined as [13]:

$$c_v = \left(\frac{\partial u}{\partial T}\right)_v \qquad \left[\frac{J}{g \cdot K}\right] \tag{2-14}$$

The change of the enthalpy with the temperature at a constant pressure ($dp = 0$) is expressed as [13]:

$$c_p = \left(\frac{\partial h}{\partial T}\right)_p \qquad \left[\frac{J}{g \cdot K}\right] \tag{2-15}$$

The heat capacities of monatomic gases are temperature-independent, which is not the case with diatomic and polyatomic gases [19]. In addition to the rotation and translation of the whole molecule of polyatomic gases, vibrations of the atoms in the molecular assembly also occur. This so-called inner degree of freedom is only stimulated by collisions in which a certain minimum energy can be transmitted. The temperature dependence becomes noticeable and substantial at higher temperatures where a sufficient number of molecules have greater velocities [20]. Due to this contemplation, we differentiate between true and average heat capacity.

The true specific heat capacity of a substance presented with equation (2-12) is defined as derivative of the quantity of heat added to the body with respect to its temperature [21]. But when heat is added to a unit mass of substance while heating it from temperature T_1 to temperature T_2, the average specific heat capacity must be considered. This property is defined with equation (2-16) [16].

$$\bar{c}_p\Big|_{t_1}^{t_2} = \frac{1}{t_2 - t_1}\int_{t_1}^{t_2} c_p dt = \frac{1}{T_2 - T_1}\int_{T_1}^{T_2} c_p dT \tag{2-16}$$

Graphical representation of the average specific heat capacity in the temperature interval $\Delta T = T_2 - T_1$ is given in Figure 2-3, where the areas A_1 and A_2 are equal. The area under the integral $\int_{T_1}^{T_2} c_p dT$ is equal to the area under the average value of the specific heat capacity in the interval ΔT [22].

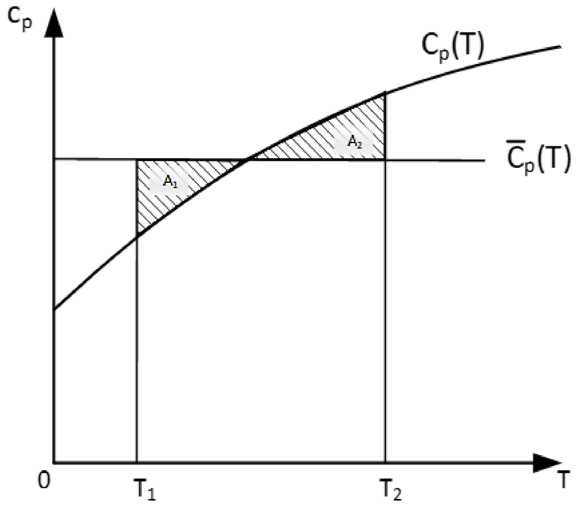

Figure 2-3: Average specific capacity $\bar{c}_p/_{T_1}^{T_2}$ *[22]*

There are several ways to calculate the value of the average specific heat capacity in a specific temperature interval:

1. If the true specific heat capacities at certain temperature are given and they increase marginally with increasing temperature, we can calculate their average using the advantage of linear interpolation, equation (2-17).

$$\bar{c}_p\Big|_{t_1}^{t_2} = \frac{c_p(t_2) - c_p(t_1)}{2} \qquad (2\text{-}17)$$

This is recommended for small temperature intervals.

2. If the true c_p is given as a polynomial function of the temperature,$c_p = a + b \cdot T + c \cdot T^2 + d \cdot T^3 + e \cdot T^4$, the average value $\bar{c}_p$ can be calculated according to equation (2-16).

3. When the average specific heat capacities for a certain substances are given between 0°C and t, it must be considered that the heat required to heat up a body from t_1 to t_2 is equal to the difference between heating up the body from 0°C to t_2 and heating it up from 0°C to t_1 [16].

$$\bar{c}_p\Big|_{t_1}^{t_2} = \frac{t_2 \cdot \bar{c}_p\Big|_{0°\mathrm{C}}^{t_2} - t_1 \cdot \bar{c}_p\Big|_{0°\mathrm{C}}^{t_1}}{t_2 - t_1} \qquad (2\text{-}18)$$

The calculation of the heat capacities for this work, presented in section 6.3, is performed with the help of equation (2-16) considering that different functions for $c_p = f(T)$ were provided for gases and hydrocarbon liquid respectively.

2.1.4 Energy changes in a system

If we consider a system in a steady state (no change of the system's internal energy, $dU = 0$) under the assumption that the potential and the kinetic energy are negligible, we can express the first law of thermodynamic in the following way [23]:

Energy Accumulation = 0 = Energy Inflow – Energy Outflow

or

$$\sum (\dot{m} \cdot h) = \sum \dot{Q} - \sum \dot{W} \tag{2-19}$$

In order to apply this equation, the system and the given data need to be analyzed.

1. Choice of System

In this case, heat integration using pinch analysis will be performed so that certain streams will be cooled down on the account that others will be heated up. This leads us to a certain piece of equipment – heat exchanger. In the heat exchanger no work is done, so we assume $W = 0;\ \Delta H = Q$ [23].

2. Available data

In the provided Heat and Material Balance for the corresponding plant the mass flow of each stream is given. A mass flow represents the flow rate of a certain mass of the fluid per unit time:

$$\dot{m} = \frac{m}{t} \qquad \left[{}^{g}/_{s}\right] \tag{2-20}$$

Considering this, and the equations ***(2-6)*** and ***(2-16)*** the heat flow (heat supplied or removed per unit time or heat load) in a certain stream when changing its temperature from T_1 to T_2 can be calculated in the following way:

$$\dot{Q}_{12} = H_2 - H_1 = \dot{m} \cdot \bar{c}_p\big|_{t_1}^{t_2} \cdot (T_2 - T_1) \tag{2-21}$$

or

$$\dot{Q}_{12} = CP \cdot (T_2 - T_1) \tag{2-22}$$

where CP presents the heat capacity flowrate:

$$CP = \dot{m} \cdot \bar{c}_p\big|_{t_1}^{t_2} \qquad \left[{}^{kW}/_{^\circ\mathrm{C}}\right] \tag{2-23}$$

This will be the equation on which the calculation of the pinch point and the design of the heat exchangers network will be grounded and explained later on in this work.

2.1.5 Heat Transfer

The main condition under which heat transfer from one system to another occurs is that there is a difference in their temperatures. The heat flows always from the system with higher temperature to the one with lower temperature. Heat can be transferred in one of the following ways: conduction, convection or radiation [12].

Conduction is transfer of thermal energy between two particles when they are in contact so that the molecules transfer energy across the interface [10]. Conduction can take place in solids, liquids and gases [12].

Convection is the transfer of energy between a solid surface and an adjacent moving fluid based on macroscopic particle movement which is always accompanied with a heat conduction. We differentiate between forced and free convection. In the first case, the fluid is forced to by external means (fan, pump, wind). Free convection is caused by density differences due to variation of the temperature in the fluid [12].

Radiation is the energy emitted by matter in the form of electromagnetic waves (or photons) as a result of the changes in the electronic configurations of the particles. All bodies at a temperature above absolute zero emit thermal radiation [12].

Our field of interest is the heat transfer between the moving fluid (gas, hydrocarbon liquid) in the pipes, the wall of the pipes and the fluid surrounding them. This can be described as a combination of a conduction and a convection, also known as a heat transmission. Consider a hot flowing hydrocarbon liquid in a streamline (Figure 2-4). The particles of the fluid, which are in contact with the wall of the pipe, transmit heat to the solid surface allowing other molecules to move into place and repeat the same. The adjacent particles will further on transfer the heat within the wall, due to conduction. The second fluid, on the other side of the wall, absorbs the heat [24].

The heat flow in a heat exchanger can be calculated in the following way:

$$\dot{Q}_{12} = k \cdot A \cdot \Delta T_{LM} \qquad [kW] \tag{2-24}$$

Where:

A - Heat transfer surface area, $[m^2]$
k - Heat transfer coefficient, $[W/m^2 \cdot K]$
ΔT_{LM} - Logarithmic mean temperature difference, $[K]$

The overall heat transfer coefficient, k, is not a property of the fluid but a function of the convective heat transfer coefficient - $\alpha\ [W/m^2 \cdot K]$ and the thermal conductivity of the wall - $\lambda\ [W/m^2 \cdot K]$ [24]:

$$k = \frac{1}{\frac{1}{\alpha_1} + \frac{L}{\lambda} + \frac{1}{\alpha_2}} \qquad [W/m^2 \cdot K] \tag{2-25}$$

The values of the heat transfer coefficient, in the scope of this work, will be considered from a literature listing for the corresponding heat exchangers and fluids (Subchapter 6.6, Table 6-8).

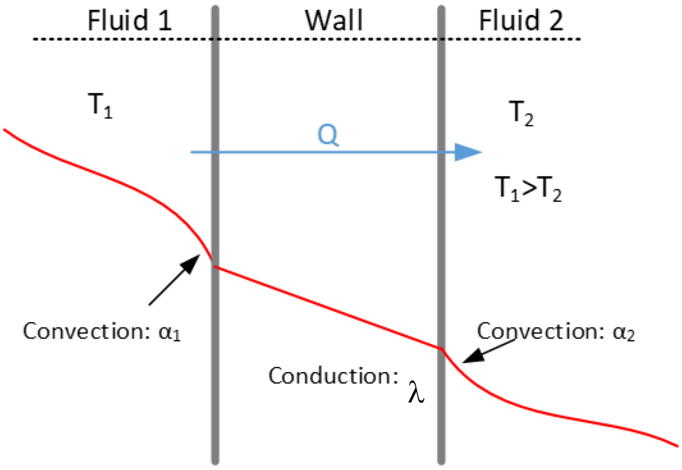

Figure 2-4: Heat transfer between two fluids through a wall

The logarithmic mean temperature difference ΔT_{LM} (also known as log mean temperature difference – LMTD) is a logarithmic average of the temperature difference between the hot and the cold end of the heat exchanger. In order to explain the calculation of ΔT_{LM}, in Figure 2-5 is shown example of a countercurrent heat exchanger. The hot stream is entering the heat exchanger at temperature t_{h1} and is leaving at t_{h2}. The cold stream is being heated up from t_{c1} to t_{c2}. In this case, t_{h1} and t_{c2} are at the hot end, and t_{h2} and $t_{c1}$are at the cold end of the exchanger. ΔT is changing along the length, as represented on the diagram in Figure 2-5 which value can be determined as the logarithmic mean temperature difference [25] [7]:

$$\Delta T_{LM} = \frac{\Delta T_2 - \Delta T_1}{\ln \frac{\Delta T_2}{\Delta T_1}} = \frac{t_{h1} - t_{c2} - t_{h2} + t_{c1}}{\ln \left(\frac{t_{h1} - t_{c2}}{t_{h2} - t_{c1}} \right)} \qquad [W/m^2 \cdot K] \tag{2-26}$$

Once the properties of the heat transfer are known, we can calculate the surface area for each heat exchanger:

$$A = \frac{\dot{Q}_{12}}{k \cdot \Delta T_{LM}} \qquad [m^2] \tag{2-27}$$

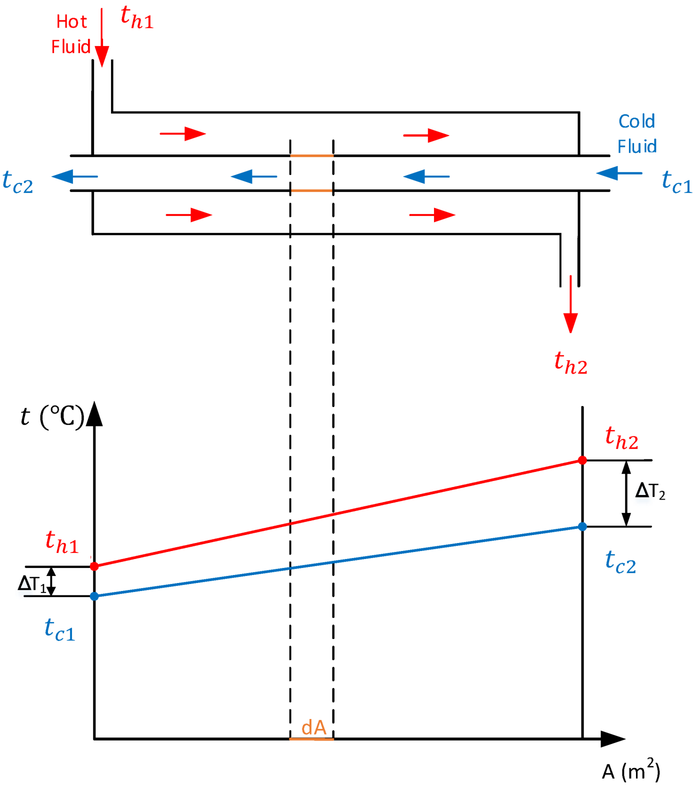

Figure 2-5: Thermal driving force in counter-current heat exchanger

The lower the temperature difference, bigger heat exchange surface area is needed in order to achieve the efficiency of the HE. This leads to expansive heat exchanger and increased capital costs. Considering this, the optimal values of ΔT should be chosen according to the balance between energy and capital costs.

2.2 Heat integration methods

Heat Integration can be realized with a graphical approach or using mathematical programming (MP) [26]. The key concept is to exchange heat between the hot and the cold process streams in the system in order to satisfy the energy targets and to reduce the duty of external utilities considering the minimum energy recovery (MER) of the system. The graphical method (as for instance Pinch Analysis) represents the heating and cooling requirements of the processes through temperature-enthalpy profiles. It relies on the concept of pinch temperature and Heat Recovery Approach Temperature (HRAT) guided by defined rules for using (re-using) the streams. This concept is used in the design phase of the processes but also for retrofit of existing heat exchangers networks [27]. The mathematical programing describes the processes in mathematical form in order to achieve process optimization and synthesis of the process schemes and process subsystems. The most used models of MP are Mixed Integer Linear Programming (MILP) and Non-Linear Programming (NLP). These methods require defining variables, constraints and defining objective functions. The MILP describes the variables with linear functions and uses only integer numbers as constants. If at least one function is nonlinear, the NLP methodology is used. The mathematical programming is based on stage-wise selection of matches from the Heat Exchangers Network (HEN) structure, where each hot stream can match any cold stream for each stage, and the temperature driving forces are regarded as optimization variables. The important advantage of these HI models is that the process streams with fixed temperatures and variable flows can be simultaneously used with process models to perform process optimization [27].

The concept of increasing the energy efficiency of single plants through heat integration using both, the graphical approach and mathematical programing, has developed in multi-plant heat integration. The exchange of heat between process streams within one plant is known as direct HI. On the other side, there is indirect HI, which uses the surplus heat from one plant and transfers it to another heat-demanding plant via intermediate fluid loops [27].

The methods for HI can be implemented in the designing phase of a certain project, referred as Grassroots Design using the available tools and methods in creating energy efficient processes and units. But more recurrent is the Retrofit Design where the focus is on the opportunities for improvement of already existing plants. The goal is to increase heat recovery and decrease energy consumption by making investments in new equipment, re-piping or changing internals in heat exchangers [28].

The most widely used methodology for heat integration with given results in numerous projects worldwide is Pinch Analysis (PA). The ultimate goal of the pinch methodology is to achieve more efficient use of the energy in the system and to reduce the amount of external utilities requirements. It is based on the understanding of heat exchange between process streams using a temperature – enthalpy diagram [3].

The Pinch Analysis, due to the simplicity of its underlying concept even for complex processes, will be used in this work in order to identify the possibilities for improving the efficiency of an existing complex Upstream plant. The methodology and concepts of the PA will be explained step by step in the next chapter.

3 PINCH ANALYSIS METHODOLOGY

The Pinch Analysis Method is based on thermodynamic principles and uses a systematic methodology for identification of the possible energy recovery by heat exchange between the hot and the cold streams. It analyses the potential of exchanging heat between the heat sources of systems or processes that use energy and the heat sinks via the use of heat exchangers.

The **hot streams** are the ones which have to be cooled down and represent the heat sources of the system.

The **cold streams**, or so-called heat sinks, are the streams that need to be heated up.

The enthalpy changes in the streams passing through a heat exchanger can be calculated with the first law of thermodynamic. The direction of the heat flow is determined by the second law of thermodynamic, according to which, the heat always flows spontaneously from hotter to colder bodies and never the reverse, unless work is performed on the system. In that way "temperature crossovers" of the hot and cold streams through the heat exchanger are prohibited. That means that a cold stream can't be heated to a temperature higher than the supply temperature of the hot stream, and a hot stream can't be cooled down to a temperature lower than the supply temperature of the cold stream. In practice the driving force allowed in the heat exchanger unit is defined by the minimum allowable temperature difference (ΔT_{min}) between the stream profiles. The temperature level at which ΔT_{min} is observed is referred to as "pinch point" [29].

The primary objective of the pinch is to maximize the heat recovery of the process and to reduce the external utility loads. The methodology is based on three steps:

1. **Selection of $\mathbf{\Delta T_{min}}$**
2. **Definition of hot and cold streams**
3. **Calculation of the energy targets**
4. **Design of the heat exchanger network (HEN)**

The 1st step, selection of $\Delta \mathrm{T}_{\mathrm{min}}$, defines the pinch point of each case study, dividing the process in two independent subsystems: below and above the pinch point. The 2nd step depends on the process unit operations and their required thermodynamic operating conditions. The minimum energy requirement (3rd step) is determined by identification of the pinch point which can be done either through representation of the hot and cold composite curves in a temperature-enthalpy diagram (see 6.4) or calculation using the cascade method (see 6.5). The both methods must give the same results. The targeted heat recovery can then be realized with the fourth step by designing the heat exchanger network.

3.1.1 Selection of $\Delta\mathbf{T}_{\mathbf{min}}$

The minimum temperature difference between the hot and the cold composite curve defined as $\boldsymbol{\Delta T_{min}}$, is based on the minimal overall cost, as well as on experience gained by solving different cases.

When analyzing the optimal value of ΔT_{min}, the following factors are important [3]:

- **Energy vs. capital costs**

In the process industry there is a trade-off between the energy savings obtained by heat exchange and the required heat exchangers investment. Although there are cases where saving in both, energy and capital, are possible, saving energy generally implies increased capital costs [3], which increase with the heat exchangers' surface.

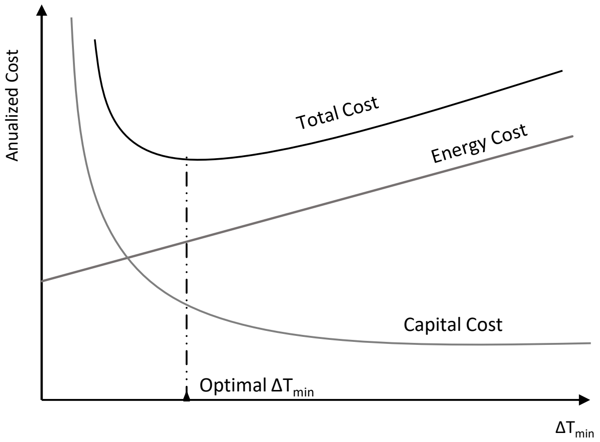

Figure 3-1: Optimal ΔT_{min} according to the trade-off between energy and capital cost [3]

Figure 3-1 shows a generalized relation between the energy and capital cost as function of $\boldsymbol{\Delta T_{min}}$ [7][3]. On this diagram is visible that an increase of the energy cost leads to a decrease of the capital cost. Therefore, an optimal minimal temperature difference $\boldsymbol{\Delta T_{min}}$ exists at the minimum value of the total annual cost of energy and capital costs. Usually the total cost curve is nearly flat around the optimum, so the nearby points around the optimal point are also acceptable.

- **The shape of the composite curves**

When the composite curves are almost parallel, a higher value of ΔT_{min} is chosen because the temperature difference between cold and hot streams, in any heat exchanger of the process, is close to the ΔT_{min} value. In this case, a small ΔT_{min} would result in a high heat exchange area for all heat exchangers (not only for the ones that transfer heat between streams close to the pinch point) and thus, high investment costs [3].

The difference in the results when changing $\Delta \boldsymbol{T}_{\boldsymbol{min}}$ are presented in the example in Figure 3-2 for two values of $\Delta \boldsymbol{T}_{\boldsymbol{min}}$: 10 °C and 20 °C.

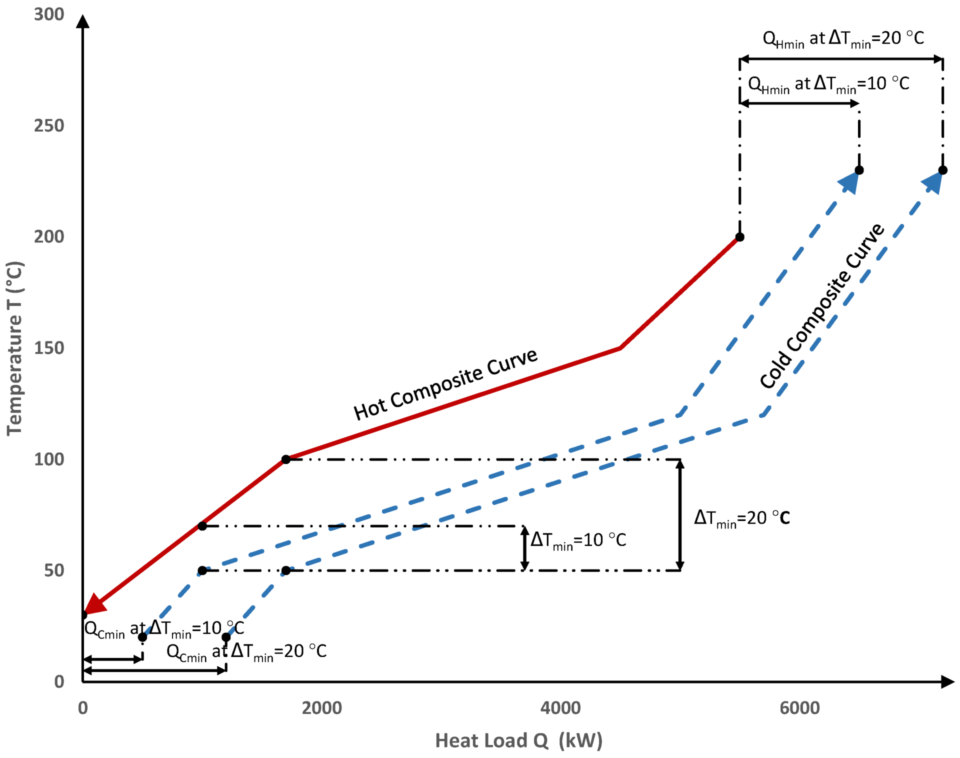

Figure 3-2: Effect of increasing $\Delta \boldsymbol{T}_{\boldsymbol{min}}$[27]

With **an increase of the value of $\Delta \boldsymbol{T}_{\boldsymbol{min}}$, the cold composite curve is further away from the hot composite curve, which means that their overlap is reduced. This leads to a lower heat recovery, but higher utility demand, meaning increased energy cost.**

At the same time, **the capital cost is decreased because bigger temperature difference in the required heat exchangers means smaller units.** In this case, the higher energy cost has been off-set with the reduced capital cost of the heat exchangers [3].

- **Experience**

In systems where fouling readily occurs, or where heat transfer coefficients are low, typical ΔT_{min} values of 30–40°C are used. For chemical processes, and where utilities are used for heat transfer, ΔT_{min} values are typically in the range of 10 to 20°C. For low temperature processes using refrigeration, lower ΔT_{min} values (3–5°C) are used to minimize expensive power demands in the refrigeration systems [3].

3.1.2 Definition of hot and cold streams

Data extraction means collecting and processing data about heating and cooling requirements of the process streams, often referred to as Stream Data [28]. Extracting the data needed for pinch analysis is a complex issue but a crucial part of the methodology considering that the results depend on this step. It is important to start from the data that you know/are given, continue with the information that you can determine following the rules and at the end calculate the rest of the data needed. Those steps lead to defining the hot and cold streams of the process, which will be used in the PA.

The information is usually being extracted from plant measurements, data acquisition systems or simulation models. It is important to take into consideration that the amount of available information is usually large, so the first step is to identify the relevant sources and sinks and their interactions in the process. The key information that needs to be extracted includes the temperature levels of the process streams and the amount of heat required to bring the desired changes in temperature [3].

For a complete optimization of the process, utility data is also required, referring the external heating and cooling systems available in the process [28], as well as the marginal utility cost [3]. When doing a case study for Retrofit Design, as in this case, data for the existing heat exchangers, heat exchanger area and heat transfer coefficient for cold and hot sides of heat exchangers is also needed.

In this case, a heat and material balance, as well as process and utilities flowsheets for the whole plant were provided, from which only the data necessary for the pinch analysis was extracted.

Data extraction must be performed carefully because the results strongly depend on this step. **At the beginning it is recommended that all process streams be included in the data extraction.** Constraints regarding issues such as distance between operations, operability, control and safety concerns can be incorporated later on.

There are **heuristic rules developed as guidelines that should be respected** when extracting data for a given process. The most important are the following:

- **Choose streams that change in heat load but not in composition**

One of the most important criteria is that a stream should change in a heat load but not in composition. Such streams are: flow of liquid through a heat exchanger, single component liquid being evaporated or a mixture which is being cooled without any separation of the components. But streams such as: flow of liquid through an absorption column or a scrubber, a mixture which is reacting or a flow through a distillation column from which a component is being removed should not be treated as single streams [7].

- **Mix the streams before taking it into consideration**

If two or more streams with the same composition leaving from different units are being mixed and heated/cooled to a common final temperature, the final, mixed stream should be considered as a single stream and the heating/cooling duty can be performed by one heat exchanger [7].

- **Do not include utility streams**

Utility streams (steam, flue gas, cooling water, refrigerant, cooling air, etc) should not be considered in the process data unless they are involved directly in the process or they cannot be replaced [3].One of the goals of using pinch analysis is to reduce the usage of utilities. Therefore, if utility streams are extracted in a similar way to process streams, they will be considered as fixed requirements and no opportunities of reduction in utility use will be identified. In some cases, utility streams can be included because it is not practical to replace them by any form of heat recovery. For example, this is often the case for steam dryers, ejectors and turbine drives [3].

- **Do not consider the existing plant layout**

When selecting the inlet and outlet parameters for a process stream, existing heat exchange equipment and plant topology should not be taken into account at first. True utility targets (for cooling and heating) should be set regardless of the existing plant layout. Current plant energy consumption can then be compared with minimum energy targets. In retrofit of existing facilities, once these targets have been determined, plant layout (existing heat exchangers and piping, distances, etc.) needs to be taken into account in order to identify practical and cost-effective projects to reach or approach these targets [3].

- **Identify hard and soft constraints on temperature levels**

For example, a hard constraint would be the inlet temperature of a reactor that cannot be changed in any way, while a soft constraint would be the discharged temperature of a product going to storage, for which the target temperature is often flexible. It is sometimes possible to change the potential for heat recovery by changing some process temperatures at the data extraction phase [3].

The crucial data for accomplishing pinch analysis is the temperature range of each stream and the heat needed to bring the streams to the required temperature. For that purpose, the **basic data** required for each stream is listed as follows:

- **Supply T_s and target T_t temperatures** $[℃]$**;**
- **Mass flowrate** $[kg/s]$;
- **Specific heat capacity** $[kJ/kg \cdot ℃]$**;**
- **Heat of vaporization for stream with a phase change** $[kJ/kg]$

When this data is known, the heat capacity flowrate and the heat load for each stream can be calculated.

3.2 Determining the energy targets

Once the data are extracted and calculated, the next step follows, which is providing a target for the minimum energy consumption. The energy targets in frames of the PA can be obtained in two ways:

- Graphical approach - **Composite Curves**
- Algebraic approach - **Cascade Method** (Problem Table).

It is important that these two methods give the same results, so that the HEN can be designed correctly.

3.2.1 Construction of the Composite Curves

The Composite Curves (CC) are representing the process' heat availability (hot composite curve) and heat demands (cold composite curve) on a Temperature(T) – Enthalpy (H) diagram. The degree to which the curves overlap is a measure of the potential for the heat recovery. That means that heat from the hot streams can be recovered and used to heat the cold streams which will decrease the necessary duties to cover the energy demands [7].

Table 3-1: Stream data for construction of the composite curves (Example)

Stream	T_s [℃]	T_t [℃]	CP $[kW/℃]$	H $[kW]$
H1	200	50	20	3000
H2	150	100	60	3000
C1	80	140	80	-4800
C2	60	180	15	-1800

The construction of the hot composite curve (HCC) for two individual hot streams with a given supply (T_s) and target temperature (T_t) will be explained on a simple example given in Table 3-1.

Steps for constructing the hot composite curve (HCC):

- **Present each stream on a T-H diagram**

Each stream is represented with a straight line starting from the stream supply to the stream target temperature (Figure 3-3, a)), with a slope equal to the reciprocated value of the heat capacity flow:

$$\frac{dT}{dQ} = \frac{1}{CP} \tag{3-1}$$

- **Temperature intervals**

In this step all the hot streams and their supply and target temperatures will be considered. The temperature intervals are defined according to the temperature levels at which enthalpy changes occur:

Interval I: 50-100 °C

Interval II: 100-150 °C

Interval III: 150-200 °C

- **CP for each interval**

Identify which streams contribute in each of the temperature intervals.

In the first interval, from 50 to 100 °C, only stream H1 is present. Therefore, the heat capacity flowrate - CP of the composite curve is equal to the CP of stream H1:

$$CP_I = CP_{H1} = 20\ kW/°\mathrm{C}$$

In the second interval, from 100 to 150 °C, both streams, H1 and H2 are present. The CP of the composite curve is the sum of the CPs of both streams:

$$CP_{II} = CP_{H1} + CP_{H2} = 20 + 60 = 80\ kW/°\mathrm{C}$$

In the third interval, from 150 to 200 °C, only stream H2 is present. This means that the CP of this part of the composite curve is equal to the CP of the stream H1:

$$CP_{III} = CP_{H1} = 60\ kW/°\mathrm{C}$$

- **Enthalpy changes for each interval**

The calculation of the enthalpy changes is done according to equation (2-22):

$\dot{Q}_I = 20 \cdot (100 - 50) = 1000\ kW$

$\dot{Q}_{II} = (20 + 60) \cdot (150 - 100) = 4000\ kW$

$\dot{Q}_{III} = 20 \cdot (200 - 150) = 1000\ kW$

- **Plotting the composite curve on a T-H diagram**

The HCC is constructed by adding the enthalpy changes of each individual stream within the corresponding interval (Figure 3-3, b)).

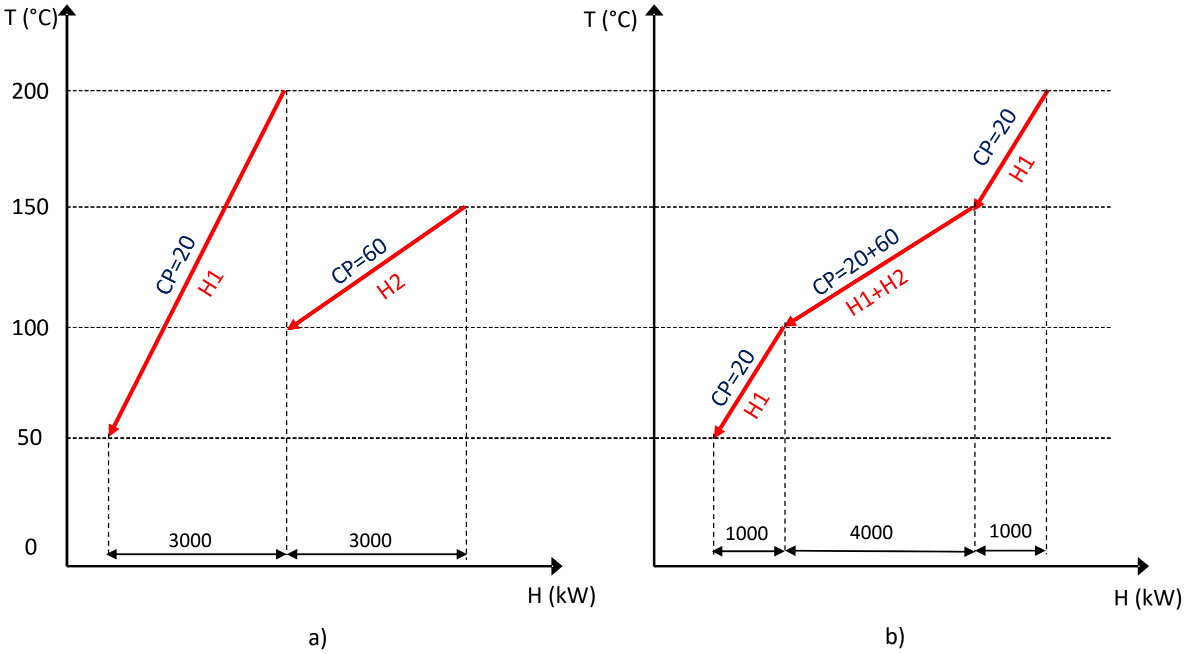

Figure 3-3: Construction of the Hot Composite Curve (HCC)

The construction of the cold composite curve (CCC), Figure 3-4, is done analog to the construction of the HCC, combining the representative curves of the cold streams:

Interval I: 60-80 °C ; $CP_I = CP_{C2} = 15\ kW/°C$; $\dot{Q}_I = 15 \cdot (80 - 60) = 300\ kW$

Interval II: 80-140 °C ; $CP_{II} = CP_{C1} + CP_{C2} = 95\ kW/°C$;

$\dot{Q}_{II} = 15 \cdot (140 - 80) = 5700\ kW$

Interval III: 140-180 °C ; $CP_{III} = CP_{C2} = 15\ kW/°C$;

$\dot{Q}_I = 15 \cdot (180 - 140) = 600\ kW$

When the heat capacity flowrate and the heat flow for each interval is calculated, the cold composite curve can be plotted in a T-H diagram, as shown in Figure 3-4.

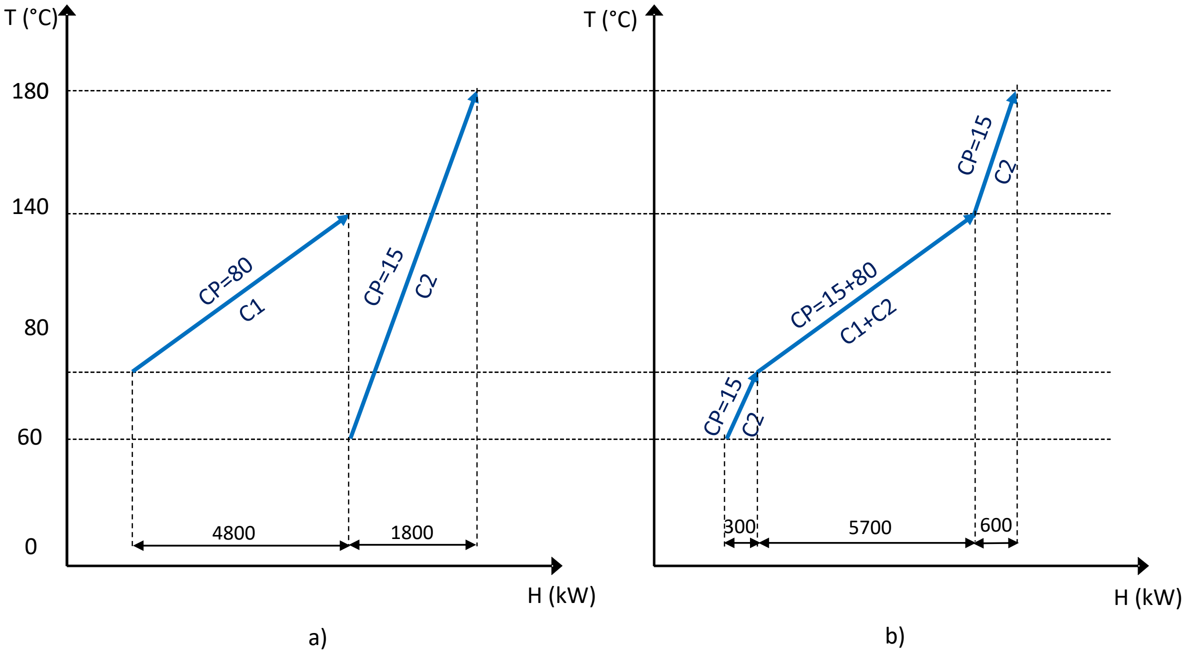

Figure 3-4: Construction of the Cold Composite Curve (CCC)

The results of the pinch analysis are represented in Temperature-Enthalpy Diagram through the composite curves (CCs) as shown in Figure 3-5. The hot streams are defined as heat sources and are graphically presented by the hot composite curve. The cold streams are heat sinks presented by the cold composite curve. The cold composite curve is mowed horizontally toward the hot composite curve.

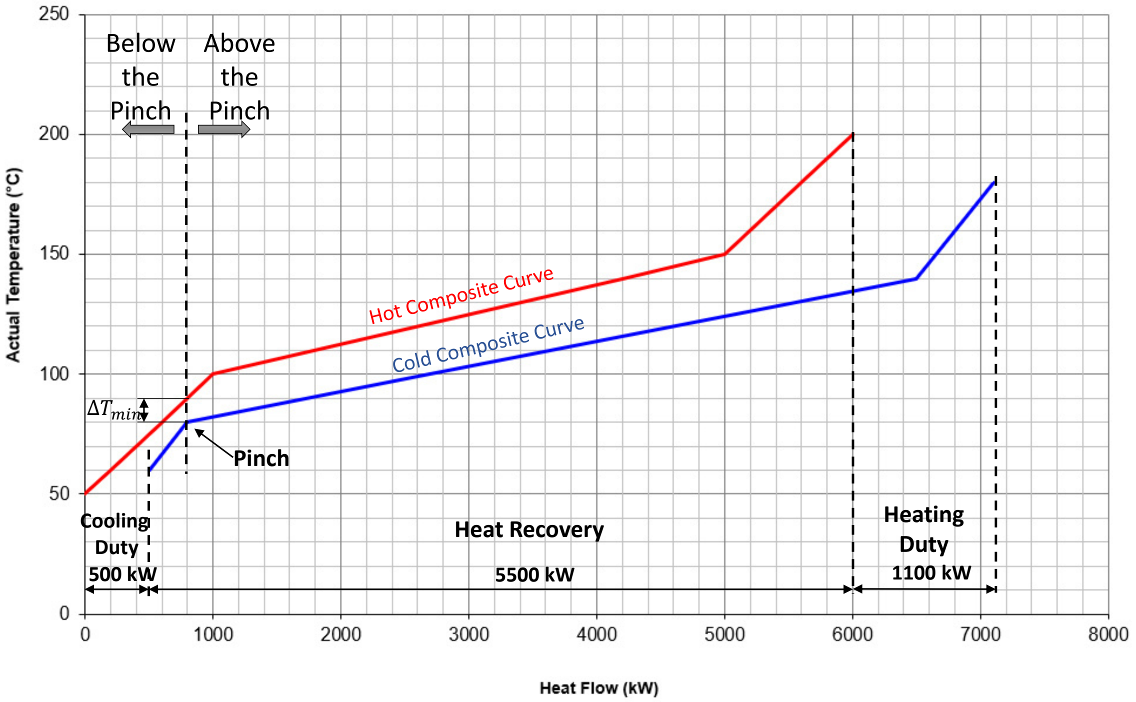

Figure 3-5: Hot and Cold Composite Curve

The point of the closest approach between the two composite curves represents the minimum temperature difference (ΔT_{min}) referred to as Pinch Point [3]. For this example, a ΔT_{min} of $10°\mathrm{C}$ has been chosen. This represents the minimum temperature difference that will be accepted in any heat exchanger.

The maximum heat recovery (MER) that can be achieved is represented by the overlap between the two composite curves. In this example (Figure 3-5), the MER is 5500 kW. The horizontal distance between the cold ends shows the value of the minimum cold utility requirement; in this example 500 kW. On the other side, the horizontal distance between the hot ends of the CCs, the minimum hot utility requirements are presented; 1100 kw for the given example.

The graphical method of the PA allows the engineer to read the energy requirements from the T-H diagram. The MER requirement is supplied by process to process heat exchange, whereas the minimum cold and hot duties are covered by utilities.

3.2.2 Cascade method – Problem Table

The Cascade Method or the Problem Table method is another approach for determining the energy targets. The enthalpy balance in this case is based on temperature intervals set up according to the supply and target temperatures of both, the hot and the cold streams. The procedure is almost the same as described for the composite curves method, with the difference that in this case needs to be ensured that within any interval, the hot and the cold streams are at least ΔT_{min} apart. This can be done in 3 different ways [7] :

1. Express all temperatures in terms of hot stream temperatures and increase all cold stream temperatures by ΔT_{min}.
2. Express all temperatures in terms of cold stream temperatures and reduce all hot stream temperatures by ΔT_{min}.
3. Use the shifted temperatures, which are a mean value; all hot stream temperatures are reduced by $1/2\ \Delta T_{min}$ and all cold stream temperatures are increased by $1/2\ \Delta T_{min}$.

The implementation of this method will be explained step by step in Chapter 6.5, applied on the corresponding case study.

3.3 Grand Composite Curve

The Composite Curves, as well as the Problem Table can be represented graphically, plotted on a temperature-enthalpy diagram, known as Grand Composite Curve (GCC). This curve shows the cumulative surplus or deficit of energy for each temperature [30]. Shifting of the stream's temperatures ensures that the minimum temperature difference of ΔT_{min} is maintained between the process streams and the utility levels [7].

The composite curves shown in Figure 3-6 are shifted for the value of $1/2\,\Delta T_{min}$ according to the 3rd rule described in section 3.2.2. The pinch temperature is at the point of nearest approach of the CCs; in this case they touch at the Pinch point. The hot and cold utility requirements didn't change with the shifting of the curves.

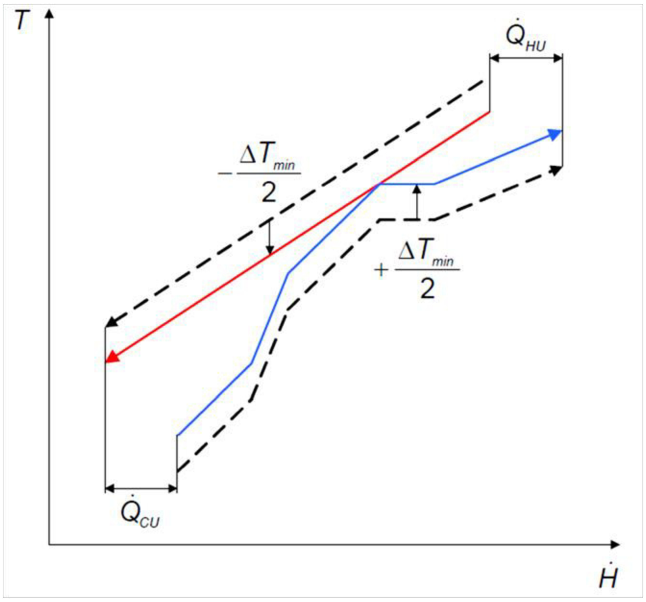

Figure 3-6: Shifted Composite Curves [31]

To construct the GCC from the shifted composite curves diagram, the horizontal distance between the shifted HCC and the shifted CCC will be plotted in a T-H diagram (Figure 3-7)

The point where the GCC touches the shifted temperature axis meaning that the net heat flow is 0 kW, represents the shifted Pinch temperature. In this way it is even more clear that the process is divided into two subsystems, below and above the pinch point [7].

The intervals A and D in Figure 3-7 which curves are marked with blue line, show positive slope. This means that between the temperatures T_0^* and T_1^*, as well as between T_0^* and T_1^*, there is a net heating demand available. The asterix "*" is a sign for the shifted temperatures. The curves with negative slope (marked with red line) show a net cooling demand. The "pockets" represented with shaded area between intervals A and B, and between D and E, represent the heat that can be recovered by the process streams. In this areas no external heating or cooling are needed [31].

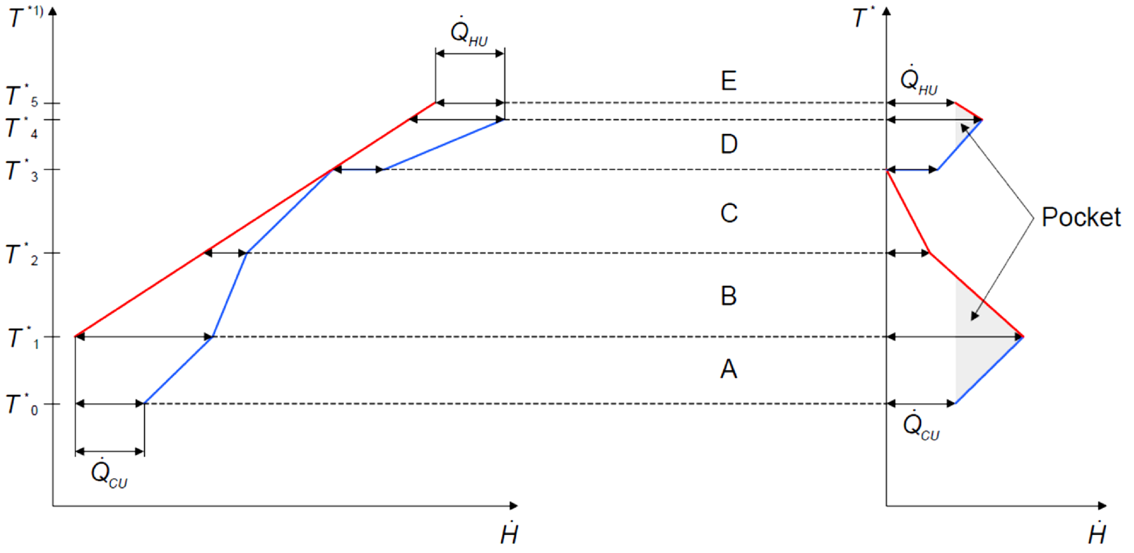

Figure 3-7: Plotting of the Grand Composite Curve (GCC) from the shifted composite curves [31]

Considering that the GCC was created from the shifted composite curves, before applying the temperature levels for the hot (T_{HU}) and cold utilities (T_{CU}), they need to be corrected for the factor $1/2\,\Delta T_{min}$ [31]:

$$T_{HU} = T^{*}_{HU} + \frac{\Delta T_{min}}{2} \tag{3-2}$$

$$T_{CU} = T^{*}_{CU} - \frac{\Delta T_{min}}{2} \tag{3-3}$$

The hot utility temperature (T^{*}_{HU}) needs to be increased for $1/2\,\Delta T_{min}$, whereas the cold utility temperature (T^{*}_{CU}) needs to be decreased for the same value, $1/2\,\Delta T_{min}$.

3.4 Golden Rules of the Pinch

Important property of the PA is that the Pinch Point divides the system into two thermally independent subsystems, above and below the Pinch (Figure 3-5). This is important when designing the heat exchangers network (HEN) because allows the both regions to be designed separately. Once the subsystems are defined, the three golden rules of the Pinch must be respected [32]:

1. **No cold utilities above the pinch.**
2. **No hot utilities below the pinch.**
3. **No transfer of heat across the pinch.**

The subsystem above the Pinch has a heat deficit, which is why needs only heating of the streams. A surplus of heat is identified in the region below the Pinch point and requires cooling duty. The last rule for meeting the energy targets helps an unnecessary cascade of energy through the entire system, from hot to cold utility to be avoided. If a certain amount of heat α, was to be transferred from the region above to the region below the pinch point (Figure 3-8), the requirement of hot utility will be decreased for the same amount of heat. This means, it has to be balanced with an additional hot utility $(Q_{hmin}+\propto)$. Since the subsystem below the pinch already had a surplus of heat before the heat transfer, additional cold utility needs to be added in order to satisfy the new requirement on cooling duty $(Q_{cmin}+\propto)$ [3].

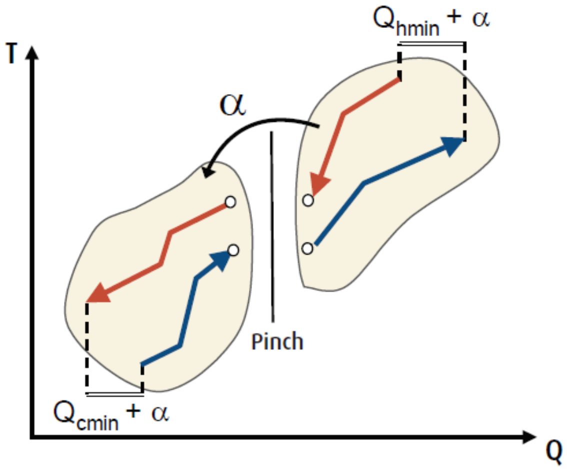

Figure 3-8: Transfer of heat across the Pinch [3]

Therefore, following the three golden rules of the pinch leads to designing a HEN that will satisfy the energy targets with suitable matches of streams without increasing the hot and cold utility consumption.

3.5 Heat transfer surface area

The required total heat transfer surface area for the entire HEN at the specified ΔT_{min} can be estimated before actually designing the HEN.

When the overall heat transfer coefficient k is known, the heat surface area may be calculated with the equation (2-27).

When multiple streams are involved in an interval, the following equation for the heat transfer coefficient is used [30]:

$$\frac{1}{k} = \sum_{i}^{hot} \frac{1}{k_i} + \sum_{k}^{cold} \frac{1}{k_k} \tag{3-4}$$

where k_i and k_k are the individual heat transfer coefficients for the i-th hot stream and for the k-th cold stream. This leads us to the following equation which gives a more accurate estimation for A_{HEN} [30]:

$$A_{HEN} = \sum_j \frac{1}{\Delta T_{LM,j}} \left(\sum_i^{hot} \frac{\dot{Q}_{ji}}{k_i} + \sum_k^{cold} \frac{\dot{Q}_{jk}}{k_k} \right) \tag{3-5}$$

$\dot{Q}_{ji}$ - rate of heat transfer from the i-th hot stream within the j-th enthalpy interval

$\dot{Q}_{jk}$ - rate of heat transfer to the k-th cold stream within the j-th enthalpy interval

3.6 Heat Exchangers' Network (HEN)

The design of the heat exchangers network uses the "Pinch Design Method" (PDM), whose application allows feasible network that achieves the energy targets set by the Pinch Analysis. The PDM incorporates two important parts [29]:

1. **It recognizes that the pinch region is the most constrained part of the problem** (it starts the design at the pinch and develops by moving away);
2. **It allows the designer to choose between match options.**

In effect, the design of network examines which hot streams can me matched to which cold streams via heat recovery. Every match brings the stream to its target temperature, meaning the hot streams will be cooled down until the Hot Pinch Temperature; the cold streams will be heated up to the Cold Pinch Temperature. Many variations can be possible and feasible, but the energy targets obtained by the design need to match the results from the Composite Curve Method and the Cascade Method.

HEN - Design Rules

1. **Stream Splitting Algorithm**
   a) N – Rule ($N_{out} \geq N_{in}$)
   b) CP – Rule ($CP_{out} \geq CP_{in}$)
2. **Start from the Pinch**
3. **Start from the highest CP_{in} in the Pinch**
4. **HEs Optimization**
   a) "Tick Off Rule"
   b) "Driving Force Plot"
5. **Next largest CP_{in} in the Pinch**
6. **Next closest to the Pinch**

Figure 3-9: Rules for designing MER HEN [31]

The MER HEN can be systematically constructed by following the HEN-Design Rules [31], Figure 3-9, and applying them for each subsystem separately.

1. Stream Splitting Algorithm

a) N - Rule $N_{out} \geq N_{in}$

N_{out} – number of streams "leaving the pinch"; the streams which do not begin directly at the pinch won't be considered [31].

N_{in} - number of streams "going in the pinch"; the streams which do not enter directly to the pinch won't be considered [31].

This rule guarantees the feasibility of the HEN for maximum heat recovery meaning [31]:

- there are enough hot streams above the Pinch that can heat up the cold streams

- there are enough cold streams below the Pinch that can cool down the hot streams

If $N_{out} < N_{in}$, one of the streams "leaving" the pinch needs to be splitted up.

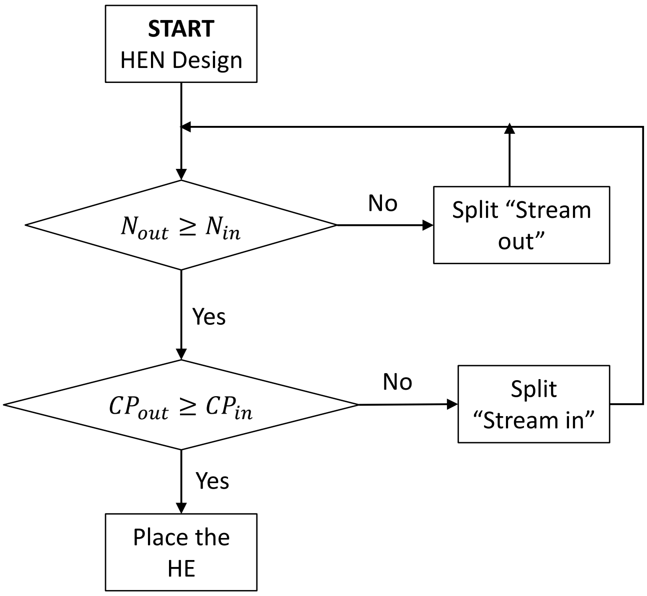

Figure 3-10: Stream Splitting Algorithm

b) CP – Rule $CP_{out} \geq CP_{in}$

CP_{out} – Heat capacity flow of streams "leaving the pinch"

CP_{in} – Heat capacity of streams "going in the pinch"

This rule ensures that by designing the MER HEN, the minimum temperature difference, ΔT_{min}, won't be crossed in any of the heat exchangers. To explain this rule, a theoretical HE between two streams will be considered (Figure 3-11).

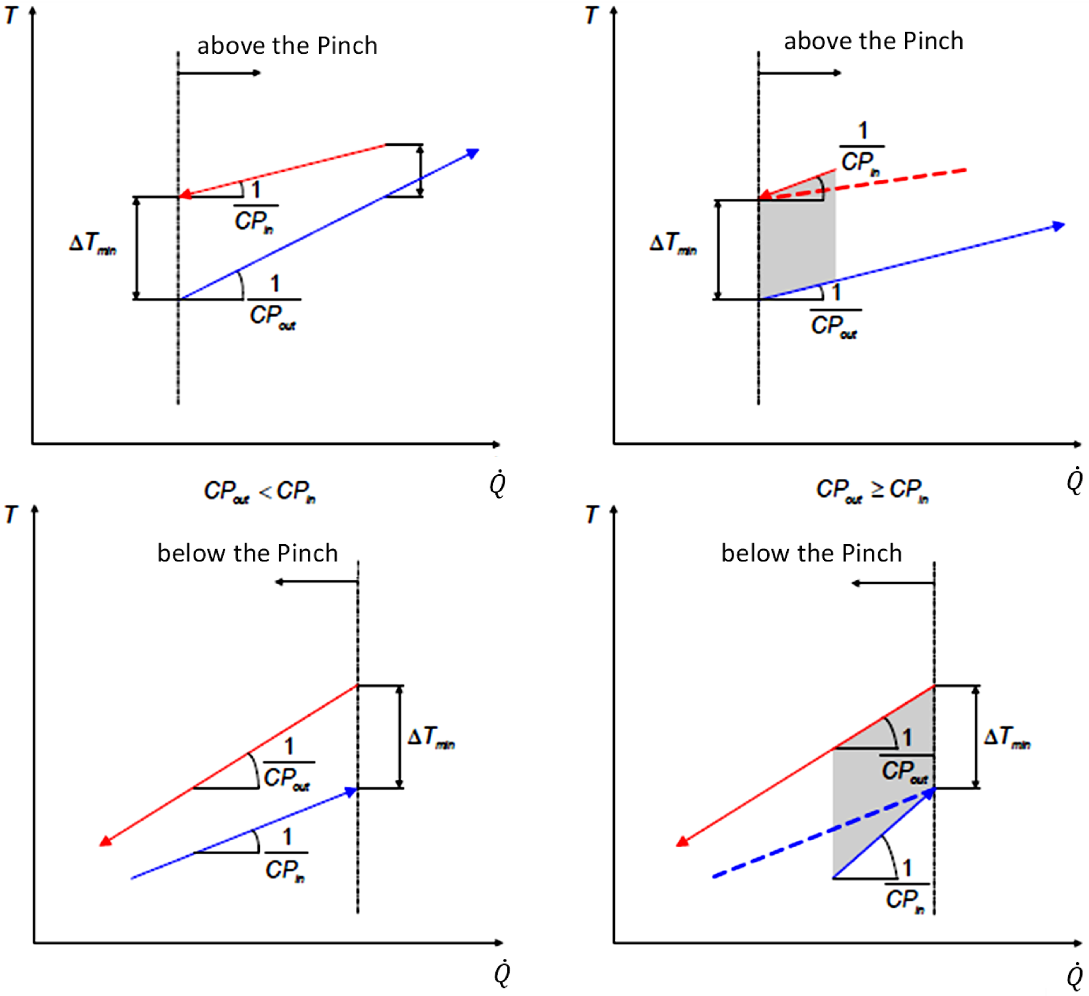

Figure 3-11: CP-Rule explained in T-H diagram

As shown in Figure 3-11, when $CP_{out} < CP_{in}$, the curves of the HE show that at some point the ΔT_{min} will be crossed over. To avoid that, the “Stream in” will be splitted in two different streams with lower heat capacity flowrate then the original stream. In this way, the slope of the curve will be steeper $\left(\frac{1}{CP}\right)$, while the supply and target temperatures stay the same. That ensures that the two curves are “divergent” or at least parallel [31].

This rule applies to the HEs at the Pinch point. For the ones who are further away from the Pinch, breaking the rule is allowed only when the minimum temperature difference is being kept [31].

Splitting of streams according to the Stream-Splitting Algorithm rule and the calculation of the corresponding heat capacity flowrates and heat flow is explained on the case study later on in this work (Chapter 6.7 Design of HEN).

2. Start from the Pinch

The HEs that are nearest to the Pinch point should be considered first, because they have the lowest temperature gradients between the hot and the cold streams [31].

3. Start from the highest CP_{in} in the Pinch

The stream with the highest capacity flowrate has the flattest slope of the curve, which is why is the most difficult to handle regarding the ΔT_{min} and needs to be considered at the very beginning when designing the HEN [31].

4. HEs Optimization

The optimization of the heat exchangers can be applied in one of the following ways:

- **“Tick Off Rule”**
- **“Driving Force Plot”**

The “Driving Force Plot” approach is being used when the goal is designing a network with minimal total area of the HEs.

In interest of this work is the other approach, **“Tick Off Rule”**, because leads to designing a network with minimal number of units. Considering that the goal of the study is a retrofit PA, it is better to implement as less as possible HEs, while maximizing their efficiency.

According to this rule, one of the streams will be “emptied”, all of its energy requirement will be covered with the placed HE. This stream can then be “thick off” and the next stream will be considered.

When the HEs nearest to the Pinch point are placed, the designing of the HEN continues with the next largest CP and the next closest to the Pinch point.

4 STATE OF THE ART OF PINCH ANALYSIS

Fifty years history of the pinch analysis started with small know-how practical applications which led to several commercial failures and divided opinions. The concepts of pinch analysis were integrated by technical experts into the design process on one side, whereas concerns existed that the PA can lead to missing big opportunities for improvement on the other side [33]. Nevertheless, PA has evolved from re-designing heat exchanger networks into a defined general methodology for improving the process efficiency, reducing the investment costs and optimizing the process control [4].

4.1 Short history of Process Integration (PI)

The historical milestones of heat integration in the period between 1944 and 1969 were marked by developments of the HEN synthesis. The research presented by Gundersen and Naess and the overview of process synthesis by Nishida et al. were considerable starting impulse for further developments [2]. In the 70s, Bodo Linnhoff at the Swiss Federal Institute of Technology (ETH) in Zurich and the Leeds University introduced the PI concept based on pinch analysis (PA). Although his first paper as a PhD Student was nearly rejected, due to its persistence the idea of PI was launched [2].

The PI was developed from simple curves representing the total heating and cooling requirements of a process in a temperature-enthalpy diagram. This graphical representation is referred to as Composite Curves (CC) method. An algebraic approach leaded to the Problem Table Algorithm (PTA) or Heat Cascade as a numerical method. In this way, the deficits and surpluses of energy in the system are presented, as well as the necessary information for constructing the Grand Composite Curve (GCC) [2].

The pinch point was introduced firstly in 1983 as the temperature level, corresponding to a zero heat flux between the hot and cold fluid (Figure 3-7) and proposed the graphical approach based on the Grand Composite Curve (GCC) in order to evaluate the pinch and the energy targets [4].

In the late 1980s and early 1990s, the pinch analysis was developed and pioneered by the Department of Process Integration at the Institute of Science and Technology within the University of Manchester (UMIST) [2]. In 1983, the Linnhoff March Ltd was established offering process design services to international clients. For instance, in the following years, 80% of the world's largest oil and petrochemical companies became its clients or sponsors [4].

Contributions at that time in the field of PI were made also in Japan, at the Chiyoda Chemical Engineering and Construction Co. Ltd., Tsurumi, Yokohama. Their publications dealt with HEN

Synthesis, optimum water reallocation in a refinery and applications of the temperature-enthalpy diagram to heat integrated system synthesis [2].

In 1990s' the researches in the field of HI further presented the heat-deficit region above the Pinch point and a heat-surplus region below the Pinch point. In that way, the guidelines for increasing the potential for heat recovery were introduced by Dhole (1994) and further developed by Linnhoff [2].

Although PA provides promising results for individual processes, heat exchange between process streams is required to reach the identified energy targets. This process-process interaction is typically impossible on industrial sites for practical reasons, such as shutdown, startup and safety issues. In order to overcome these drawbacks the Total Site Heat Integration (TSHI) method was initially introduced by Dhole and Linnhoff [34] and further developed by Raissi [35]. It includes indirect heat transfers between processes meaning that the excess heat of one process can be used as a heat source for another process identified as heat deficit. The remaining heat deficit is than supplied by utility.

The total site analysis (TSA) was developed into a more implementable methodology by a research group at the University of Pannonia, Hungary led by Klemes, in a collaboration with the Center of Process Integration (CPI) at the University of Manchester and the University of Maribor. Further on, the focus of TSHI practical implementations was put on a Combined Heat and Power (CHP) processes [2].

As analogy to the heat integration, developments were made also in the field of mass transfer. Driving force for heat integration is the temperature difference that leads to a heat transfer between the substances. On the other hand, mass is transferred as a result of concentration differences. In that way, the Mass Pinch, developed by El-Halwagy and Manousiouthakis has various industrial applications in the units where process stream are exchanging mass, such as absorbers, extractors, etc. [2]

4.2 Developments in the PI by using Pinch Analysis

This thesis studies the possibilities for heat recovery between different units of a complex Upstream plant regarding a retrofit design. The Phase 1 of the plant is well-deigned in terms of energy efficiency and in function in the last ten years. However, it will be investigated if there is still place for improvements between the different units of the plant. There is Phase 2 planned that should increase the capacities of produced gas and condensate. Developing methodology for heat recovery between the two plants (Phase 1 and Phase 2) can lead to Total Site Analysis (TSA). So far, in the upstream sector the same concept of PA as in the downstream have been used. Because of that, in this part, complex studies from the petrochemical industry, showing different methods for retrofit design between units as well as between plants were chosen.

The pinch analysis (PA) started as an optimization tool for individual processes or units, analyzing only the efficient use of their utilities and improving their energy efficiency. For refineries and petrochemical plants, but also for large industrial units of other sectors, the PA was broadened, considering the fact that they are usually serviced by centralized utility system. In this case PA can be used to determine the energy targets for the entire site and integrate the different departments, which operate independently (Total Site Analysis-TSA) [36]. One more step forward is Regional Energy Analysis representing the identification of the potential of a whole area by studying the energy demands of the companies in that region and their potential to share heat amongst them. This concept can give an insight about the amount of waste heat available for export, investigating if it is enough to be used for district heating or power generation, depending on the temperature level of the waste heat [36].

One of the successfully implemented cases was presented by Matsuda et. al. with a comprehensive Total Site Heat Integration (TSHI) study applied in Kashime industrial area, one of the largest chemical and petrochemical complexes in Japan [37]. The study shows that even though the individual sites of one complex have high efficiency, there is a potential for energy savings among different sites. It demonstrates the use of R-Curve and Site Source Sink Profile (SSSP) analysis. The R-Curve is a representation of the power to heat ratio (W/Q) and shows the maximum achievable efficiency, which compared to the existing efficiency shows the possibility for improvement. The SSSP curves were generated from the heat exchanger of the process utility interfaces such as heaters, coolers and steam generators. Other projects were also included in forming a long-term energy saving plan for the plant in Kashima, which resulted in rearranging the steam header conditions and defining new specifications of utility conditions according to the SSSP analysis and installing a 400 MW gas turbine and 300 MW steam turbine in order to satisfy the energy targets defined by the R-Curve method. This methodology has shown that the pinch technology tools and techniques can be successfully used for enormous and complex industrial areas [37].

The PA framework in combination with a non-convex Mixed Integer Nonlinear Programming (MINLP) model has been developed for establishing energy targets for waste HI not only among sites but also between plants.

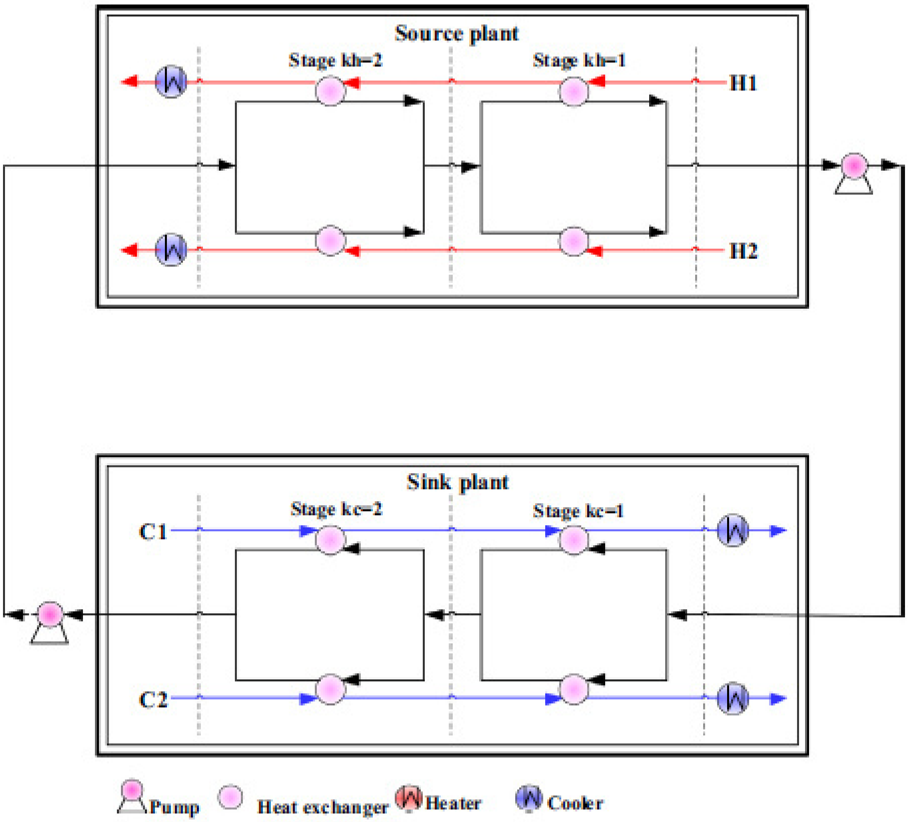

Figure 4-1: Waste HI between two plants using HRL [38]

For that purpose, an efficient optimization algorithm using a heat recovery loop (HRL) between two plants was presented in the paper of Chang et. al.[39]. The plant which demands heat is the sink plant and the plant which supplies heat is presented as a source plant (Figure 4-1). The heat integration was achieved due a heat recovery loop (HRL) which uses water as an intermediate fluid and is responsible for transferring heat from the source plant to the sink plant. The heat recovery is influenced by the mass flow rate of the intermediate fluid. When the fluid has a high mass flow rate, the gradient of the line is small, which means bigger heat recovery (Figure 4-2, left). In case of low mass flow rate, the value of the heat recovery is also low (Figure 4-2, right).

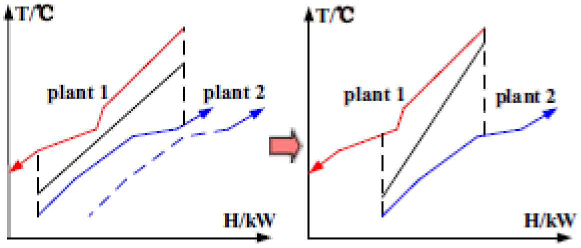

Figure 4-2: Dependance of the heat recovery from the mass flow rate of the HRL [39]

The dimensions of the pipeline, more precise its diameter, through which the recovery fluid is transported, directly influences the mass flow rate. For a higher mass rate, contributes larger diameter and more power for fluid transportation is required. This results in higher investment costs, meaning that a trade-off between the energy recovery and the distance related costs is necessary. The case study was implemented in an industrial plant in China. The structure as shown in Figure 4-1, and a corresponding mass flow rate optimization of the recovery fluid have resulted in a decrease of the total annual cost (TAC) from around 50% [39].

Another area of interest in the development of PA is the Heat Exchanger Network retrofit method with accent on the need to avoid cross-pinch transfer. Its application in a large petrochemical complex consisting of several interconnected processing units was presented in two case studies by Feng et. al [40]. This case studies explain the rules of how to define a boundary for heat integration in order to maximize the energy saving potential. The boundary for heat integration can be the whole plant or its individual processing units. The first case study was based on an aniline plant which has four processing units: nitrobenzene unit, aniline unit, natural gas unit and waste acid treatment unit. Considering that the total energy saving potential of all subsystems was close to the energy saving potential of the whole system, the heat integration was carried out in each subsystem itself, resulting in a retrofit design with total energy recovery of 76.2 % The second case study explains the choice of the boundaries of aromatic hydrocarbon plant with three units: hydrocracking unit, aromatic hydrocarbon extraction unit and isomerization unit. In this case the boundary for heat integration was the whole system because its energy saving potential was considerably higher than the one of all subsystems. The new design resulted in 61.05 % energy recovery compared to the original design [40].

Another method for identification of the possibilities for HEN retrofit was presented in a study by Bonhivers et. al. in 2014 [41]. This method called Energy Transfer Diagram (ETD) provides a graphical representation of the current performance and driving forces of the existing HEN (Figure 4-3). The inefficiencies are than identified with a GCC of an individual heat exchanger [2]. The enhanced version of this method is called Modified ETD (METD) where the individual heat exchangers are represented as heat recovery pockets of the GCC showing the temperature and quantity of heat in surplus and deficit with respect to the minimum approach temperature. This method has a purpose on reducing the heat flow from the utilities to the environment in order to optimize the energy consumption. The heat savings modifications imply bridging heat outlets to hot utility users [41]. For large plants as complex as oil refineries the Modified Energy Transfer Diagram (METD) lead to developing the Heat Surplus Deficit

Table (HSDT) into an automated retrofit targeting model for identifying new utility paths as a result of a new heat exchanger units [42].

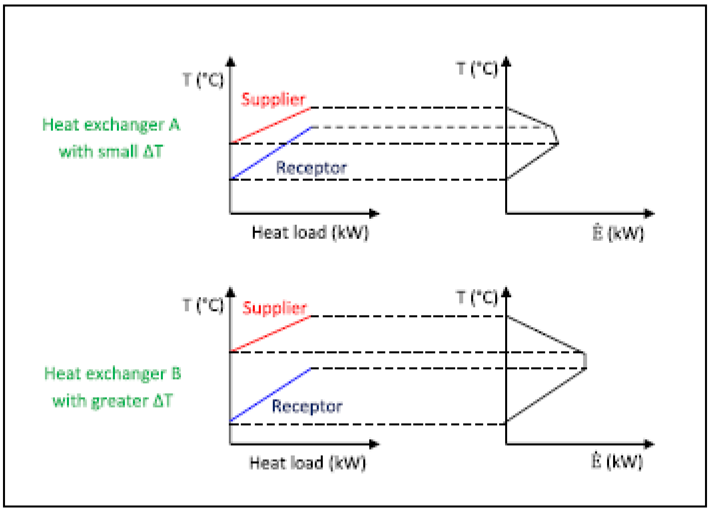

Figure 4-3: Connection between heat load curves of PA and energy transfer curves [41]

The study of Gadalla et.al. [43] presents a new graphical approach which is based on PA and requires only simple data of process stream temperature. With this approach each heat exchanger is represented as a straight line in a diagram formed from a hot stream temperature as y-axis and cold stream temperature as x-axis. The gradient of the line depends on the ratio of the heat capacity flowrates for the selected streams. Each point on the graph is identified by the x-coordinate representing the cold stream temperature and the y-coordinate showing the driving force of the HE.

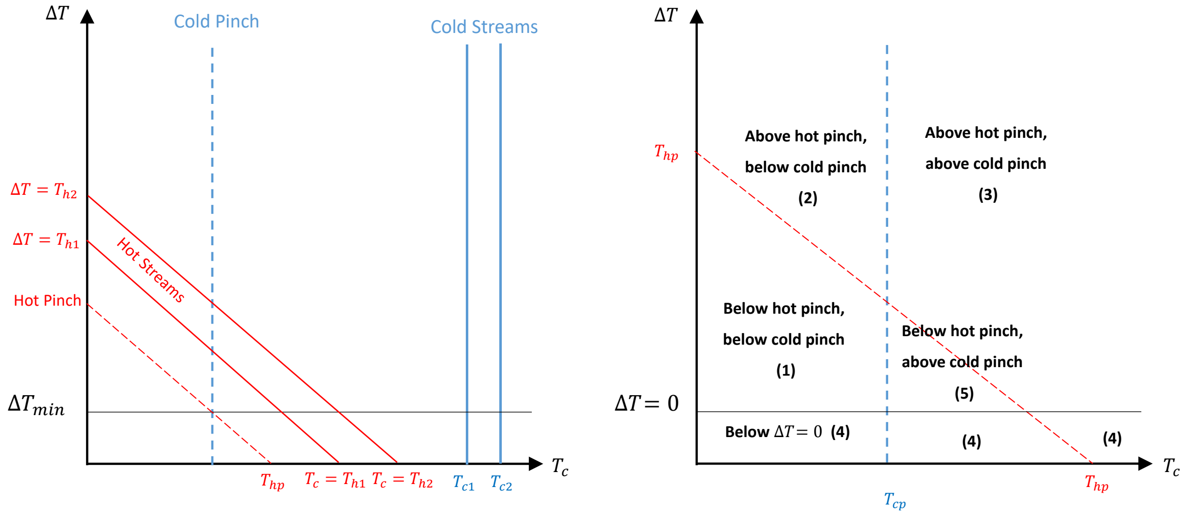

Figure 4-4: Graphical representation of: a) hot and cold streams; b) feasible regions for heat integration

The vertical lines, starting at T_c on the x-axis represent the cold streams. The straight lines starting from T_h on the y-axis and ending at T_c on the x-axis are representation for the hot streams. All the hot streams are parallel to the hot pinch line, and all the cold streams are parallel to the cold pinch line. $\Delta T_{min}$is represented as a horizontal line at $\Delta T = \Delta T_{min}$. This graphical approach shows five different regions (Figure 4-4) according to which the placement for a corresponding heat exchangers can be determined. Region 1 and 3 are convenient for implementation of heat exchangers, coolers (region 1) and heaters (region 3). Any heat exchanger in region 4 is infeasible, whereas regions 2 and 5 represent a non-optimal area for any HE, as they cross the pinch. This method was used as a tool for HI in an existing Egyptian oil refinery, resulting in 10% energy saving and a payback period of no more than half a year [43].

Another significant development of the retrofit design based on a PA is the Retrofit Tracing Grid Diagram (RTGD) developed as a follow up from the Grid Diagram Table. This method uses a temperature scale (x-direction) in grid diagram format without any shift for the ΔT_{min}. In this diagram the locations of the coolers, heaters and recovery units are highlighted [2].

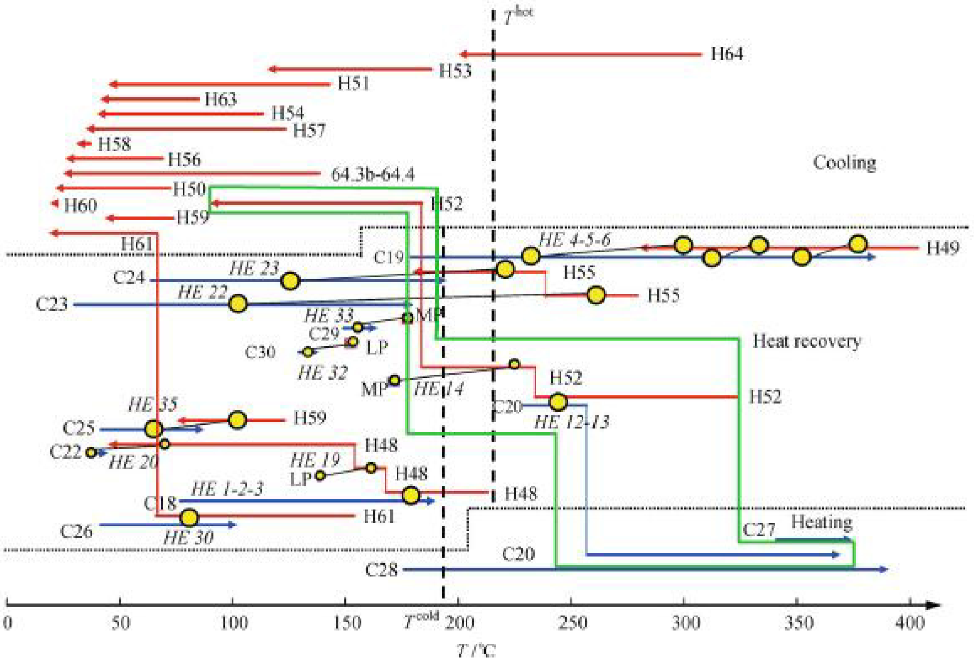

Figure 4-5: Retrofit Tracing Grid Diagram (RTGD) [44]

It has the ability to reveal additional options for modification compared to the previous methods. The application of this method is explained in a case study for an oil refinery considering four operating scenarios as a result from the seasonal temperature situation (winter and summer) and the type of the processed crude oil (high and low Sulphur content). The RTGD can be analyzed considering three regions (Figure 4-5):

a) cooling region, presented by the hot streams;

b) heat recovery region, presenting the heat exchangers by circles whit a small distance between the hot and the cold stream;
c) heating region showed by the cold streams.

This representation provides a clear indication of that which streams, or part of streams are not already integrated in the existing HEN. Involved streams are partitioned to different level on vertical axes, presenting the connections between the streams. When the heat transfer is close to vertical, the heat exchangers are presented with one (yellow) circle. However, when the heat transfer is highly non-vertical it is presented with two smaller yellow circles connected with a line (Figure 4-5). This gives already some initial indication regarding the current network performance, as networks with highly non-vertical heat transfers can usually be enhanced. In that case, the heat exchangers can be removed and reconnected with other newly integrated streams. Such modification can be reasonable when a hot stream with lower temperature and a cold stream with higher temperature are available compared to currently integrated streams. The results of the case study have shown heat recovery from around 2 MW and payback period in less than a year. The same method was applied to retrieve any remaining waste heat which was used for a district heating of the town of Busalla, Italy [44].

The PA as a tool and a technique for a process integration via heat recovery has a variety of applications. In the recent years, a subject of intensive studies in the frames of numerous research centers and institutes, has been the Total Site Heat Integration (TSHI). The further developments in this direction, have to face the challenges coming from such a technique. The key issues of the Total Site targeting include automation of the targeting procedure, investment costs, environmental impact, reliability, maintenance and regulatory issues [45]. These problems can’t be ignored and when in large quantity, can make the total site targeting complicated to study and evaluate. But not considering them, can lead to unfeasible designs. A properly resolved system and integration of the method can contribute in a high rates of heat recovery and reducing the total energy consumption of whole sites.

Based on the TSHI, several authors have worked on industrial symbiosis of industrial parks considering not only energy and water but also combinations of them both, as well as integrating products and waste. Dealing with the waste-to-energy and waste-to-wealth problems opens possibilities for implementation of the PA for achieving long-term sustainability [45].

4.3 “Time-resolved” Pinch Analysis

In the last years, the PA is being used as basis for indirect heat recovery via energy storage integration, especially in continuous, batch and semi-continuous processes. Here two methods will be presented. The first one is graphical developed from the composite curves approach, and the other one is a numerical method based on the problem table, or cascade method.

The batch processes are a complex optimization problem because of their time-dependent behavior. Olsen et. al. have presented a methodology for optimization of a batch processes through three types of improvements: direct heat recovery (DHR), indirect heat recovery (IHR) and utility system optimization. The IHR is done using a thermal energy storage design based on the Time Average Model (TAM). In this case the process heating and cooling demands are distributed over the duration of the batch. This model uses source/sink profile (ISSP) which includes temperature shifting of the streams [46].

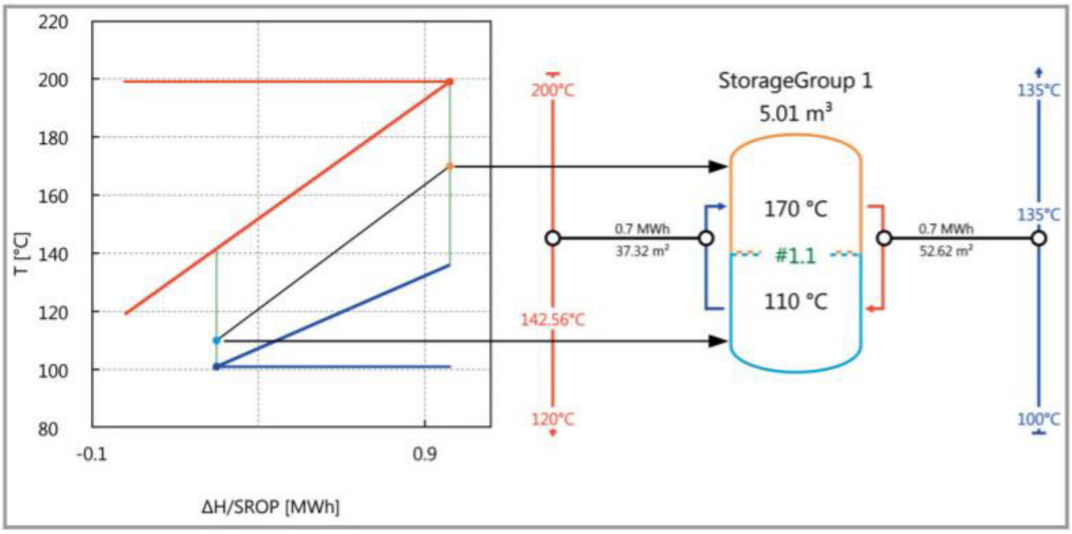

Figure 4-6: Placement of an IL/HS system within the ISSP [46]

The intermediate loop and heat storage (IL/HS) systems are placed between the source and sink profiles in real temperature as shown in Figure 4-6 with a black line. The IL/HS systems extract heat from the source profile, transfer it to the heat storage, and distribute it to the sink profile later. Once the IL/HS system has been conceptually placed within the ISSP, the streams can be allocated to the individual IL/HS system as shown in the heat exchanger and storage network (HESN) on the right in Figure 4-6 [46].

This allocation enables the computation of the required heat exchanger areas for heat recovery. A heat balance at each time slice within the single batch defines the loading and unloading profile of each heat storage from which the required capacity and volume is derived. The model used distributes the heat recovered between streams over the whole batch duration rather than at the time when heating and cooling demands are simultaneous. Therefore, this model does not minimize the required storage volume but provides a conservative design based on the expected variability in the heating and cooling demands [46].

A case study of Jamaluddin et.al. have presented a developed numerical method for trigeneration with energy storage design known as TriGenCT. A trigeneration system is a technology that can produce power, heating and cooling from a single energy source. Construction of TriGenCT with energy storage systems is used to determine the minimum target for outsourced power, cooling and heating, amount of excess power, heating and cooling for storage during the first day and continuous 24 h operations and maximum storage capacity. The energy efficiency was increased by reusing the access heat for district heating and for heating and cooling utilities of the plant and by selling the access power to the grid [47].

5 PLANT DESCRIPTION

5.1 Categorization of the oil and gas industry

The oil and gas industry includes the exploration, extraction, refining, transportation and distribution of petroleum products. It is divided in three main sectors: Upstream, Midstream and Downstream processes. This categorization comes from the petroleum value chain, according to which the oil and gas industry includes activities for finding and producing hydrocarbons; refining the hydrocarbons and producing saleable petroleum products; and storage and transportation of the resources and the products. There isn't a clear border between the three sectors because of different opinions and approaches. Nevertheless, there is a general, mostly accepted concept that gives an overview of the processes and facilities in each sector [5].

The upstream processes, often referred to as Exploration and Production (E&P) processes include searching for potential underground or underwater crude oil and natural gas fields, drilling exploratory wells and subsequently drilling and operating the wells that recover and bring the crude oil or the natural gas to the surface [5]. The upstream activities are often divided in two groups [48]:

a) "subsurface" – the activities up to the producing well head (drilling, casing, completion, wellhead);
b) "surface" – hydrocarbon lifting technologies and surface facilities for conditioning the fluids up to the export product's specification.

The midstream sector refers to transportation and storage of the crude oil and natural gas before they are refined and processed into products. It includes pipelines, shipping, storage tanks and all the infrastructure needed to move the resources to long distances [5].

The downstream sector involves the petrochemical plants and refinery processes for production of a variety of petroleum products [5].

5.2 Upstream processes

This case study is about a real-time onshore upstream gas and condensate production plant, in which the facilities and processes for conditioning the well fluids are our sphere of interest.

Once a natural gas or oil well is drilled and it has been confirmed that there are commercially viable quantities present for extraction, the well must be completed in order to allow the crude oil or natural gas to flow out of the formation up to the surface. On the top of the well, sits the wellhead which's structure is often called Christmas tree. The well head has a task to maintain the well conditions and to ensure an efficient flow of natural gas from the well. The well flow is controlled with a choke valve [48].

The individual well streams through a network of gathering pipelines and manifold systems are brought to the main production facilities. In the case considered in this work, the well flow consists of a full range of hydrocarbons from gas (methane, butane, propane, etc.), condensates (medium density hydrocarbons) to crude oil. It also contains a variety of unwanted components, such as water, carbon dioxide, salts, sulfur and sand. The well fluid from the gathering manifold enters the central processing facility (CPF) where is processed into clean marketable products; in this case natural gas and condensate [48].

The natural gas and condensate exported from the production installation is monitored and managed with metering stations which allow measuring of the flowarate of the gas/condensate without impeding its movement. Usually a metering installation consists of several meters so that the full capacity range is not handled by only one meter. The meter accuracy is being tested and calibrated at regular intervals [48].

The facilities of the gas and condensate production plant being investigated are situated in an arid environment and mountainous terrain. The production capacity of 847 564 m^3/day (30 MMSCFD) natural gas, 525 m^3 /day (3300 BPD) stabilized condensate and 159 m^3 /day (1000 BPD) produced water is covered by three wells. The working conditions of the well are 65°C - 100°C well head temperature and 227 bar(g) well head shut-in pressure [5].

The layout of the plant consists of the following facilities [5]:

- Well head facilities
- Transfer and flow lines
- North Gathering Manifold
- CPF inlet manifold
- Gas Sweetening Unit
- Gas Dehydration Unit
- Dew Point Control Unit
- Sales Gas Metering
- Flash Separator
- Flash Gas Compressor
- Export Sales Gas Compressor
- Condensate Stabilization Unit
- Produced Water Treatment Unit
- Condensate Storage and Loading Facilities

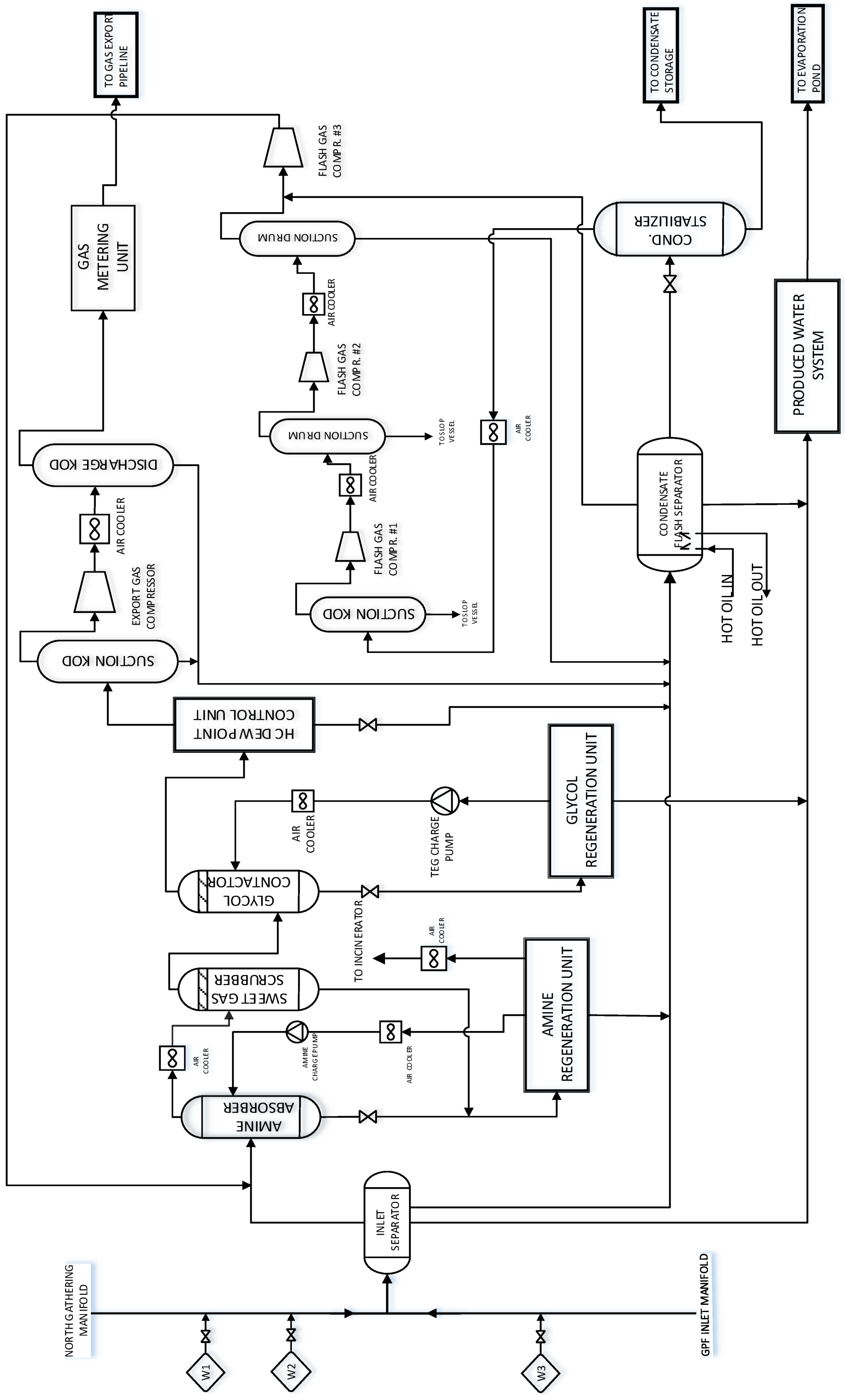

Figure 5-1: Representative flowsheet of the gas processing facility [5]

The whole production system is supported by the utilities, which do not handle the hydrocarbon process flow, but provide services to the main process. In this plant common facilities will be provided, such as: high pressure (HP) and low pressure (LP) flare system, utility air system, raw/service water system, evaporation ponds, fuel gas system, hot oil system, power generator, emergency power generator, pig launcher/receiver, fire water, diesel storage and transfer system, water system, refrigeration system, corrosion, wax and hydrate inhibition packages, pipeline venting or flaring facilities etc. [5]

The central processing facilities (CPF) are approximately 7 km away from the farthermost wells and around 30 km away from the nearest town. This position was chosen considering the distance from community, the land ownership, the site flood risk, the ground water prospects, the production loss risk due to access closure and the incremental cost [5].

5.3 System configuration

The required production of gas and condensate is met by three wells: W1, W2 and W3.

Well fluid flowing temperature and pressure downstream of choke valve is 65°C (max) and 77 barg (max) respectively. The maximum flow through each well varies between 23543 m^3/h and 30000 m^3/h (20 and 25 MMSCFD) [5].

The wells W1 and W2 are connected through flow lines to the North Gathering Manifold from which a transfer line transports the fluid to the Central Processing Facility (CPF). The well W3 is directly connected to the CPF [5]. The well fluid composition at standard conditions (at 0 bar(g) and 15,5 °C) is given in Annex A, Table 9-1 and Table 9-2.

The north gathering manifold has a pig launcher and a pig receiver facility. The CPF has two pig receivers: one to receive the pig scrapper form the north gathering manifold, and the other one to receive the pig scrapper from the south wells (W3). The pigging is a procedure of forcing a solid object through a pipeline for cleaning or technological purposes, without stopping the flow of the product in the pipeline.

Each well head is provided with pig launchers and Chemical Injection Skids [5]:

- Wax Inhibitor
- Corrosion Inhibitor
- Hydrate Inhibitor

The task of the Wax Inhibitor is to avoid wax formation problems in the flow-lines due to wax precipitation. The injection occurs when the temperature of the well-fluid is below the wax deposition temperature.

In order to protect the carbon steel wellhead piping and the flow-lines from corrosion caused from the CO_2 and H_2S in presence of moisture, continuous injection of the corrosion inhibitor is needed. This inhibitor and the wax inhibitor are injected after the choke valve.

The Hydrate Inhibitor reduces the hydrate formation when the well-fluid temperature falls below hydrate formation temperature in the flow-lines and transfer lines. Methanol is used for hydrate inhibition. The hydrate inhibitor is injected prior to the choke valve.

There are two test headers, one at the North Gathering Manifold for W1 and W2 and another including a test separator at the CPF for W3. Test separators are mandatory equipment in CPF and have the task to measure (test) the main parameters of the fluid, such as temperature, pressure and flow rates of each separated phase (gas, oil, water). This is a legal and technological requirement from reservoir engineering and production in order to keep tracking of the reservoir production and evolution. In this way, it is possible to diagnose well problems, evaluate production performance of individual wells and manage reserves properly. The well fluid from the test separator is sent to the inlet separator [5].

The Inlet separator in this process is a horizontal separator with big slug retention, which is designed to handle large gas capacities and liquid slugs on a regular basis. In this case, the vessel is a three-phase separator that separates the hydrocarbon liquid and the liquid water from the gas. It is absolutely essential that no liquid, condensate or water enters the absorber section.

The operating pressure of the test- and the inlet-separator is 69 bar(g), and the operating temperature is 24/65 °C (W/S). The role of the inlet separator is based on separating the fluid phases according to the density difference between the liquid and the gas [5].

The gas stream from the Inlet Separator mixed with recompressed flush gases from low pressure equipment, flows further to the Gas Sweetening Unit (GSU) consisting in an Monoethanolamine (MEA) plant where H_2S and CO_2 content of the gas will be reduced to the required sales specification. In case of reduction of the wellhead pressure that leads to insufficient pressure before the Gas Sweetening Unit, a front-end compressing system will be activated.

The sweet gas passes through a Gas Dehydration Unit, consisting of a Triethylene Glycol (TEG) unit, where its water content will be reduced to meet sales gas specification. The dehydrated gas flows further through the Hydrocarbon Dew Point Control Unit (HDPC). In this unit the heavier HC content of the gas will be stripped off by cooling via a mechanical refrigeration unit and low temperature separation (LTS). The condensate recovered from the HDPC Unit is sent to the condensate stabilization unit.

The liquid from the Inlet Separator is flashed in the 3-phase Flash Separator. The Hydrocarbon Liquid from the Flash Separator is stabilized in the Condensate Stabilizer. The stabilized condensate is being cooled before being sent to the Storage Unit. The acid gas recovered from the Condensate Stabilization Unit (CSU) is sent to the incinerator.

Overheads of the Condensate Stabilizer and vapors from the Flash Separator are compressed to a pressure equal to HP gas from the inlet separator by Flash Gas Compressor and mixed with the main sour gas stream entering the MEA unit. [49].

Sales gas flows through Sales Gas Metering to the export pipeline network. The sales gas and condensate specifications are given in Appendix A Table 9-3.

The field instrumentation used to control the process is a SMART type with HART protocol. All transmitters have integral digital indicators configured in engineering units. The control elements are pneumatic, electric or hydraulic, depending on the requirements. The use of switches is avoided and transmitters are used for measurements, alarms and protection [5]

The design characteristics of the individual units of the G-Plant are listed in section 9.2 in Appendix A.

5.3.1 Gas Sweetening Unit

The high pressure (HP) sour gas stream, after leaving the inlet separator flows in the Gas Sweetening Unit, which removes the carbon dioxide and the hydrogen sulfide from it, so that the sweetened gas complies with the sales gas quality regulations.

A natural gas is defined as “sour” when the H_2S content of the gas mixture exceeds the limit imposed by the purchaser of the gas. A sour gas can vary over a wide concentration of H_2S and CO_2, as well as other sulfur compounds. When the H_2S content exceeds the sales gas specification limit, the excess H_2S must be separated from the sour gas. This process of removal of the H_2S from the sour gas is called “sweetening” [50]. In this case, the limit set by the sales gas specification (Table 9-3: Quality specification of the products, Appendix A) can not cross 3.8 ppm.

In Figure 5-2 a process flow diagram of the gas sweetening unit of the plant is shown which uses an amine solution, in this case, Methildiethanolamine (MDEA), as a regenerative chemical solvent for sweetening the gas. The sour gas, after being separated from the well fluid, flows into the lower part of the amine absorber which represents an absorption column. In the upper part of the absorber a lean amine solution is pumped in and it flows down from tray to tray. As the sour gas flows upwards a high interfacial contact area is provided so that the mass transfer of H_2S from the gas to the liquid can be enhanced. The absorption process prefers conditions of low temperature and high pressure in order to increase the amount of H_2S dissolved in the liquid and to prevent the volatization of the solvent. These parameters allow higher solubility of the gas, increased mass transfer and reduced solvent losses. H_2S is being absorbed at temperature of 40°C, adjusted by an air cooler the pressure is maintained at 66 bar(g). When the gas reaches the top of the vessel, almost all of the H_2S is removed. The sweet gas, leaving the amine absorber at 70.25°C is being cooled down to 48.89°C by an air cooler before entering the sweet gas scrubber. The scrubber has a task to "polish" the gas eliminating any residual contaminants before sending the gas flow to the sweet Gas Dehydration Unit (GDU).

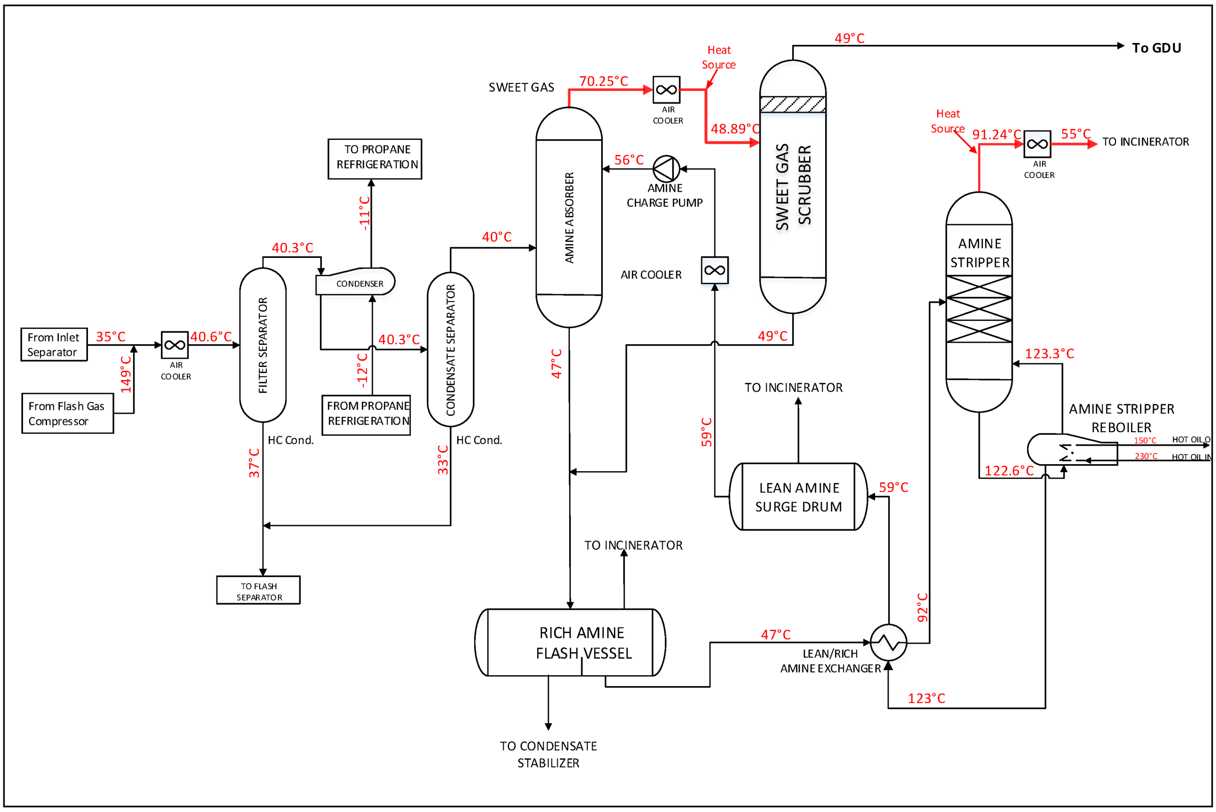

Figure 5-2: Gas Sweetening Unit (GSU)

At the bottom of the Amine Absorber, the rich solution after reduction of the pressure to around 4.5 bar(g) with a pressure drop valve, is sent to the Rich Amine Flash Vessel where most dissolved hydrocarbon gas and some acid gas flash off. After that, the solution will be heated up to 92°C using the hot regenerated lean solution stream. The heated rich solution then enters the amine stripper where the regeneration of the solvent occurs at a low pressure and high temperature. To achieve the needed temperature level for regeneration (100°C) an external source, hot oil circuit, is used. The desorbed acid gas and any hydrocarbon gas not flashed off in the flash drum leave the stripper at the top at 91.24°C , containing some solvent and a lot of water vapor. Afterwards, the stream is sent through a condenser, in this case air cooler before going to incinerator. The regenerated solution is cooled down to 59℃ in the lean/rich amine exchanger and being sent to a lean amine surge drum, where the acid gas is separated from the liquids and sent to the incinerator. From here, the lean amine will be cooled down to 56℃ with an air cooler before entering the amine absorber which working temperature is 40.3℃.

As mentioned before, in this case an amine solution or more precisely Methyldiethanolamine (MDEA) was used for sweetening the gas. Amines are weak organic bases that when reacting with the acid gases in the contactor, form unstable salts. The salts break down under the elevated temperature and low pressure in the stripper. The amines are highly suitable for removing the acid gases from the hydrocarbon gas stream, because the chemical reactions are reversible by changing the physical conditions of temperature and pressure between absorber and still [50].

In this unit, two possible heat sources were detected. One is the stream before entering the sweet gas scrubber, being cooled down from 70.25℃ to 48.89℃ . The second, is the gas stream leaving the amine stripper with 91.24℃ being cooled down to 55℃ before entering the incinerator.

After leaving the GSU the sweetened gas goes into the Gas Dehydration Unit.

5.3.2 Gas Dehydration Unit

The main task of the Gas Dehydration Unit is to ensure that the water content of the sales gas is within specification limit. According to the sales gas specification (Table 9-3: Quality specification of the products, Appendix A), the water content is limited to 0.147 g/kg at tie point to the customer.

Dehydration of the gas can be done in the following ways: absorption with glycol; adsorption with dry desiccant; absorption with a deliquescent salt; and refrigeration and hydrate suppression with a chemical. There are four types of glycols used for gas dehydration: ethylene glycol (EG), diethylene glycol (DEG), Triethylene glycol (TEG) and tetraethylene glycol [50]. In our case, the water vapor is removed from the gas with Triethylene glycol (TEG). This type of glycol is mostly used because of the advantages that it has in comparison to diethylene glycol (DEG): is more easily regenerated to a higher degree of purity, vapor losses and operating costs are lower (45).

The process for glycol dehydration is shown on the scheme in Figure 5-3. The gas flow is sent through a separator for removing the condensed liquids or any solids that might be in the gas, to the lower part of the Glycol Contactor. The glycol TEG, after being cooled by an air cooler, flows down from the upper part of the contactor. The cooling of the chemical solvent has the purpose of maintaining low temperature in the contactor. In this case, as well as in the amine absorber, low temperature and high pressure are preferred so that the solubility of H_2O is increased and the loss of solvent is limited. As the gas rises upwards, it comes to a direct contact between the gas and the glycol. With specific internal equipment configurations, a large surface area between the gas and the liquid is accomplished.

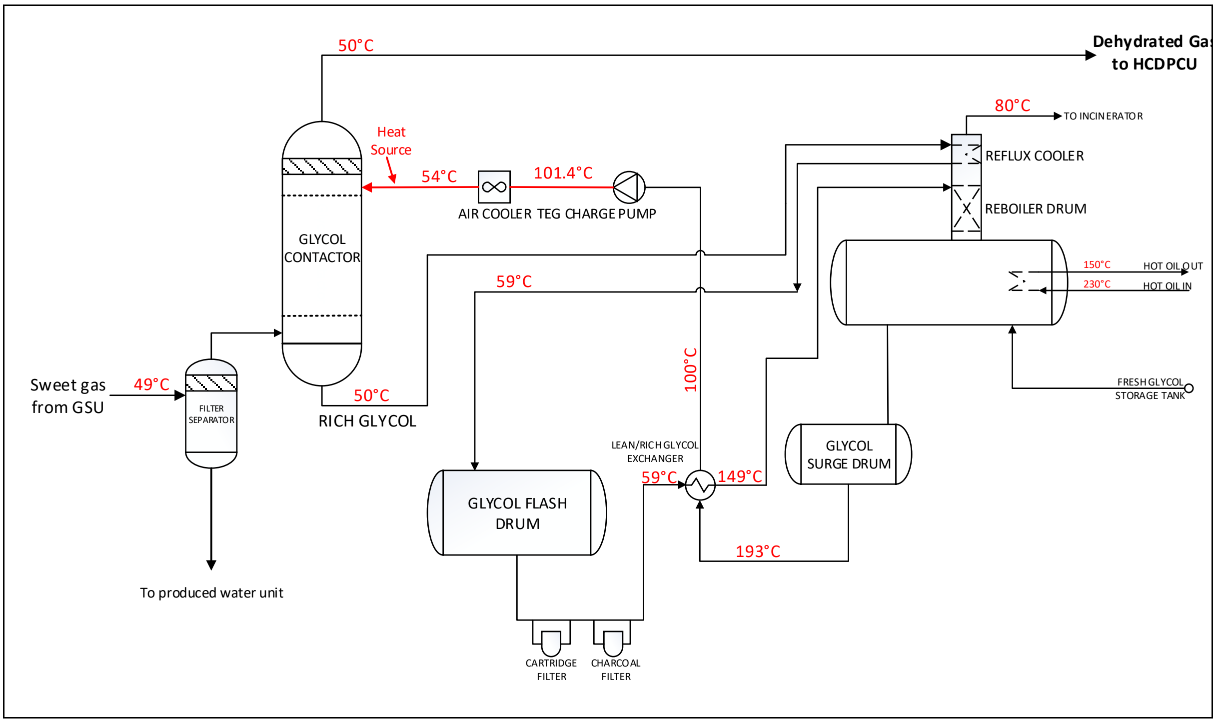

Figure 5-3: Gas Dehydration Unit (GDU)

H_2O is being removed at temperature of around 50℃, while a pressure of 64 bar(g) is maintained. Most of the water in the gas phase will be absorbed by the liquid glycol phase due to its hygroscopic characteristic. The rich glycol that contains the absorbed water, is withdrawn from the bottom of the contactor and is sent to the regeneration section. The treated gas leaves the contactor at the top of the column at temperature of 50℃.

The rich glycol that leaves the absorber must be regenerated to a high level of purity before it is recirculated to the absorber. The regeneration starts with heating up the rich glycol from 50 ℃ to 59 ℃, , with a heat exchange coil at the top of the glycol re-boiler known as reflux cooler or still. The rich solution then passes through a flash drum where the absorbed hydrocarbon gas is separated from the glycol. The hydrocarbon gas goes to low pressure (LP) Flare header. The rich glycol solution is being cleaned in cartridge and charcoal filter with a purpose of maintaining a high degree of solution cleanliness to avoid solution foaming. After that, is heated up to 149 ℃ as a cold stream of the lean/rich glycol exchanger, and through the still goes to the glycol re-boiler. In the re-boiler with the help of the hot oil system, the glycol is heated up to the necessary regeneration temperature of 193℃, because of which the glycol loses its ability to hold water, the water is vaporized and leaves at the top of the still. The regenerated glycol first goes to a glycol surge drum, that has a task to handle any surges in the circulation rate. The lean glycol represents the hot stream of the lean/rich heat exchanger, being cooled down to 100℃ by heating up the stream with the rich glycol. Before the regenerated glycol can be used for dehydration of the gas, the working conditions of the glycol contactor must be accomplished. After cooling the lean glycol, it is sent through a TEG surge pump that boosts its pressure from 0.014 bar(g) to 68.3 bar(g), after which using an air cooler the temperature of the glycol will be adjusted from 101.4℃ to 54℃. This stream will be considered as a heat source in the heat integration analysis, with the possibility to decrease the air cooler duty or to cut it off from the system.

The dehydrated gas at temperature of 50℃ is then sent to the Hydrocarbon Dew Point Control Unit (HCDPCU).

5.3.3 Hydrocarbon Dew Point Control Unit

The Hydrocarbon Dew Point Control Unit (HCDPCU) has a task to adjust both hydrocarbons and water dew point in order to inhibit the formation of hydrates in the gas stream and to avoid liquids formation which can affect export quality of the gas. For that purpose, the hydrocarbon liquid is being removed from the gas in order to satisfy the hydrocarbon dew point specification of the sales gas. The hydrocarbon dew point is defined as the temperature (at a given pressure) at which the hydrocarbon components of the gas will start to condense out of the gaseous phase [50].

As shown in Figure 5-4, the hydrocarbon content is reduced by cooling the treated gas stream with propane refrigeration utility, as well as a low temperature separation (LTS). The gas flow with temperature of 50 ℃ is firstly cooled down to 8.3 ℃ by the gas leaving at the top of the low temperature separator. Any condensate produced at this point is removed in the cold separator. After that, the gas stream is once again cooled down to -3.61 ℃ by a propane refrigeration unit before entering the low temperature separator (LTS). This LTS unit uses the Joule-Thompson effect to reduce the gas temperature upon adiabatic expansion low to -17 ℃. The LTS system can only be used where sufficient pressure is available to provide the desired processing and separation, here 61.2 bar(g). Not only HC condensation, but also a water condensation is achieved with this temperature reduction. The water is generally removed as hydrates in this process.

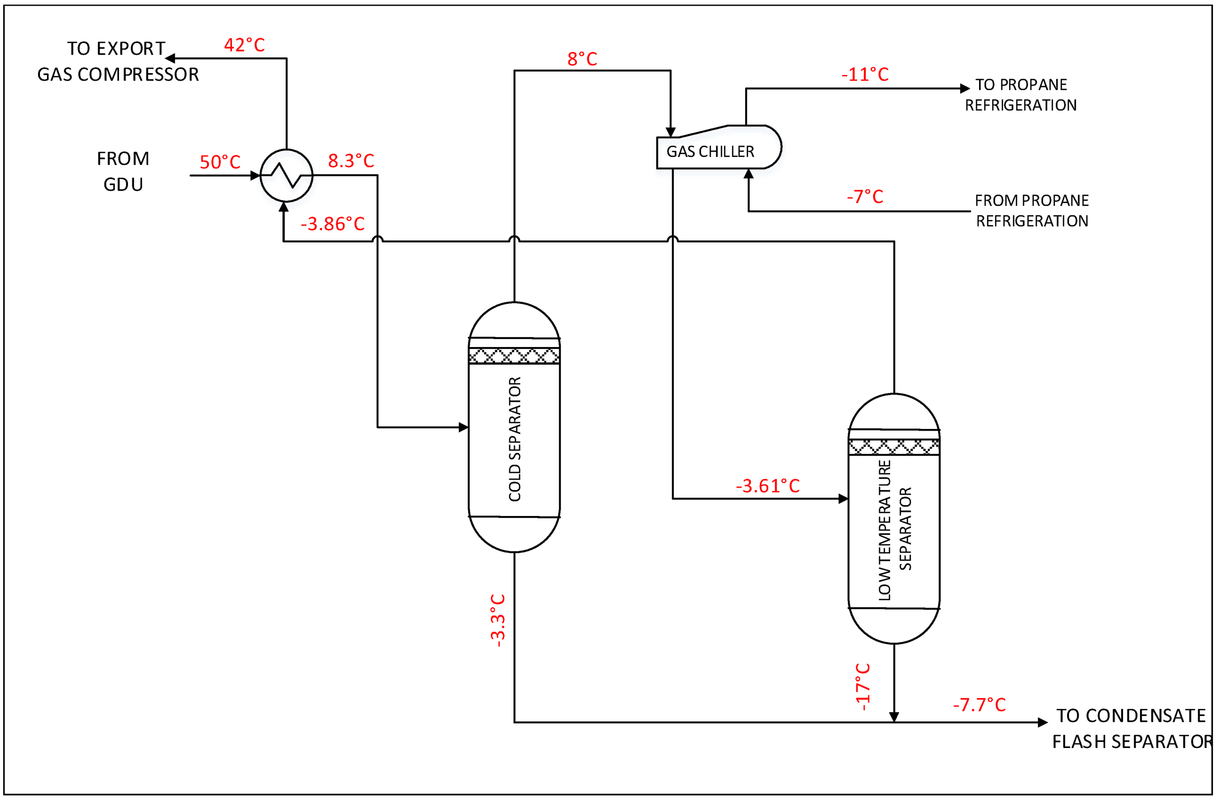

Figure 5-4: Hydrocarbon Dew Point Control Unit (HCDPCU)

Thus, the process can actually accomplish dew point control of both water and hydrocarbon at a single unit. The gas leaving the LT separator has achieved the hydrocarbon dew point is being heated up to 42 °C in a gas/gas heat exchanger by the gas stream coming from the GDU.

The heated gas is then sent to the export gas compressor unit at a temperature of 42 °C.

5.3.4 Condensate Stabilization Unit

The condensate stabilization unit (CSU) achieves a stabilization of the separated condensate in the individual processes, so that its storage and shipment are enabled. The condensate which is collected from different units (Flash Gas Compressor Unit-FGCU, HCDPCU, GSU, inlet separator), after mixing has a temperature of 28.15 °C. In the condensate flash separator, the condensate is preheated up to 46 °C by a hot oil system after which through a heat exchanger a temperature of 101°C is achieved.

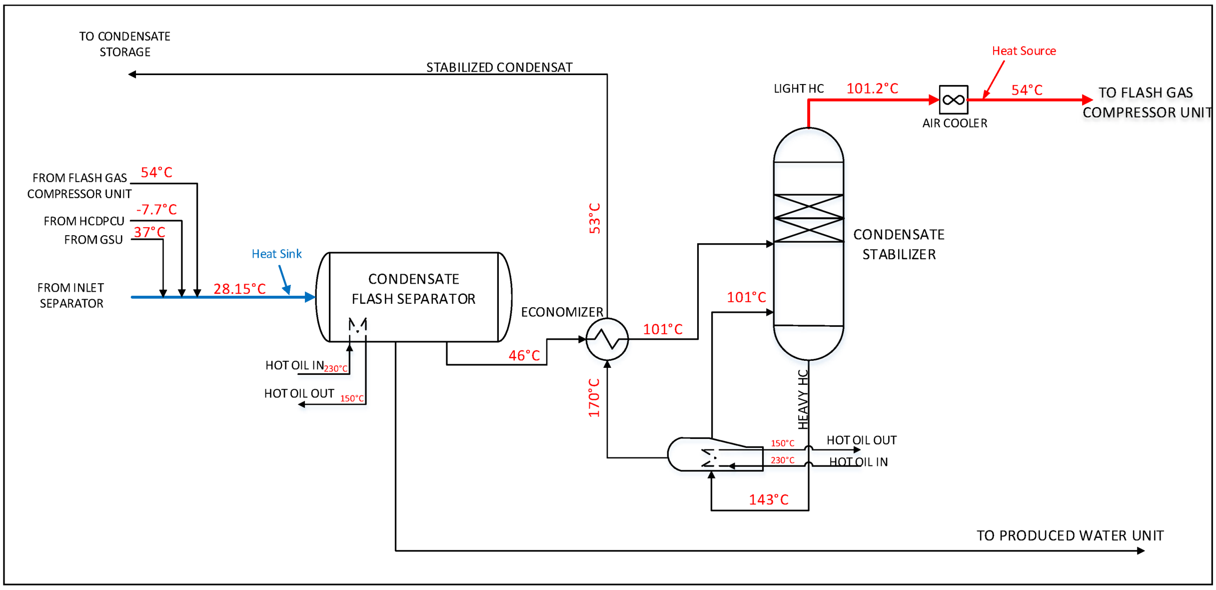

Figure 5-5: Condensate Stabilization Unit (CSU)

The separation and the stabilization of the condensate prefer higher temperatures because in this way the lighter hydrocarbons evaporate and are removed from the condensate. The heavier hydrocarbons in a liquid phase are removed at the bottom of the stabilizer and are heated up once again by a re-boiler using the hot oil system up to 170 °C. This stream is being cooled down to 53 °C by heating up the condensate in a heat exchanger before entering the condensate stabilizer. The resulting stable condensate has a low vapor pressure of 0.21 bar(g) and a temperature of 53 °C so it can be stored in tanks for shipping.

The vapor that leaves the stabilizer is being cooled down from 101.2 °C to 54 °C before entering the FGCU. This stream has a potential of being a heat source in the system for the heat integration, with the idea of reducing the duty of the air cooler. A heat sink, on the other side, is marked after mixing the condensate from the different units and before entering the condensate flash separator with the opportunity to reduce the duty of the hot oil system.

5.3.5 Gas Compression Unit

The lighter components removed in the gas phase during the stabilization process will be at a lower pressure than the main gas stream. These components must be re-compressed to the HP-separator pressure so they can be processed with the rest of the gas.

The overheads of the condensate stabilizer and vapors from the flash separator are being compressed through three stages Flash Gas Compressor to a pressure equal to HP gas from the Inlet Separator, 69 bar(g). The compressed gas is injected upstream of the Gas Sweetening Unit.

The Export Sales Gas Compressor, in case #600 ANSI rating, compresses the treated gas from HDPC Unit to the required limit pressure of 83 bar(g). A compression is not needed if the well flow lines and plant are operated on a higher pressure (case: #900 ANSI Rating) [5].

The ANSI (American National Standard Institute) rating refers to a pressure and temperature ratings for steel pipe flanges and flanged fittings. It defines the maximum allowed pressure that a flange can withstand at increasing temperatures. There are seven classes: 150, 300, 400, 600, 900, 1500 and 2500 [51].

5.3.6 Produced Water Treating

The water separated in the Gas Sweetening Unit, the Gas Dehydration Unit and the Condensate Stabilization Unit still contains a certain amount of oil, dissolved gases, solid particles and other impurities which must be removed to acceptable levels before the water can be disposed of. The produced water is sent to a water degassing boot where the gas left in the stream is removed and further sent to LP flare header. The oil will be removed in a separator and distributed to a slop vessel with recovered oil pumps. The separated water is disposed at an evaporation pond.

The capacity of the water treatment system not only cater the produced water at the GPF, but also the additional water from pigging operations or any unforeseen plant upset conditions.

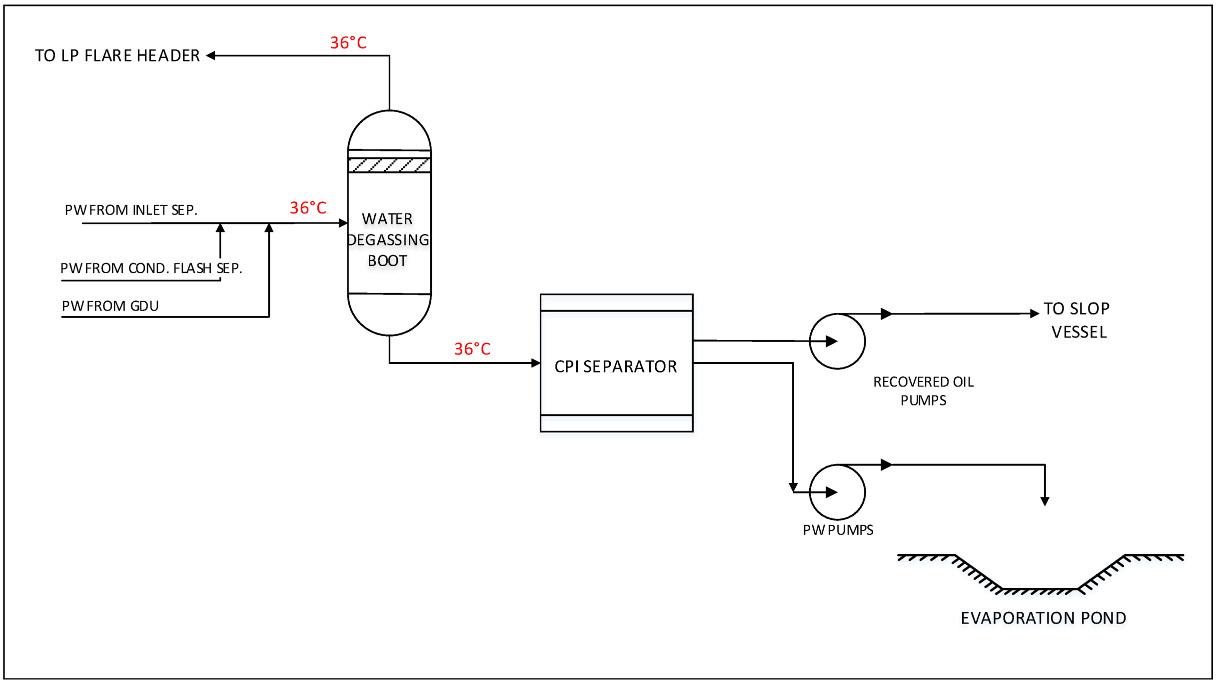

Figure 5-6: Produced Water System (PWS)

6 APPLICATION OF THE PINCH METHODOLOGY FOR AN UPSTREAM PLANT

6.1 Problem statement

The energy optimization via Pinch Analysis aims on developing methodology for heat integration which can be implemented in the design process of any complex upstream plant.

The main unit operations are based on modification of the physical properties, such as pressure and temperature. The idea is to analyze the different heat requirements and to identify the sources and sinks of energy. A "**source**" corresponds to a stream that has available heat to be recovered and is presented through the hot streams; whereas a "**sink**" requires heat, representing the cold streams. For that purpose, the overview of the process shall be done based on the existing process and utilities flow diagrams (PFD's, UFD's), as well as on the heat and material balance (H&MB) that contains the working conditions of each stream in the plant.

In order to determine the key areas for possible improvements, the following **selection guideline**, according to the operations within the plant, was made:

1. The separators need, in many cases, lower temperature;
2. The columns involved in absorption process, such as amine absorber (GSU), TEG absorber (GDU) etc., require high pressure and as low as possible temperature (limited by the physical properties of the corresponding stream and the material resistance);
3. The units for regeneration of the chemical solvents TEG and MDEA using desorption process as in amine stripper (GSU), still columns (GSU), glycol reboiler (GDU); or desorption/stripping process (CSU) require low pressure and as high as possible temperature;
4. Cryogenic /cold process as LTS with mechanical refrigeration or turbo expander system for C_{2+} recovery have usually, a surplus of low temperature and can be used to cool down the other streams which request lower temperature;
5. The streams containing liquid (condensate) have more energy to offer then the gas streams because of the higher heat capacity coefficient of the liquid.
6. Streams which are already part of heat exchanger network won't be taken into account.

According to this guideline, the streams will be selected and identified in the following subchapter.

Before performing the analysis, accordingly to the rules explained in section 3.1.1 a minimum temperature difference of $\Delta \boldsymbol{T}_{\boldsymbol{min}} = \mathbf{10}$℃ will be considered.

This value has shown as an optimal in numerous projects in the oil and gas industry. It provides designing HEN with high efficiency while providing acceptable investment costs.

6.2 Selection of streams and data extraction

Following the selection guidelines 2, 3 and 4 from section 6.1, looking for possibilities for heat integration, three areas were chosen: the Gas Sweetening Unit, the Gas Dehydration Unit and the Condensate Stabilization Unit. The Amine and Glycol regeneration units need high temperatures in order to extract the chemical component from the HC liquid and gas mixture. This streams need to cooled down before entering the amine absorber (Figure 5-2) and the glycol contactor (Figure 5-3), or before going to the incinerator (Figure 5-2). A sink was spotted in the Condensate Stabilization Unit with an opportunity to reduce the hot oil duty in the condensate flash separator if this stream was to be heated up with the other (hot) streams.

The supply temperatures for each stream, their composition and the mass flowrate were given in the heat and material balance, but the target temperatures were defined considering the process requirements and limitations of the equipment given in the Process Flow Diagrams (PFD) (

Table 6-1).

Table 6-1: Operating temperatures of the equipment units of interest for the PA

Equipment	Operating Temperature (winter/summer) [°C]
Sweet Gas Scrubber	48.9/55
Glycol Contactor	48.4/54.6
Condensate Flash Separator	28/50.6
Suction KOD	54.4/55

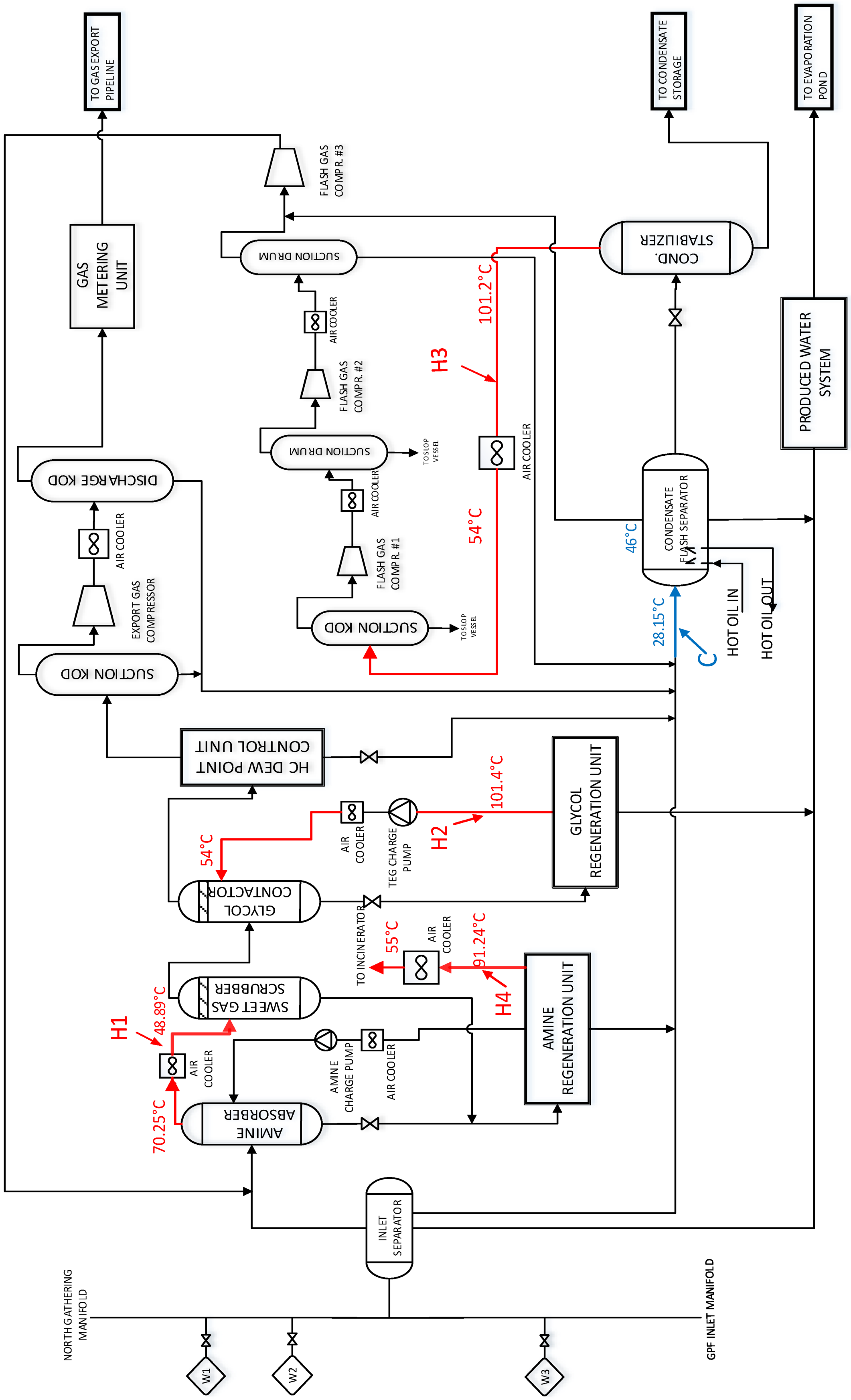

Figure 6-1: Selected hot and cold streams

The hot streams were chosen as streams that don’t change in composition and cooling them down would reduce the duty of four air coolers. The following streams were selected (Figure 6-1):

H1 - before entering the sweet gas scrubber (GSU)

H2 - before entering the glycol contactor(GDU)

H3 - before going to the flash gas compressor unit (CSU)

H4 - after leaving the amine stripper and before going to the incinerator (GSU).

According to the second rule mentioned prior in section 3.1.2, the cold stream (C) was considered after mixing the condensate from the other units together, but before entering the separator.

Table 6-2: Provided data for the selected streams

Stream Name	Stream Type	Stream composition	Supply Temperature (℃)	Target Temperature (℃)	Mass Flowrate (kg/s)
H1	Hot	gas	70,25	48,89	37498,07
H2	Hot	aquaous liquid	101,4	54	2084,398
H3	Hot	gas	101,2	54	7864,284
H4	Hot	gas	91,24	55	2312,216
C	Cold	gas+aq.liq.+ HC liquid	28,15	75	28451,96

6.3 Specific heat capacity calculation

The heat capacity of a substance is an indicator of how much heat can one stream offer, according to its composition. The mass flowrate and the specific heat capacity of each stream were given in the H&MB. With this information and the equations (2-10) and (2-16) it seems pretty simple to calculate the heat capacity flowrate, as well as the stream heat load. But the first task is to determine the missing data for the specific heat capacity of each stream in the target state. To be more precise, the average specific heat capacity between the supply ($T_s = T_1$) and the target temperature ($T_t = T_2$) needs to be found. Due to the fact that three different fluids are present, the calculation will be explained for each of them separately.

1. Average specific heat capacity for gases

The specific heat capacity of a gas at a constant pressure is expressed as a polynomial function of the temperature [52]:

$$c_p = a + bT + cT^2 + dT^3 \tag{6-1}$$

The coefficients a, b, c and d are depending on the constants given in Table 6-3 and the specific gravity of the gas.

Specific gravity of a gas, γ_g (also known as relative density) is the ratio of the density of the gas to the density of the air at standard conditions (15°C, $1bar$) [53].

$$\gamma_g = \frac{\rho_g}{\rho_{air}} \tag{6-2}$$

Where:

γ_g – specific gravity of gas

ρ_g – density of gas $[kg/m^3]$

ρ_{air} – density of air, normally 1.204 $[kg/m^3]$

In this case, the values of the specific gravity for each stream were given.

Table 6-3: Constants of linear regression of ideal gas under constant pressure [52]

Constant	Estimated Value	Calculated constants
a_1	-10.9602	$a = a_1 \cdot \gamma_g + a_2$
a_2	31.9033	
b_1	0.21517	$b = b_1 \cdot \gamma_g + b_2$
b_2	$-6.8687 \cdot 10^{-2}$	
c_1	$-1.3337 \cdot 10^{-4}$	$c = c_1 \cdot \gamma_g + c_2$
c_2	$8.6387 \cdot 10^{-5}$	
d_1	$3.1474 \cdot 10^{-8}$	$d = d_1 \cdot \gamma_g + d_2$
d_2	$-2.8396 \cdot 10^{-8}$	

Now that the function of the specific heat capacity is known, we can calculate the average specific heat capacities of each stream between 0°C and T (T_1 and T_2) respectively. Using equations (2-16) and (6-1) we get the following expression:

$$\boldsymbol{\overline{c_p} = \frac{1}{T_2 - T_1}\int_{273,15}^{T}(a + b \cdot T + c \cdot T^2 + d \cdot T^3)\, dT} \qquad \left[{}^{kJ}/_{kmol \cdot {}^\circ\mathrm{C}}\right] \tag{6-3}$$

Important here is to apply the values of the temperatures expressed in Kelvin (K), and the boundaries of the integral to be from 273,15 K (equivalent to 0°C) and the corresponding temperature. Another hint to follow is the unit of the calculated average specific heat capacity. Equation (6-3) expresses the molar heat capacity, so that equation (2-13) needs to be applied in order to get the value of the average specific heat capacity.

In our case, the hot streams H1, H3 and H4 consist of gaseous fluid. The provided calculation accordingly the steps explained above is presented in Table 10-1, Appendix B.

2. Average specific heat capacity for hydrocarbon liquid

The specific heat capacity for hydrocarbon liquid depends on the specific gravity of the fluid and was estimated with the function [23]:

$$\boldsymbol{c_p = 2.96 - 1.34 \cdot \gamma_{HC} + t \cdot (0.00620 - 0.00234 \cdot \gamma)} \tag{6-4}$$

Specific gravity of the hydrocarbon liquid is the ratio between its density and the density of water.

$$\gamma_{hc} = \frac{\rho_{fluid}}{\rho_{water}} \tag{6-5}$$

Where:

γ_{hc} – specific gravity of the hydrocarbon

ρ_{fluid} – density of the fluid $[kg/m^3]$

ρ_{air} – density of water, normally 1000 $[kg/m^3]$

The value of specific gravity is used to measure the density of a liquid. If the specific gravity is more then 1, that means that the liquid has a greater density then water. Liquid with lower densities, have a specific gravity value between 0 and 1 [54]. In the petroleum industry uses API (American Petroleum Institute) gravity as a gravity scale. The connection between API and the specific gravity is given with equation (6-6) [53]:

$$\gamma_{API} = \frac{141.5}{\gamma_{HC}} - 131.5 \tag{6-6}$$

In our case, API gravity was given, which leads to the calculation of the specific gravity with equation (6-7).

$$\gamma_{HC} = \frac{141.5}{\gamma_{API} + 131.5} \tag{6-7}$$

The rest of the calculation was done with the equations (2-16) and (6-4), but this time the temperature was expressed in °C [23]:

$$\overline{\boldsymbol{c_p}} = \frac{\mathbf{1}}{\boldsymbol{t}} \int_{\mathbf{0}}^{\boldsymbol{t}} (\mathbf{2.96} - \mathbf{1.34} \cdot \boldsymbol{\gamma} + \boldsymbol{t} \cdot (\mathbf{0.00620} - \mathbf{0.00234} \cdot \boldsymbol{\gamma}))\, \boldsymbol{dt}$$

3. Average specific heat capacity for aqueous liquid

The specific heat capacity for aqueous liquid between the standard state conditions and the corresponding temperature was determined by a simulation in the VMGSim Program. This is a simulation program in ownership of the ILF company, so with respect to the confidentiality agreement it won't be referred in this work. The program uses each chemical element/compound of which the composition of the streams consists, its molecular weight and the temperature.

If we have a look at the composition of the cold stream (Table 6-2), this fluid consists of gas, aqueous liquid and hydrocarbon liquid.

The next step is to calculate the mixture of the corresponding fluids which are found in each of the streams respectively.

$$\boldsymbol{c_{p_{mix}}} = \boldsymbol{c_{p1}} \frac{\boldsymbol{m_1}}{\boldsymbol{m_{mix}}} + \boldsymbol{c_{p2}} \frac{\boldsymbol{m_2}}{\boldsymbol{m_{mix}}} + \boldsymbol{c_{p3}} \frac{\boldsymbol{m_3}}{\boldsymbol{m_{mix}}} \tag{6-8}$$

And then, using equation ***(2-16***(2-18), the average specific capacity between t_1 and t_2 can be calculated.

$$\bar{c}_p\Big|_{t_1}^{t_2} = \frac{t_2 \cdot \bar{c}_p\Big|_{0°C}^{t_2} - t_1 \cdot \bar{c}_p\Big|_{0°C}^{t_1}}{t_2 - t_1}$$

6.4 Composite curves

The composite curves are a graphical representation of each stream in a T-H Diagram, giving information about the heat availability and the heat demands in the system. As a result, there should be only one hot and one cold composite curve as representatives of the corresponding heat sources and sinks in the processes. That representation was gained through the following steps:

1. Heat load calculation

With the provided data, presented in Table 6-2 for the mass flowrate, and the calculated average specific heat capacity in subsection 6.3, the heat transferred per unit time (heat load) in each stream can be determined using the equation (2-21). The results of the heat load calculation are presented in Table 6-4.

Table 6-4: Calculation of the heat transferred in each streams when changing the temperature from T_1 to T_2

Stream Name	Stream Type	Supply Temperature (°C)	Target Temperature (°C)	Mass Flowrate (kg/h)	Average Specific Heat Capacity (kJ/kg°C)	Heat Capacity Flowrate (kW/°C)	Heat Load (kW)
H1	Hot	70,25	48,89	37498,07	2,51342	26,18	559,33
H2	Hot	101,4	54	2084,39	2,68827	1,56	73,76
H3	Hot	101,2	54	7864,28	1,98763	4,34	204,94
H4	Hot	91,24	55	2312,22	1,13536	1,41	51,03
C	Cold	28,15	75	28451,96	2,36038	18,65	-873,98

In Figure 6-2 and Figure 6-3 the composite curves between the of the supply and target temperature of each stream, with slope defined as:

$$\frac{dT}{dQ} = \frac{1}{CP} \tag{6-9}$$

The space between the composite curves in Figure 6-2 doesn't have thermodynamic meaning. It serves only as a graphical representation of the CCs for each hot stream.

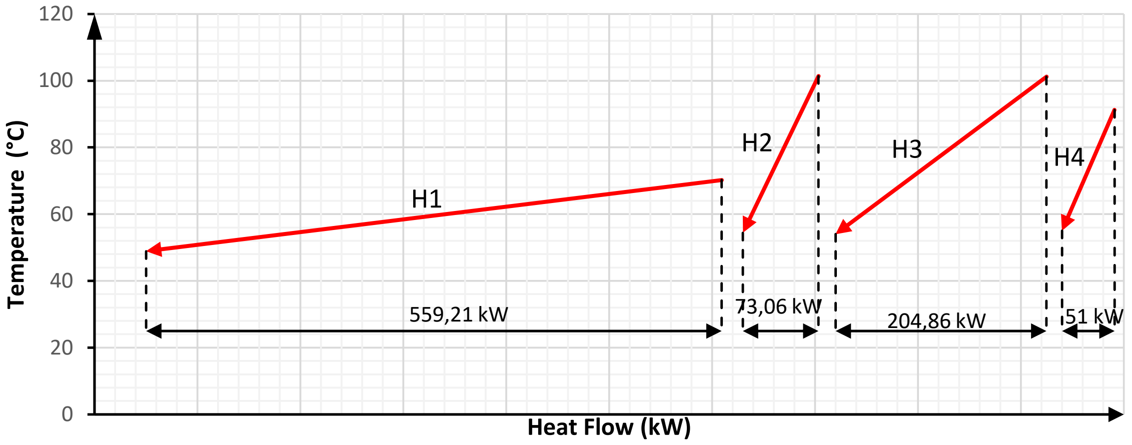

Figure 6-2: Composite curves for each hot stream

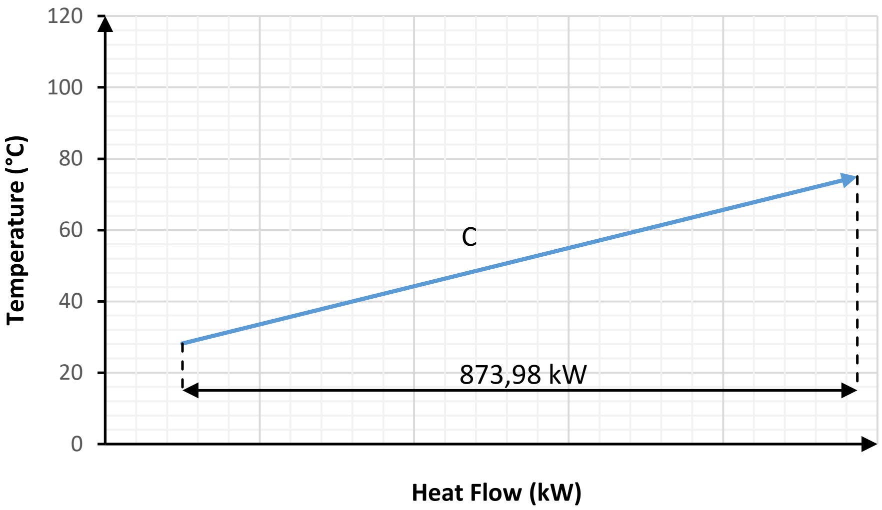

Figure 6-3: Composite curve of the cold stream

2. Determination of temperature intervals

The process will be divided in temperature intervals depending on the temperature level of each stream. For that purpose, we analyze the supply and target temperatures of the hot streams and sort them in intervals as shown in Table 6-5. For each interval, the heat capacity flowrates of all streams existing in the given temperature interval will be added. The heat content will be calculated as a product of the temperature difference and the heat capacity flowrate of the interval.

In our case we have four hot streams, but six temperature intervals formed by the supply and target temperatures of each stream. In the first interval, between 48.89 °C and 54 °C, exists only stream H1, which means that the heat available in the first interval is:

$$\Delta\dot{Q}_I = CP_{H1} \cdot (T_2^I - T_1^I)$$

The second interval, between 54 °C and 55 °C includes three streams, H1, H2 and H3 so the heat load in this case will be calculated as:

$$\Delta\dot{Q}_{II} = (CP_{H1}+CP_{H2}+CP_{H3}) \cdot (T_2^{II} - T_1^{II})$$

The values of ΔH for the rest four intervals will be calculated following the same steps:

$$\Delta\dot{Q}_{III} = (CP_{H1}+CP_{H2}+CP_{H3}+CP_{H4}) \cdot (T_2^{III} - T_1^{III})$$

$$\Delta\dot{Q}_{IV} = (CP_{H2}+CP_{H3}+CP_{H4}) \cdot (T_2^{IV} - T_1^{IV})$$

$$\Delta\dot{Q}_V = (CP_{H3}+CP_{H4}) \cdot (T_2^V - T_1^V)$$

$$\Delta\dot{Q}_{VI} = CP_{H2} \cdot (T_2^{IV} - T_1^{IV})$$

The results of the calculation are presented in the table below, and their graphical representation is shown in Figure 6-4.

Table 6-5: Temperature intervals for the hot streams

Temperature Interval ΔT			Heat Capacity Flowrate	Heat Load
	T_1	T_2	$\sum CP$	$\Delta\dot{Q}$
I	48.89	54	26.1800593	133.780103
II	54	55	32.07858503	32.078585
III	55	70.25	33.48701535	510.676984
IV	70.25	91.24	7.30695605	153.373007
V	91.24	101.2	5.89852573	58.7493163
VI	101.2	101.4	1.55650873	0.31130175
				$\sum\Delta\dot{Q} = 888.97$ kW

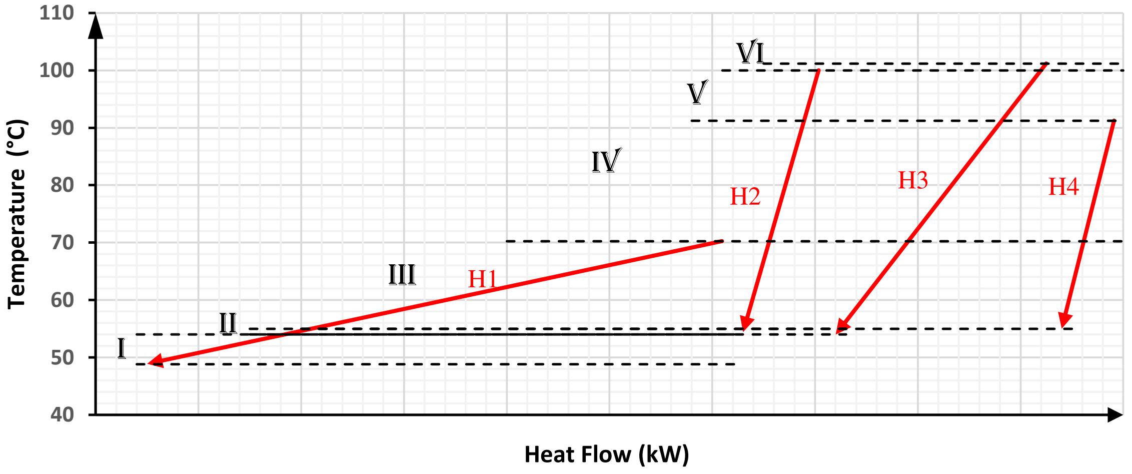

Figure 6-4: Temperature intervals for construction of the hot composite curve

3. Construction of the hot and cold composite curve

There are four hot streams, consequently four composite curves. These need to be illustrated as one, Hot Composite Curve (HCC), describing the changes in temperature and heat load at all points in the overall temperature range. This is accomplished by adding the enthalpy changes in each interval against the temperature levels.

The same procedure should be applied for all cold streams so that the cold composite curve can be plotted. In our case, there is only one cold stream, which means no further calculation is needed.

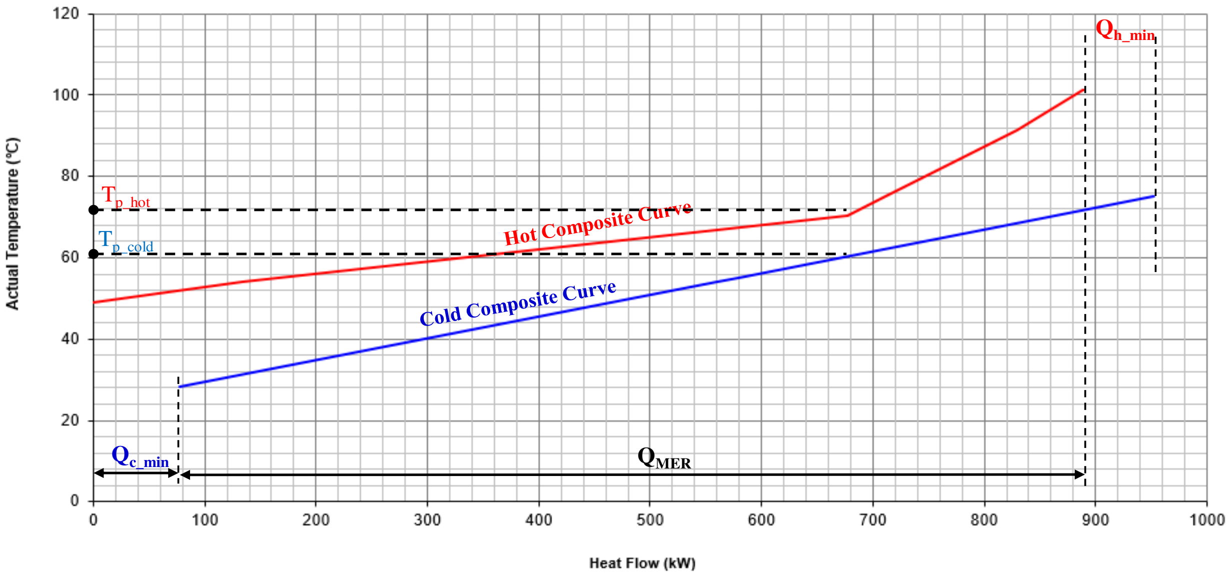

Figure 6-5: Energy targets for MER

Figure 6-5 shows the hot composite curve represented with red line and the cold composite curve represented with blue line. The hot stream must, at all points, be hotter than the cold stream for feasible heat exchange.

After plotting the two curves, we can notice the minimum temperature difference between the two streams. This represents the point of closest approach which is called pinch point. In this case we have chosen $\Delta T_{min} = 10\ ℃$ as the minimum temperature difference that will be accepted in any heat exchanger. From the graphic we can see that the hot pinch point is at $70.25\ ℃$ and the cold pinch point is at $60.25\ ℃$, which represents exactly the difference of $10\ ℃$.

The overlap between the hot and the cold composite curve is the maximum amount of heat (MER) which can be recovered in the process. The part at the bottom of the hot composite curve which can't be recovered by the cold stream, graphically shown as the horizontal distance between the low temperature ends of the CCs (Figure 6-5) represents the minimum amount of external cooling required (Q_{c_min}). The minimum hot utility (Q_{h_min}) required, is determined graphically as the horizontal distance between the high-temperature ends of the CCs [30].

The results of the graphical method of pinch analysis are the following:

- Amount of heat that can be recovered: $\dot{Q}_{MER} = 811\ kW$;
- Minimum heating duty: $\dot{Q}_{h\_min} = 63\ kW$
- Minimum cooling duty: $\dot{Q}_{c\_min} = 72\ kW$.

6.5 Cascade Method

Prior to forming a feasible cascade in order to determine the energy targets of the process, a so called ‘Problem Table’ should be constructed. This table is based on temperature intervals set up accordingly to the shifted supply and target temperatures for both, hot and cold streams (Table 6-6). To calculate the shifted temperatures, the temperatures of the hot streams are decreased for $1/2\,\Delta T_{min}$ (5°C); and the temperatures of the cold stream are increased for the same value.

Table 6-6: Shifted temperatures of the cold and hot composite curves

Stream Name	Supply Temp. (℃)	Target Temp. (℃)	Heat Capacity Flowrate (kW/℃)	Heat Load (kW)	Shifted Supply Temp. (℃)	Shifted Target Temp. (℃)
H1	70,25	48,89	26,180	559,329	65,3	43,9
H2	101,4	54	1,556	73,762	96,4	49
H3	101,2	54	4,342	204,943	96,2	49,0
H4	91,24	55	1,408	51,026	86,2	50,0
C1	28,15	75	18,655	873,987	33,2	80,0

Each interval has either surplus or deficit of heat but can’t have the both. The enthalpy balance for each interval can be calculated according to equation (6-10).

$$\Delta H_i = (T_{si} - T_{s(i+1)})\left(\sum CP_H - \sum CP_C\right)_i \qquad (6\text{-}10)$$

for each interval i.

The results are presented in Table 6-7.

The last column of the Problem table is a good tool for building a feasible heat exchanger network based on the assumption that all “surplus” intervals reject heat to the cold utility, and all “deficit” intervals take heat from hot utility.

Table 6-7: Problem Table representing the demand of energy for each interval

Shifted Temperature T_s (°C)	**Interval**	$T_{si} - T_{s(i+1)}$ **(°C)**	$\sum CP_{Hot} - \sum CP_{Cold}$ **(kW/°C)**	ΔH_i **(kW)**	**Surplus or deficit**
96.4					
	1	0,19	1,556	0,31	surplus
96.2					
	2	9,96	5,898	58,75	surplus
86.24					
	3	6,24	7,306	45,591	surplus
80					
	4	14,75	-11,35	-167,355	deficit
65.25					
	5	15,25	14,83	226,229	surplus
50					
	6	1	13,42	13,423	surplus
49					
	7	5,11	7,53	38,461	surplus
43.89					
	8	10,74	-18,66	-200,334	deficit
33.15					

With the calculated data is possible to set up a cascade assuming that any heat available in interval i is hot enough to supply any duty in interval $i + 1$. We start the cascade with 0 kW supposing that no heat is supplied to the first interval. After that, the demand from interval 1 is cascaded into the surplus of interval 2 resulting in 59,06 kW. This surplus joins the heat available in interval 3, so it results into 104,65 kW. Interval 4 has a 167,35 kW deficit, so after accepting the 104,65 kW surplus, only 62,7 kW deficit are left, which are further passed on the heat from interval 5. The calculation continues in that why until the heat of the last interval is considered. The result at the end is the energy that actually represents the net enthalpy balance on the whole problem.

Analyzing the heat flows between the intervals in Figure 6-6, a), it is clear that the negative heat of 62,7 kW is thermodynamically infeasible. To solve this problem, we set up another, feasible cascade where the 62,7 kW need to be added from hot utility as shown in Figure 6-6, b). After adding 62,7 kW of heat, it will be cascaded through the system in the same way as explained above.

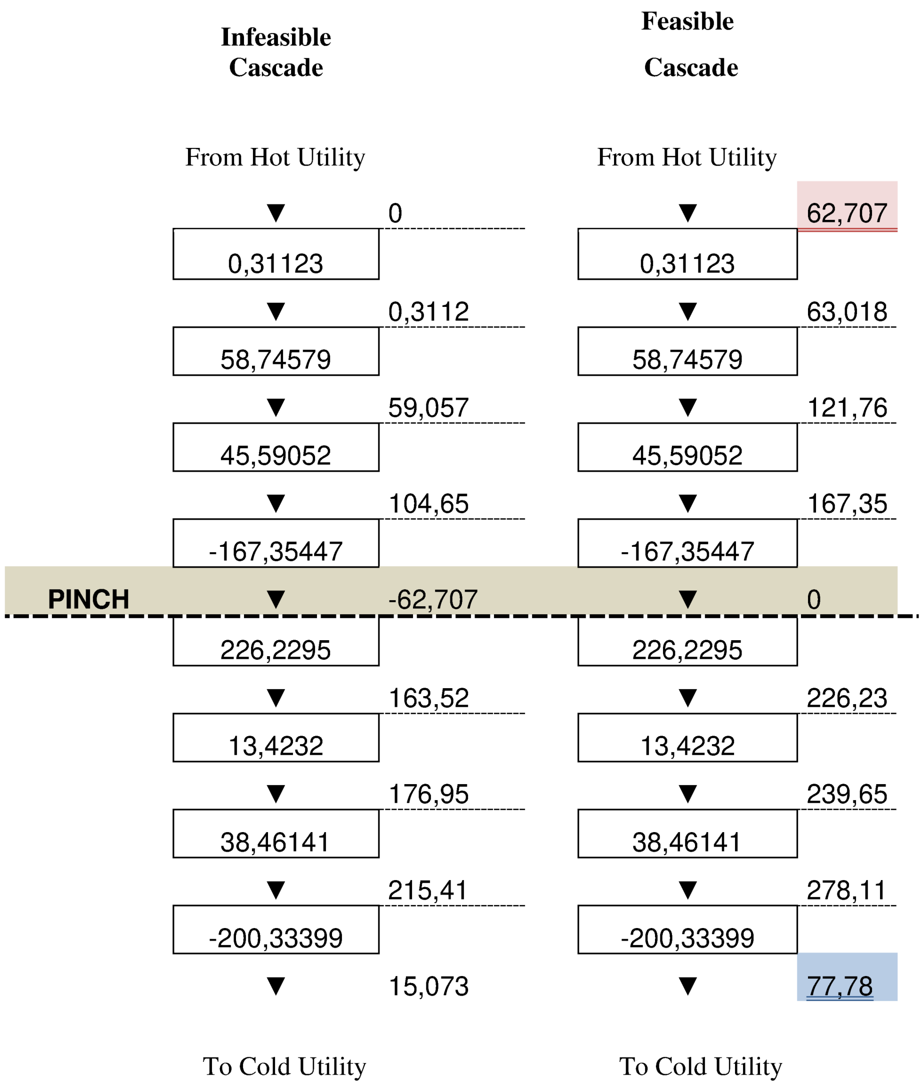

Figure 6-6: Infeasible and feasible cascade for determining the energy targets

The results of this cascade are representing the energy targets defining the minimum required hot and cold utilities:

Min hot utility: 62,7 kW

Min cold utility: 77,8 kW

The position of the pinch temperature is determined at the point here the net heat flow equals 0 kW. In this case, the pinch point is between the intervals 4 and 5, at shifted temperature of 65,25 (°C). This value, ${}^{1}/_{2}\,\Delta T_{min}$ (5°C in our case) will be added to select the Hot Pinch Temperature, whereas the Cold Pinch Temperature is ${}^{1}/_{2}\,\Delta T_{min}$ (also 5°C in our case) below that value. This results in the following:

$T_{p_{hot}} = 70{,}25\ ℃$ $\qquad$ $T_{p\_cold} = 60{,}25\ ℃$

If we compare the results obtained by the Composite Curves Method with the Problem Table approach we can conclude that the results are the same. The difference is that the Problem Table provides a framework for numerical analysis.

The total heat that can be recovered is found by adding the heat loads for all the hot streams and subtracting the minimum cold utility, which results in 811 kW. Considering the cold stream heat, and subtracting the minimum hot utility from it, we get the same results, which leads us to the conclusion that the heat recovery obtained by two different routes is 811 kW.

6.5.1 Grand Composite Curve

If we plot the shifted temperatures shown in Table 6-6 against the heat flow in a T-Q diagram, we obtain the graphical representation of the Problem Table, known as the Grand Composite Curve – GCC (Figure 6-7).

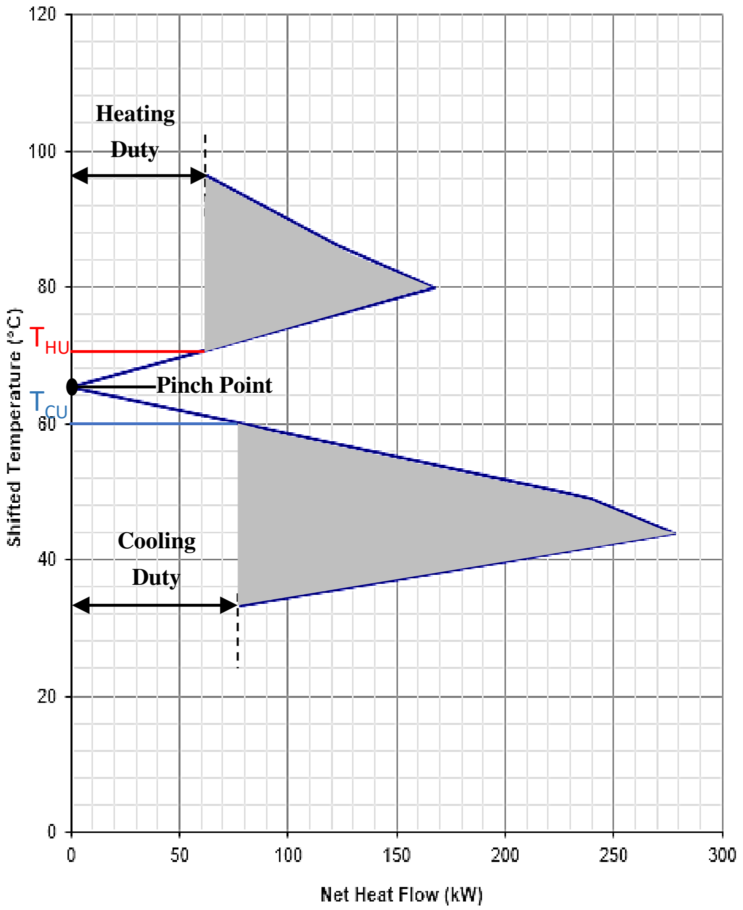

Figure 6-7: Grand Composite Curve (GCC)

As we can see, there is a difference between the heat supplied from the hot streams and the heat required from the cold streams. The possibility for heat transfer within the process, between the hot and the cold streams, is visible on the GCC where it bends towards itself. This areas, where no external cooling or heating is needed are known as "pockets" (grey-coloured regions in Figure 6-7). [31]

Not only that at the top and bottom end the duty of the hot and cold utility targets are presented, but also at which temperature are they needed [7]. Due to the fact that for plotting the GCC, shifted temperatures are used, the temperatures of the hot streams have been reduced, whereas of the cold streams increased for $\Delta T_{min}/2$. This is the reason for which the temperatures read from the GCC can't be directly used for the design of the utilities. In order to calculate the optimal temperatures, $\Delta T_{min}/2$ needs to be added to the value of the shifted hot utility temperature (T_{HU}^{*}), equation (6-11). On the other hand, the value of the shifted cold utility temperature (T_{CU}^{*}) needs to be decreased for $\Delta T_{min}/2$, equation (6-12) [31].

$$T_{HU} = T_{HU}^{*} + \frac{\Delta T_{min}}{2} \tag{6-11}$$

$$T_{CU} = T_{CU}^{*} - \frac{\Delta T_{min}}{2} \tag{6-12}$$

In this case, it is sufficient that the hot utility is available at 76 °C (Figure 6-7):

$$T_{HU} = 71 + 5 = 76°\mathrm{C}$$

6.6 Estimation of the total heat transfer surface area

In this thesis, the type of heat exchangers and the heat transfer coefficients won't be studied in details. The aim is only to give an overview of how the calculation is done and how large the heat transfer area is. For that purpose, three assumptions will be made:

1. A complete matching between the hot and the cold stream is achieved, which means the hot and the cold streams are used in a thermodynamically optimal way.
2. The heat transfer is accomplished in a shell-and-tube countercurrent flow heat exchanger at a log mean temperature difference ΔT_{LM} calculated with equation (2-26).
3. The heat transfer coefficients of the heat exchangers will be used as given in the literature sources [7, 55], and shown here in Table 6-8.

Table 6-8: Heat transfer coefficient for each stream

Stream	**Heat Transfer Coefficient (W/m^2K)**
H_1	600
H_2	1000

H_3	1000
H_4	110
C	1000
HU	800
CU	2500

For the purpose of the calculation of the total heat transfer area, the composite curves will be divided in intervals according to the change of temperature, as shown in Figure 6-8.

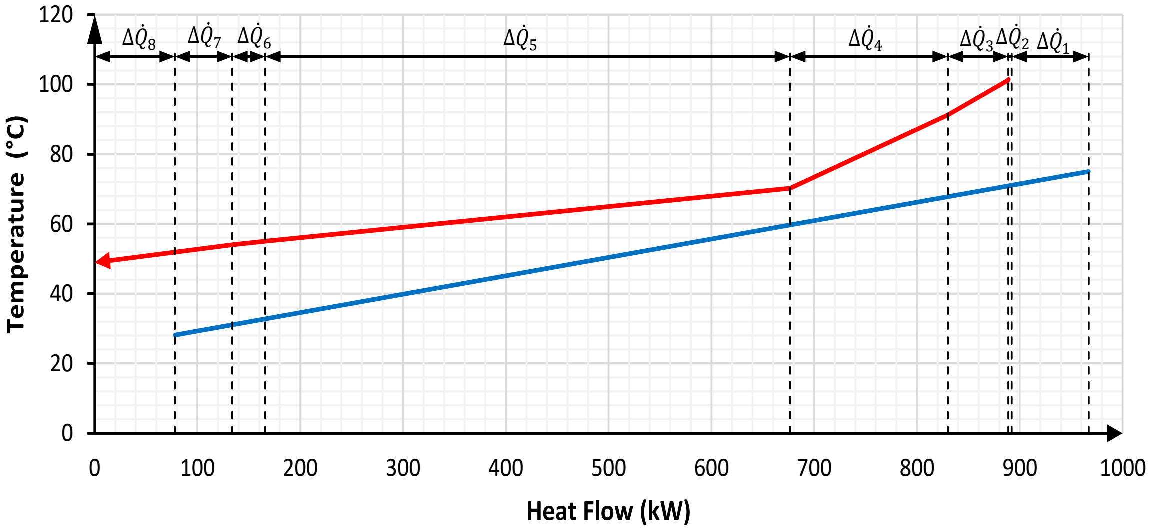

Figure 6-8: Heat flow rates for the corresponding interval

The first interval is between 75°C and 71,64 °C of the cold composite curve. Here, heat will be transferred only from the hot utility to the cold stream:

$$\Delta\dot{Q}_1 = Q_{HU} = 18.655 \cdot (75 - 71.64) = 62.7\ kW$$

The corresponding logarithmic mean temperature difference is:

$$\Delta T_{LM} = \frac{(230 - 71.6) - (230 - 75)}{\ln\frac{(230 - 71.6)}{(230 - 75)}} = 156.7\ K$$

The second interval is between 101.4°C and 101.2°C of the hot stream H_2, and between 71.64°C and 71.62°C of the cold stream. The transferred heat from the hot stream is:

$$\Delta\dot{Q}_2 = \Delta\dot{Q}_{H2} = (101.64 - 101.62) \cdot 1.556 = 0.3112\ kW$$

This heat load will be transferred to the cold stream, heating it up from temperature $T_2$to 71.64°C :

$$\Delta\dot{Q}_2 = \Delta\dot{Q}_C = (71.64 - t_2) \cdot 18.655 = 0.3112\ kW \qquad t_2 = 71{,}62\ °C$$

Table 6-9: Heat transfer rates for each stream in the corresponding interval

Interval (j)	$\Delta\dot{Q}_j$ $[_{kW}]$	CP_j $[_{kW}/_{K}]$	Temperature intervals				ΔT_{LM} $[_K]$	Heat transfer rates Q_{ih}, Q_{ik}					**Utilities**	
			Hot side		Cold side			H₁	H₂	H₃	H₄	C	HU	**CU**
1	62.7	18.655	230	230	75	71.64	156.67					62.7	**62.7**	
2	0.3112	1.556	101.4	101.2	71.64	71.62	29.67		0,3113			0.3113		
3	58.749	5.898	101.2	91.24	71.62	68.47	25.62		15.503	43.24		58.75		
4	153.373	7.3069	91.24	70.25	68.47	60.25	10.22		32.67	91.14	29.56	153.4		
5	510.677	33.487	70.25	55	60.25	32.87	15.27	399.25	23.74	66.22	21.48	510.67		
6	32.079	32.078	55	54	32.87	31.16	22.46	26.18	1.56	4.34		32.078		
7	56.091	26.18	54	51.85	31.16	28.15	23.18	56.09				56.09		
8	77.689	26.18	51.85	48.89	30	30	20.34	77.69						**77.69**

With this temperature t_2, the ΔT_{LM} for section $\Delta\dot{Q}_2$ can be calculated.

Following the same procedure, the heat rates for each stream are calculated and presented in Table 6-9.

With known heat duties and ΔT_{LM} (Table 6-8), the HE areas can be determined according to equation (3-5). The total heat transfer area was estimated to be 172.6 m^2.

6.7 Design of HEN

For a better visualization and representation of the heat exchanger network, the grid diagram represented by Linnhoff [32] will be used. The streams are presented with horizontal lines where the high temperatures are on the left side. The heat exchange pairs are shown as circles at each stream affecting the exchange, connected with vertical line. The pinch is presented with vertical lines for the hot and the cold pinch temperature respectively.

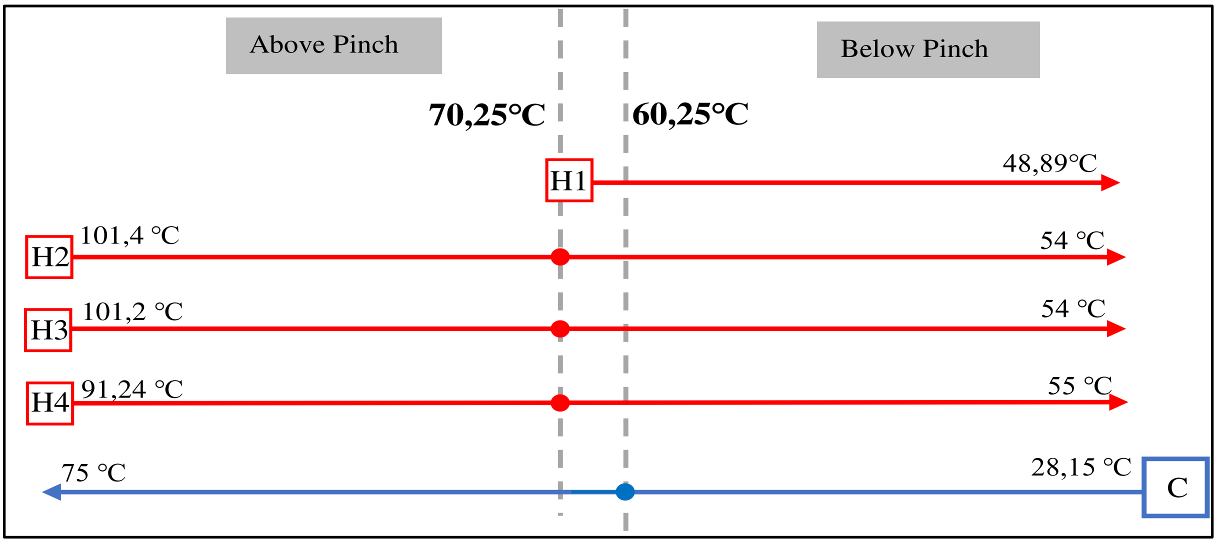

Figure 6-9: Representation of the streams and the pinch point temperature

6.7.1 Above the Pinch point

In order to design the HEN, the rules according to Figure 3-9 have to be applied.

Firstly, the Stream Splitting Algorithm will be checked:

- $\boldsymbol{CP_{out} \geq CP_{in}}$

In the subsystem above the Pinch Point, there are three hot streams and only one cold stream. The hot streams are entering the pinch point, which is why $CP_{hot} = CP_{in}$; the cold stream is leaving the pinch point, so $CP_{cold} = CP_{out}$. Considering that, the heat capacity criteria, $CP_{out} \geq CP_{in}$, for this part of the network, can be formulated in the following way:

$\boldsymbol{CP_{cold} \geq CP_{hot}}$.

If we look at the heat capacity flowrates for the streams in Table 6-4, we can conclude that the heat capacity flowrate of the cold stream is higher than any of the heat capacity flowrates of the hot streams (H3, H4 and H5). That means that the criterion is fulfilled and that any match between the hot and cold streams can be made.

- $\boldsymbol{N_{out} \geq N_{in}}$

The number of the streams leaving the pinch point (cold stream, $N_{out} = N_{cold}$) is not bigger than the number of streams entering the pinch point (hot streams, $N_{in} = N_{hot}$).

$\boldsymbol{N_{out} < N_{in}}$

That means there is insufficient number of cold streams. At least three cold streams are needed, so that every hot stream has its match. A solution of this problem is to split the cold stream into three separate streams (Figure 6-10) which have the same supply and target temperature. The three separate streams are called "branches". The heat load of each branch will be calculated according to the heat which can be delivered from each of the hot streams.

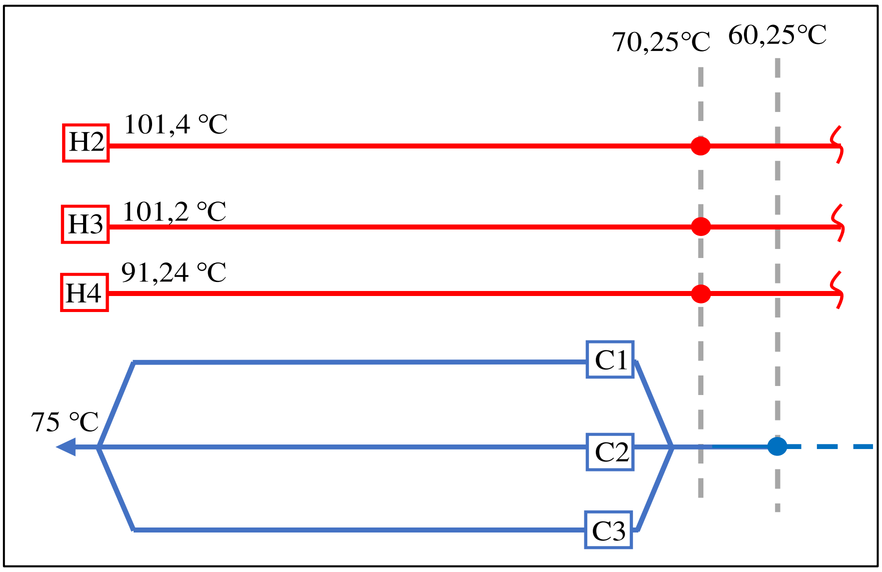

Figure 6-10: Splitting the cold stream above the pinch

According to the 2nd and 3rd rule, Figure 3-9, we start with the stream nearest to the pinch point (C1) and the stream that has the highest heat flow (H3):

1. **Stream H3 and Stream C1**

Stream H3 can deliver: $(101{,}2 - 70{,}25) \cdot 4{,}342 = 134{,}298\ kW$

If stream C1 receives all the energy from H3, we can calculate the heat capacity flowrate of C1:

$$134{,}298 = (75 - 60{,}25) \cdot CP_{C1}$$

$$CP_{C1} = \frac{134{,}298}{(75 - 60{,}25)} = 9{,}105\ kW/°\text{C}$$

This is possible because the heat cap flowrate of C1 is smaller than the overall heat capacity flowrate of the cold stream $CP_C = 18{,}655\ kW/°\text{C}$, but it is bigger than the heat capacity flowrate of the hot stream H3, $CP_{H3} = 4{,}342\ kW/°\text{C}$.

Stream H3 can deliver all its energy to the stream C1, which means it will no longer be considered. This stream will be "ticked off" ("Tick off Rule''). The heat exchanger duty is 134,3 kW. Its in- and outlet temperatures are shown in Table 6-10.

2. **Stream H2 and Stream C2**

Stream H2 has the next largest heat capacity flowrate.

Stream H2 can deliver: $(101{,}38 - 70{,}25) \cdot 1{,}556 = 48{,}47\ kW$

If the whole heat from H2 is transferred to C2 :

$$48{,}47 = (75 - 60{,}25) \cdot CP_{C2}$$

$$CP_{C2} = \frac{48{,}47}{(75 - 60{,}25)} = 3{,}29\ kW/°\text{C}$$

The calculated CP is higher than the CP of the hot stream H2 ($CP_{H2} = 1{,}56\ kW/°\text{C}$), which means that the HE is feasible, and its duty is 48,47 kW (Table 6-10). Stream H2 will be "ticked-off after delivering all its energy to the stream C2.

3. **Stream H4 and Stream C3**

Stream H4 can deliver: $(91{,}24 - 70{,}25) \cdot 1{,}408 = 29{,}2\ kW$

To see how much energy C3 can receive, we have to calculate CP_{C3}:

$$CP_{C3} = CP_C - CP_{C1} - CP_{C2}$$

$$CP_{C3} = 18{,}655 - 9{,}105 - 3{,}29 = 6{,}26\ kW/°\text{C}$$

Stream C3 can receive: $(75 - 60{,}25) \cdot 6{,}26 = 92{,}34\ kW$

Stream H4 can deliver all its energy to the stream C3, which means will be ticked-off. The heat exchanger duty is 29,2 kW (Table 6-10).

The output temperature of the cold side is calculated according to equation (2-22):

$$29{,}2 = \left(T_{out_c} - 60{,}25\right) \cdot 6{,}26$$

$$T_{out_c} = 64{,}9\ °\text{C}$$

In stream C3 are left: 92,34 – 29,56 =62,8 kW which represents exactly the required minimum hot utility.

Table 6-10: Inlet and outlet temperatures of the HEs above the pinch

Heat Exchanger ID	Heat Exchanger Duty (kW)	Hot/Cold Side	T_{in} (°C)	T_{out} (°C)
HE1	134.29	Hot Side: H3	101.2	70.25
		Cold Side: C1	60.25	75
HE2	48.45	Hot Side: H2	101.4	70.25
		Cold Side: C2	60.25	75
HE3	29.6	Hot Side: H4	91.24	70.25
		Cold Side: C3	60.25	64,97
HU	62.8	Hot Side	Any dep.on c_p	64,97+ ΔTmin
		Cold Side: C3	64,96887	75

The corresponding heat exchanger network above the pinch point is represented in Figure 6-11.

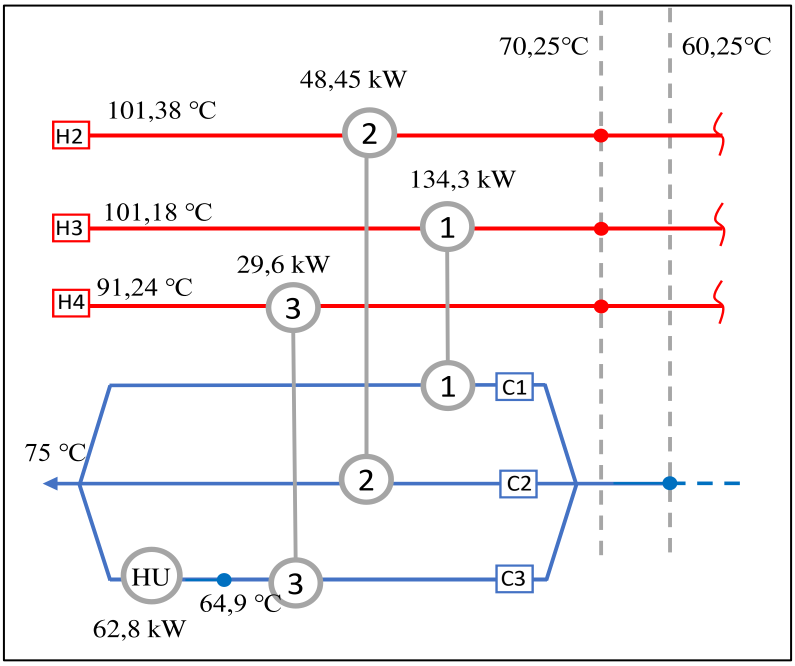

Figure 6-11: HEN above the pinch point

6.7.2 Below the Pinch point

The rule $CP_{out} \geq CP_{in}$, for this part of the network, can be formulated in the following way: $\boldsymbol{CP_{hot} \geq CP_{cold}}$.

Below the pinch, in general, the cold streams are entering the pinch point, which is why CP_{cold} is actually CP_{in}; the hot streams are leaving the pinch point : $CP_{hot} = CP_{out}$. In this case, we have only one hot stream (H1) which's CP is higher than the CP of the cold stream. With a short analysis, we can see if that stream has enough energy to warm up the cold stream:

Stream H1 can deliver: $(70{,}25 - 48{,}89) \cdot 26{,}18 = 559{,}2\ kW$

Stream C can receive: $(60{,}25 - 28{,}15) \cdot 18{,}655 = 598{,}83\ kW$

This means that only stream H1 is not enough, but no other stream has a CP higher then CP_C. If we connect Stream C with hot stream with lower CP, we will get an unfeasible heat exchanger because the ΔT of the HE will be less than ΔT_{min}. To solve this problem, we will split the stream C into two branches, C4 and C5 (Figure 6-12).

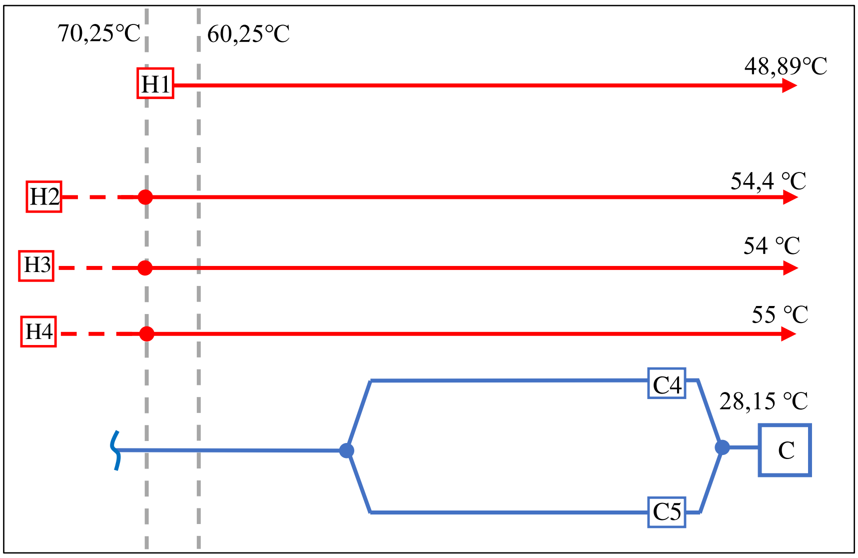

Figure 6-12: Splitting the cold stream below the pinch point

Now that we've solved the problem with the CP-rule, we will check if the N- criteria is fulfilled. According to the rule, $N_{out} \geq N_{in}$,and considering that we are in the subsystem below the pinch, we can define: $N_{hot} \geq N_{cold}$. In our case the number of the hot streams is higher than the number of the cold streams ($N_{hot} = 4, N_{cold} = 2$), which means we can proceed with the HEN design.

1. **Stream H1 and C4**

We start with H1 because it has the highest CP and C4 as the one closest to the PP:

H1: $(70{,}25 - 48{,}89) \cdot 26{,}18 = 559{,}2\ kW$

According to the calculation above, stream C4 can receive all the energy from H1, but to see if the match is possible, we will calculate the heat capacity flowrate of C4:

$$559{,}2 = (60{,}25 - 28{,}15) \cdot CP_{C4}$$

$$CP_{C4} = \frac{559{,}2}{(60{,}25 - 28{,}15)} = 17{,}42\ kW/℃$$

This match is possible because CP_{C4} is smaller than the overall heat capacity flowrate of the cold stream $CP_C = 18{,}655\ kW/℃$, and smaller than the heat capacity flowrate of the hot stream H1, $CP_{H1} = 26{,}18\ kW/℃$.

The duty of the heat exchanger is 559,2 kW, and it's inlet and outlet temperatures are shown in Table 6-11.

In stream C are left: $598{,}83 - 559{,}2 = 39{,}63\ kW$, which is the heat load of C5.

2. <u>Stream H3 and Stream C5</u>

Stream H3 has the next largest CP and can deliver: $(70{,}25 - 54) \cdot 4{,}342 = 70{,}56\ kW$

Stream C5 can receive: $(60{,}25 - 28{,}15) \cdot 1{,}23 = 39{,}6\ kW$

We calculated CP_{C5} in the following way:

$$CP_{C5} = CP_C - CP_{C4} = 18{,}655 - 17{,}42 = 1{,}23\ kW/℃$$

Stream H3 can satisfy the energy demand of the stream C5, which means the duty of the heat exchanger is 39,6 kW (Table 6-11).

The outlet temperature of the hot side is calculated according to (2-22):

$$39{,}6 = \left(70{,}25 - T_{out_h}\right) \cdot 4{,}342$$

$$T_{out_h} = 70{,}25 - \frac{39{,}6}{4{,}342} = 61{,}13\ ℃$$

In stream H3: $70{,}56 - 39{,}6 = 31\ kW$ are left. This energy must be provided from cold utility (CU1, Table 6-11).

The streams H3 and H4 still have to be cooled down to their target temperatures.

Stream H2 has a surplus of: $(70{,}25 - 54) \cdot 1.556 = 25.28 kW$

Stream H4 has a surplus of: $(70{,}25 - 55) \cdot 1.408 = 21.48\ kW$

There are no more cold streams to match them with, which leads us to the conclusion that in this case we have to use cold utilities (Table 6-11).

Table 6-11: Inlet and outlet temperatures of the HEs below the pinch

Heat Exchanger ID	Heat Exchanger Duty (kW)	Hot/Cold Side	T_{in} (°C)	T_{out} (°C)
HE4	559.21	Hot Side: H1	70.25	48.89
		Cold Side: C4	28.15	60.25
HE5	39.6	Hot Side: H2	70.25	61.13
		Cold Side: C5	28.15	60.25
CU1	31	Hot Side: H3	61.13	54
		Cold Side	54 - ΔTmin	Any dep.on c_p
CU2	25.3	Hot Side: H2	70.25	54
		Cold Side	54 - ΔTmin	Any dep.on c_p
CU3	21.5	Hot Side: H4	70.25	55
		Cold Side	55 - ΔTmin	Any dep.on c_p

The cold utilities, CU1, CU2 and CU3 can't be integrated in only one cold utility because no mixing of the streams is allowed considering the differences in the composition of each stream.

All the above calculations are presented in one MER HEN design shown in Figure 6-13.

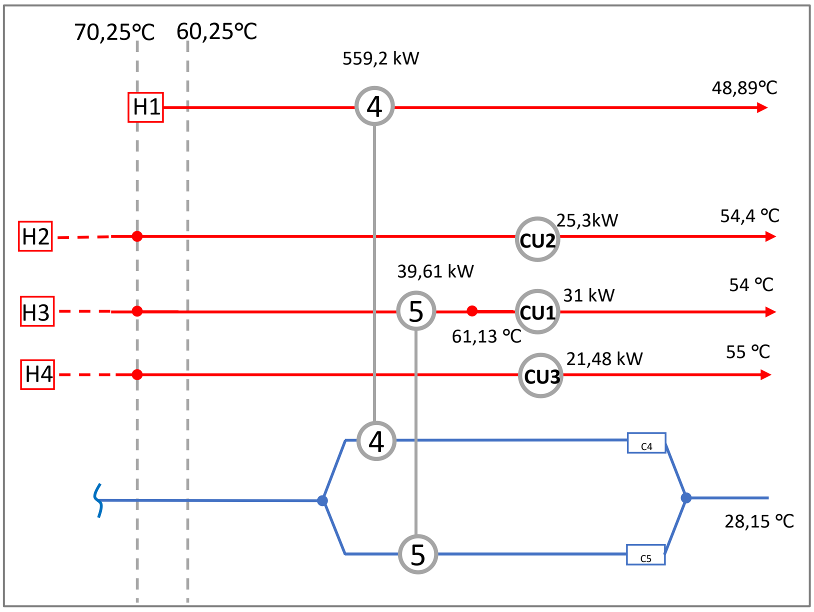

Figure 6-13: HEN below the pinch point

6.8 Minimum number of units

If we summarize the necessary utilities, we get:

$$Q_{\min\_hot} = Q_{HU} = 62{,}8\ kW$$

$$Q_{\min\_cold} = Q_{CU1} + Q_{CU2} + Q_{CU3} = 77{,}1\ kW$$

The MER HEN design resulted in the same energy targets as the cascade and the composite curves methods. This is an indicator that the HEN was correctly designed.

Besides the question of remaining utilities and their duty, the capital cost of the HEN is crucial. The costs have the tendency to be dominated by the number of units included. That is the reason why there is a great incentive to reduce the number of matches between hot and cold streams [32].

When designing MER network, usually there is a loop in the system in order to satisfy the utility requirements and to avoid heat crossing the pinch [30]. A loop is defined as a closed path between two matches, by two heat exchangers [7]. Having a loop in the system is an indicator that there is at least one HE more than the minimum number of units. A loop can be resolved by an open path between the hot and cold utilities in the system.

Referring to the HEN designed and shown in Figure 6-14, we will check if this is the minimum number of heat exchangers or if there is space for improvement.

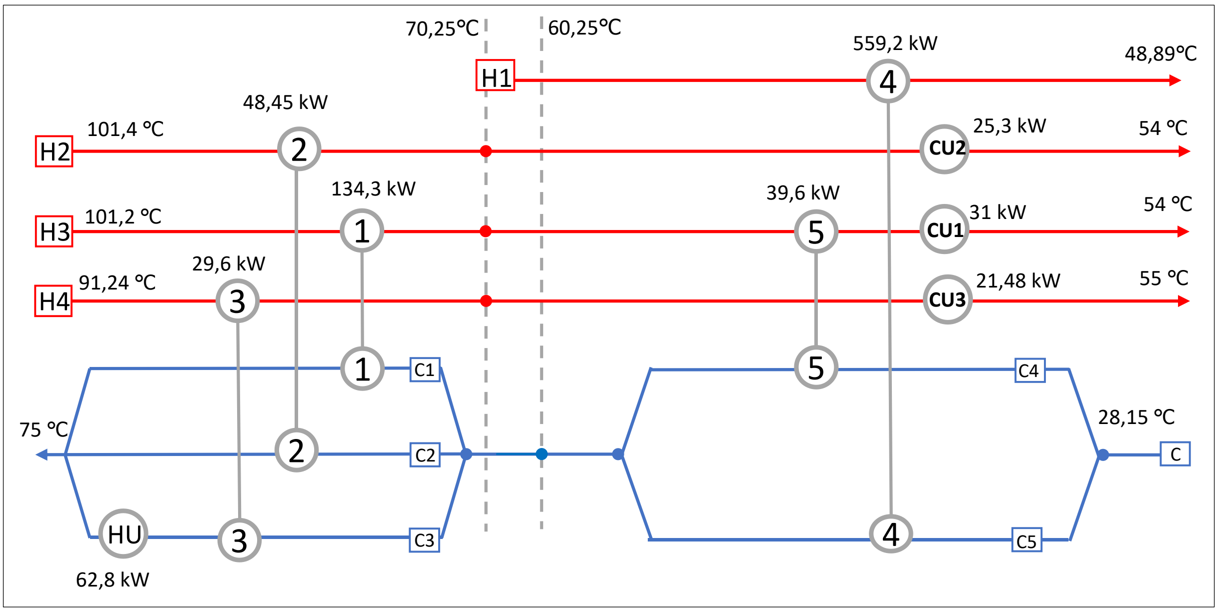

Figure 6-14: HEN for maximum heat recovery

The minimum number of units is defined as [32]:

$$N_{min} = N + L - s \tag{6-13}$$

where:

N_{min} – Minimum number of units (including heaters and coolers)

N – Number of streams (including utilities)

L – Number of loops (closed paths in the network)

s – Number of separate components.

The number of separate components represents subsystems in the network, for the given data set, which by enthalpy balance can form separate networks.

Usually, the goal is to avoid extra units and to achieve a design where the number of loops is L=0. And also, is preferable not to have subset equalities in the data set and hence s=1. This leads to the targeting equation [32]:

$$N_{min} = N - 1 \tag{6-14}$$

This equation applies for simple HENs without any loops and with no more than one subsystem. But in this case it is not convenient to use this simplification because of the fact that the designing of the HEN was done in two subsystems (s=2), above and below the pinch point. Additionally, if we analyze the HEN in Figure 6-14, we notice a loop between HE1 and HE5, which leads to L=1. So, referring to our case and applying equation (6-13) for the whole problem, with four hot streams, one cold stream, one heater and three coolers, we obtain:

$$N_{min} = 4 + 1 + 1 + 3 + 1 - 2 = 8 \tag{6-15}$$

But the design shown in Figure 6-14 has nine units, which means there is still place for improvements. This problematic will be treated in the next section, where network relaxation will be explained and implemented for the given case.

6.9 Network relaxation

The methodology of network relaxation and the procedure for reducing units at minimum energy sacrifice is [7]:

- **Identify a loop across the pinch if one exists**
- **Break the loop by subtracting and adding loads**
- **Recalculate network temperatures and identify the ΔT_{min} violations**
- **Find a relaxation path and formulate $T = f(x)$**

- **Restore ΔT_{min}**

The procedure can then be repeated for any loops and paths to give a range of options with different numbers of units and energy usage.

The designed MER HEN of this work has nine HE units, which is one more than the target number of units (number of streams – 1). This leads to the loop in the designed network, the closed path between match 1 and match 5, shown in Figure 6-15, traced out with dotted line.

To resolve the loop in the system, the heat load of one of the matches must be eliminated and an open path between two utilities must be considered.

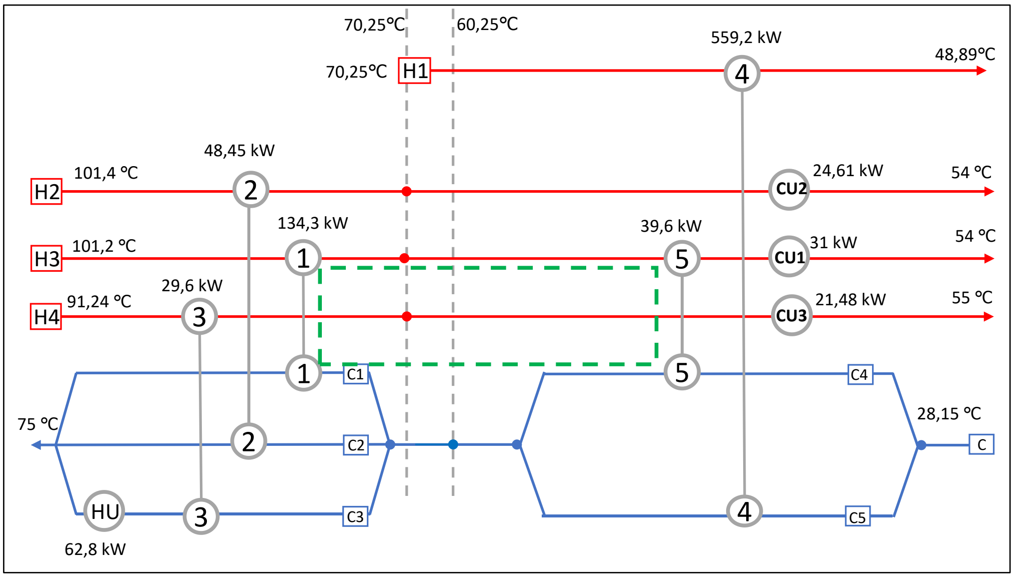

Figure 6-15: Identifying a loop in the heat exchangers network

First, the match HE5 will be eliminated because has a smaller heat load. Considering that this choice will lead to subtraction of 39,6 kW load from the design value, this heat flow must be carried by HE1 (Figure 6-15):

$$Q_{HE1} = 134.3 + 39.6 = 173.9$$

This will lead in changes in the temperatures (Figure 6-16). Considering that now the load of the HE1 is 173,3 kW, the output temperature on the hot stream will be 61,3 °C :

$$Q_{HE1} = CP_{H3}(101.2 - t_2) = 4.342 \cdot (101.2 - t_2) = 173.9\ kW$$

$$t_2 = 61.3\ ℃$$

The inlet temperature on the cold stream must be 56 °C:

$$Q_{HE1} = CP_{C1}(75 - t_2) = 9.105 \cdot (75 - t_2) = 173.9\ kW$$

$$t_2 = 56\ ℃$$

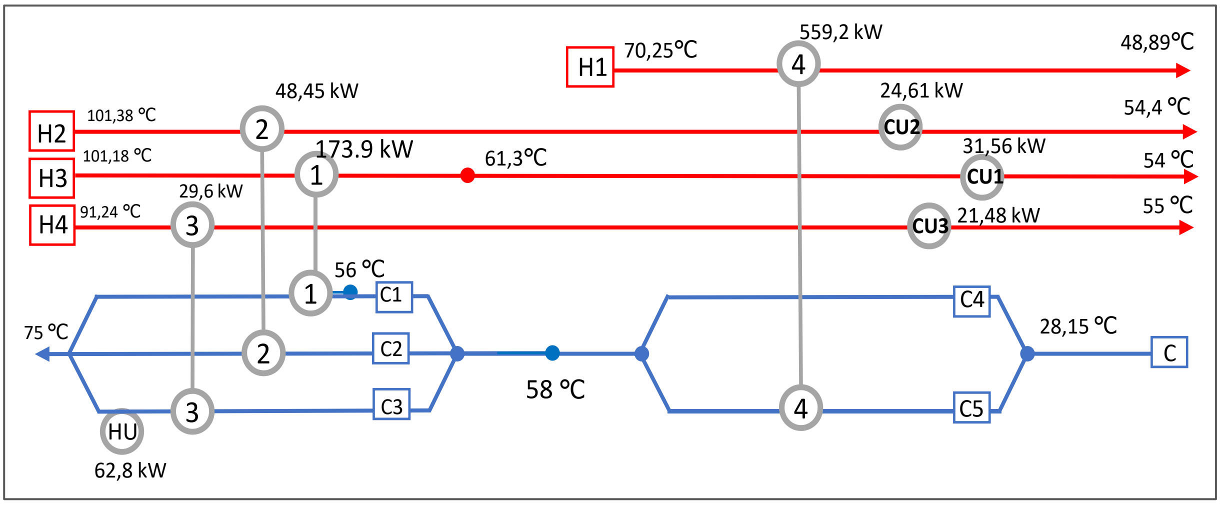

Figure 6-16: HEN after eliminating HE5

These steps lead to violation of the value. This was expected by breaking the loop, because the closed path straddles the pinch. To solve this, the utilities load must be changed.

In our network an additional problem appears because of the stream splitting on the cold end of the system. As we eliminated the HE1, stream C5 will be mixed with the heated stream C4, which will result into $T_{mix} = 58$ °C. But we saw before that the inlet temperature of the cold stream must be 56 °C. If we cool down the stream to 56 °C not only the minimum temperature difference will be broken, but also the whole network on the hot end of the system must be redesigned. To avoid that, we will calculate the allowed load of the HE1, with inlet temperature on the cold end $T_{in\_c} = 58$ °C:

$$Q_{HE1} = (75 - 58) * 9{,}105 = 154{,}8\ kW$$

Once we have defined the load of HE1, we can calculate the outlet temperature of the hot stream:

$$Q_{HE1} = \left(101{,}18 - T_{out\_h}\right) * 4{,}342 = 154{,}8\ kW$$

$$T_{out\_h} = 65{,}5\ ℃$$

Now that the new temperatures are calculated, we see that the difference $T_{out\_h} - T_{in\_c} < \Delta T_{min}, so$ we continue to find a solution on how to restore the minimum temperature difference $\Delta T_{min} = 10°\mathrm{C}$. We exploit a path through the network. A path is a connection through streams and exchangers between hot utility and cold utility [7].In this case the path is shown with dotted line, going from the cooler CU1, along stream H3 to match HE1, to branch C1 and along the branch to HU2, which we need to add (Figure 6-18).

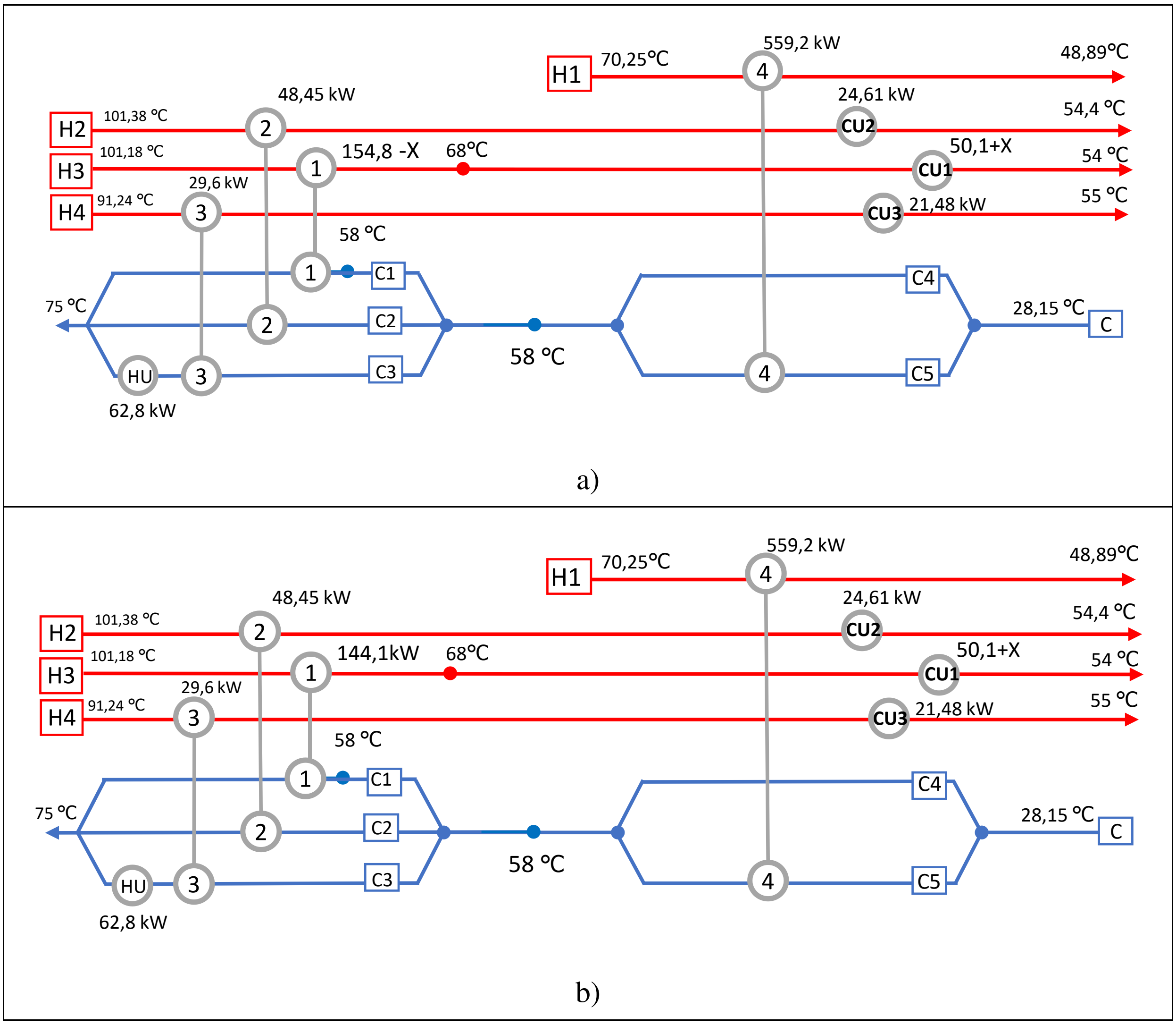

Figure 6-17: Breaking the loop and adjusting the HE duty

If we add load X to the heater HU2, the load of HE1 will be reduced for the same value X and by enthalpy balance the load of CU1 will be increased by X. Hence the temperature of the cold stream remains 58°C. Reducing the load of HE1 by X must increase $T_{out\_h} = T_2$, thus opening the ΔT on the cold end. This is exactly what we need to restore ΔT_{min}. There is clear relation between T_2 and X:

$$Q_{HE1} - X = (101{,}18 - t_2) \cdot 4{,}342$$

$$Q_{CU1} + X = (t_2 - 54) * 4{,}342$$

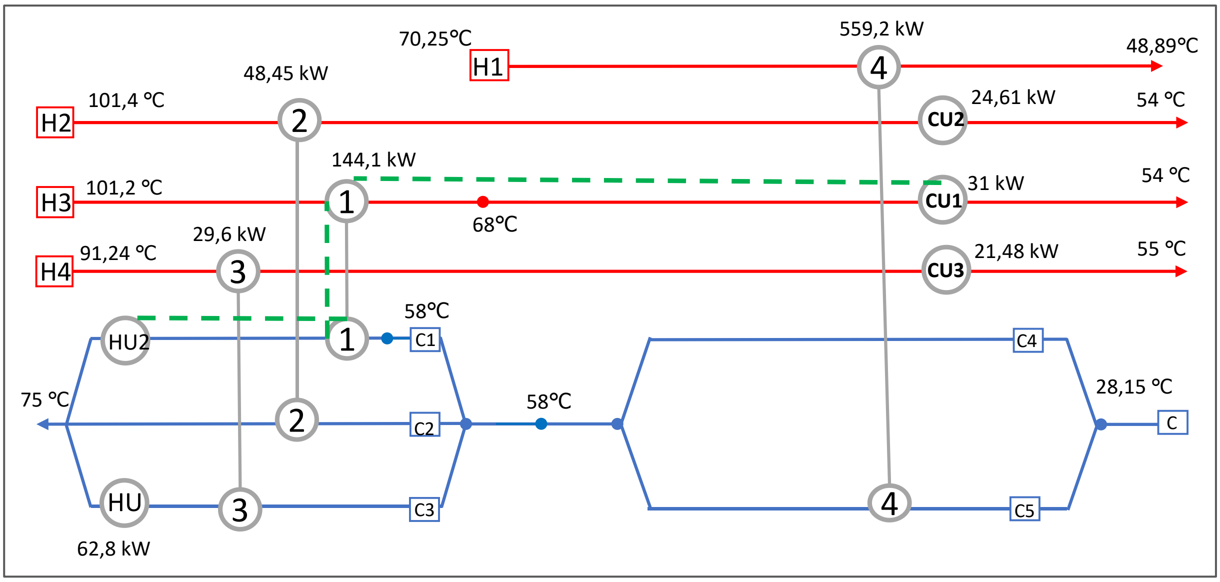

Figure 6-18: Identifying a path in the HEN

Since $\Delta T_{min} = 10°C$, we want to restore t_2 to 68 °C. Solving either of the equations above for $T_2 = 68$ °C we get $X = 10{,}7\ kW$. Since ΔT_{min} is restored, 10,7 kW seems to be the sacrifice required to produce Nmin MER solution. The new design, shown in Figure 6-19 includes the new duties of HE1 and CU1 as follows:

$$Q_{HE1} = 154{,}785 - 10{,}7 = 144{,}1\ kW$$

$$Q_{CU1} = 50{,}06 + 10{,}7 = 60{,}8\ kW$$

It was not expected, we got one unit more than one unit less. This additional problem in our case is because of the cold stream branches. To solve this, we will mix C1, C2 and C3 and afterwards define the utility of the heat exchanger.

Knowing the inlet temperatures of every branch, we can calculate the mixing temperature in the following way:

$$T_{mix} = \frac{T_{C1} \cdot CP_{C1} + T_{C2} \cdot CP_{C2} + T_{C3} \cdot CP_{C3}}{CP_{C1} + CP_{C2} + CP_{C3}}$$

$$T_{mix} = 71{,}06\ °C$$

Now, we can obtain the duty of the hot utility:

$$Q_{HU} = (75 - 71{,}06) * 18{,}655 = 73{,}5\ kW$$

The changes in the duty and the inlet/outlet temperature of the HE1, the cold and the hot utility are presented in Table 6-12.

Table 6-12: Characteristics of the heat exchangers HE1, CU1 and HU after optimizing the HEN

Heat Exchanger ID	Heat Exchanger Duty (kW)	Hot/Cold Side	T_{in} (°C)	T_{out} (°C)
HE1	144.1	Hot Side: H3	101.2	68
		Cold Side: C1	58	73.82
CU1	60.8	Hot Side: H3	68	54
		Cold Side	54 - ΔTmin	Any dep. on c_p
HU	73,5	Hot Side	Any dep. on c_p	71.06 + ΔTmin
		Cold Side: C	71.06	75

The new configuration of the MER HEN as shown in Figure 6-19 has the minimum number of units as obtained with equation (6-15). Hence, by transferring energy across the pinch, the scope for reducing the number of units by one was achieved.

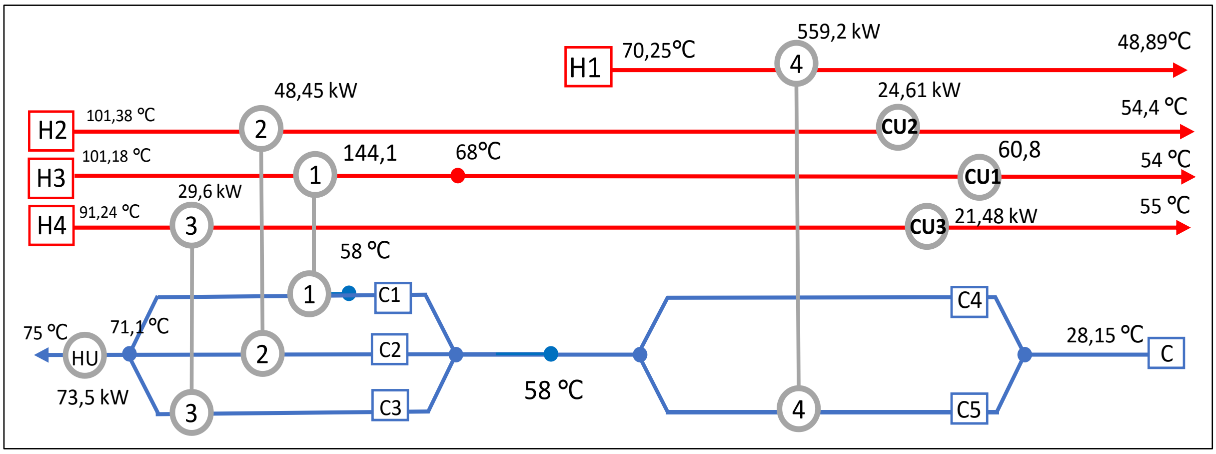

Figure 6-19: Energy relaxation using a path

A path does not have to include loops. As we can see in Figure 6-19, an alternative path exists via exchangers HE4 and HE3. In this case the 29,6 kW from HE3 should be transferred to HE1, breaking the pinch point and the enthalpy balance of this subsystem. However, the energy penalty in this case is almost three times bigger than the one by the loop-breaking method. So we can conclude that breaking-loops is usually preferable to using simple paths.

6.10 Cost estimation

A complete optimization of a system includes not only thermo-dynamical, but also economical aspects. The economic analysis and its benefits is not a part of this thesis. However, a rough estimation of the additional costs according to the heat exchanging area were made. For that purpose, Dace Price Booklet was used. This handbook provides prices which are applicable within the process industry [56].

Table 6-13: Cost estimation for the additional HEs

Heat Exchanger	Duty (kW)	Heat Transfer Area (m^2)	Cost (x1000, €)
HE1	144.1	16.7	28
HE2	48.45	5.7	19
HE3	29.6	17.7	28
HE4	559.21	101.3	52
HE5	9.6	4.1	17
			∑=144 000 €

The costs depend on the heat transfer area, as well as on the material used for the heat exchangers. In the practice shell and tube heat exchangers made of carbon steel satisfy the requirements of the plant. According to that, the prices for the additional five heat exchangers are shown in Table 6-13. That resulted in total investment cost of 144 000 euros.

7 RESULTS AND POSSIBLE IMPROVEMENTS

Nowadays has become imperative that the processes and the plants become more energy efficient. This study confirmed that Pinch Technology is a very practical and intuitive method for attaining retrofit process heat integration for a complex, already optimized plant design.

This case study is to be used as basis for development of a feasible Upstream dedicated methodology for Pinch analysis between different units.

The plant had an already optimized network of heat exchangers, which is the reason why the focus was not to retrofit the existing HEN, but to find new possibilities for heat recovery. The results have shown that the excess heat from the amine and glycol regeneration units can be used to preheat the un-stabilized condensate before entering the flash separator. In that way, potential 811 kW of energy can be recovered. Unfortunately, due to confidentiality restrictions, I didn’t have access to information about the total energy consumption of the plant. But taking into account its capacity, it can be concluded that the contribution of the heat recovery in the frames of the whole plant are minor. When analyzing the subsystems of the separate units, the benefits consist of:

- elimination of the air cooler in H1,
- reducing the duty of the other air coolers up to 40% and
- reducing the duty of the hot oil system in the condensate flash separator by 20%.

Considering that hot oil and utility water systems are already in use in the plant, the same will be considered for the hot and cold utility requirements correspondingly.

The HEN was improved by satisfying the minimum number of eight units through relaxation of the network by resolving the loop with an open path. The sacrifice in this case, were 10 kW, which are to be covered by the external utilities.

The economic contributions and the payback time of the investment costs were not considered in the frames of this work. These factors must be investigated additionally before implementing the recommendations.

Even the plant was optimized during initial design, appliance of more accurate Pinch analysis highlights new ways for improvement. This methodology consists of concise guidelines for determining the MER of a process and designing an optimized HEN. The outlined improvements have the potential to be used in the design phase of future complex projects, even for brownfield developments.

The magnitude of the benefits is constrained by the layout of the plant, the distance between the units, as well as their independent dynamic operations. The feasibility of the integrated process recommendations is a trade-off between the operational performance and the thermo-economic improvements. Overcoming these challenges and implementation of the methodology is basis for further evaluation and contributions in Total Site Heat Integration in a typical upstream plant.

8 BIBLIOGRAPHY

[1] NPTEL- NATIONAL PROGRAMME ON TECHNOLOGY ENHANCED LEARNING: *Process integration, methods and area of application*

[2] KLEMES, Jiri. J. (Hrsg.): *Handbook of Process Integration (PI)* : *Minimisation of energy and water use, waste and emissions* : Woodhead Publishing, 2013

[3] CANMET ENERGY TECHNOLOGY CENTRE: *Pinch Analysis: For the efficient use of Energy, Water and Hydrogen*. 2003

[4] CAPOCELLI, Mauro: *Oil & Gas Portal* : *Pinch Analysis in the Oil and Gas Industries*. URL http://www.oil-gasportal.com/pinch-analysis-in-the-oilgas-industries/#_ftn21 – Überprüfungsdatum 2019-06-12

[5] ILF-CONSULTING ENGINEERS: *Basis of Design of the upstream plant; Process Flow Diagrams and Heat andMaterial Balance*. (Adressat)

[6] GUNDERSEN, Truls: *Implementing Agreement on Process Integration* : *A Process Integration Primer* (2002). URL http://www.ivt.ntnu.no/ept/fag/tep4215/innhold/Retrofit-new.pdf – Überprüfungsdatum 2019-09-05

[7] KEMP, Ian C.: *Pinch Analysis and Process Integration* : *A user guide on Process Integration for the efficient use of energy* : Elsevier Ltd., 2007 (Second edition)

[8] EL-HALWAGI, Mahmoud M.: *Pollution Prevention through process integration*. In: *Clean Products and Processes* (1998)

[9] FOLORUNSO, Olusegun ; ADEWALE, Gladys ; OGUNDE, Adewale Opelouwa ; OKESOLA, Julius Olatunji: *Pinch Analysis as a Knowledge Management Tool for Optimization in Supply Chain*. In: *Computer and Informtaion Science* (2011), Vol. 4. URL DOI:10.5539/cis.v4n1p79

[10] LUCAS, Jim: *What is Thermodynamics?* URL https://www.livescience.com/50776-thermodynamics.html

[11] MIFFLIN HARCOURT, FIFTH EDITION: *The American Heritage Dictionary of the English Language* : *Definition of the term "Temperature"* – Überprüfungsdatum 2019-10-14

[12] CENGEL, Yunus ; BOLES, Michael: *Thermodynamics- An Engineering Approach*. 8th Edition : McGraw Education

[13] RAUPENSTRAUCH, Harald ; SPIJKER, Christoph ; HOLZER, Alexandra ; KAINZ, Samuel: *Technische Thermodynamik (Technical Thermodynamic)* : Lehrstuhl für Thermoprozesstechnik (Chair of Thermal Process Engineering), 2018 (1 Auflage (1st edition))

[14] NIČ, Miloslav ; JIRÁT, Jiří ; KOŠATA, Bedřich ; JENKINS, Aubrey ; MCNAUGHT, Alan: *IUPAC Compendium of Chemical Terminology*. Research Triagle Park, NC : IUPAC, 2009

[15] Lecture notesKIENBERGER, Thomas: *Thermische Energietechnik (Thermal Energy Technology)*. Lecture notes

[16] CERBE, Günter ; WILHELMS, Gernot: *Technische Thermodynamik (Technical Thermodynamics)*. München : Carl Hanser Verlag GmbH & Co. KG, 2008

[17] CHEMISTRY LIBRETEXTS: *Entropy and the Second Law of Thermodynamic*. URL https://chem.libretexts.org/Bookshelves/General_Chemistry/Map%3A_Chemistry_-_The_Central_Science_(Brown_et_al.)/19%3A_Chemical_Thermodynamics/19.2%3A_Entropy_and_the_Second_Law_of_Thermodynamics – Überprüfungsdatum 2019-10-12

[18] SAYLOR.ORG ACADEMY: *Heat Capacity*. URL https://resources.saylor.org/wwwresources/archived/site/wp-content/uploads/2011/04/Heat_capacity.pdf – Überprüfungsdatum 2019-10-15

[19] BAEHR, Hans Dieter ; KABELAC, Stephan: *Thermodynamik (Thermodynamic)* : *Grundlagen und technische Anwendungen*. 14th. Berlin, Heidelberg : Springer, 2009 (Springer-Lehrbuch)

[20] SHABER, Stefan P. ; MAYINGER, Stefan: *Thermodynamik* : *Grundlagen und technische Anwendungen*. 18. Aufl. Berlin, Heidelberg : Springer Berlin Heidelberg, 2009 (Springer-Lehrbuch)

[21] DEPARTMENT FOR TREATMENT OF WATER AND FUEL TECHNOLOGY: *Concept of heat capacity*. URL http://twt.mpei.ac.ru/TTHB/2/KiSyShe/eng/Chapter1/1-6-Concept-of-heat-capacity.html

[22] LABUHN, Dirk ; ROMBERG, Oliver: *Keine Panik vor Thermodynamik! ((Do not panic over Thermodynamics!)*. 6th Edition. Wiesbaden : Vieweg + Teubner, 2013 (Studium)

[23] *Thermodynamics Volume 1: The basic principles* : *Basic Thermodynamic Concepts*

[24] MAREK, Rudi ; NITSCHE, Klaus: *Praxis der Wärmeübertragung (Practice of heat transfer)* : *Grundlagen, Anwendungen, Übungsaufgaben (Basics, applications, exercises)*. 2nd : Hanser

[25] NPTEL - NATIONAL PROGRAMME ON TECHNOLOGY ENHANCED LEARNING: *Fundamental Concepts related to heat integration*. URL https://nptel.ac.in/courses/103/107/103107093/ – Überprüfungsdatum 2019-10-15

[26] BUTUN, Hur ; KANTOR, Ivan ; MARECHAL, Francois: *A heat integration method with multiple heat exchange interfaces*. In: *Energy* (2018), Nr. 152

[27] KLEMES, Jiri J. ; KRAVANJA, Zdravko: *Forty years of Heat Integration: Pinch Analysis (PA) and Mathematical Programming (MP)*. In: *Current Opinion in Chemical Engineering* 2 (2013), Nr. 4. URL https://www.sciencedirect.com/science/article/pii/S2211339813000944?via%3Dihub

[28] GUNDERSEN, Truls: *Heat Integration-Targets and Heat Exchanger Network Design* : *Handbook of Process Integration, Chapter 2.1.*

[29] THE CHEMICAL ENGINEERS' RESOURCE PAGE: *Pinch Technology: Basics for the Beginners*

[30] BEJAN, Adrian ; TSATSARONIS, George ; MORAN, Michael: *Thermal Design and Optimization* : Wiley, 1996

[31] BRUNNER, Florian ; KRUMMENACHER, Pierre: *Einführung in die Prozessintegration mit der Pinch-Methode (Introduction to process integration with the pinch method)* : *Handbuch für die Analzse vo kontinuierlichen Prozessenund Batch-Prozessen (Handbook for the Analysis of Continuous Processes and Batch Processes)*, 2015

[32] LINNHOFF, March: *Intorduction to Pinch Technology*, 1998

[33] LINNHOFF, Bodo: *Pinch Analysis: A state of the art overview* : *Techno-economic analysis*. In: *Chemical Engineering Research and design* (1993), Abstract;. URL https://scinapse.io/papers/784564648

[34] LINNHOFF, Bodo ; DHOLE, Vikas: *Total site targets for fuel, cogeneration, amissions and cooling*, 1993

[35] RAISSI, K.: *Total SIte Heat Integration* : The University of Manchester, 1994

[36] ROKNI, Masoud: *Introduction to Pinch Technology* : Technical University of Denmark (DTU), 2016

[37] MATSUDA, Kazuo ; HIROCHI, Yoshiichi ; TATSUMI, Hiroyuki ; SHIRE, Tim: *Applying heat integration total site based pinch technology to a large industrialarea in Japan to further improve performance of highly efficient process plants*. In: *Energy* (2009)

[38] YOON, Sung-Geun ; LEE, Jeongseok ; PARK, Sunwon: *Heat integration analysis for an industrial ethylbenzene plant using pinch analysis*. In: *Applied Thermal Engineering* (2007)

[39] CHANG, Chenglin ; CHEN, Xiaolu ; WANG, Yufei ; FENG, Xiao: *An efficient optimization algorithm for waste Heat Integration using a heat recovery loop between two plants*. In: *Applied Thermal Engineering* (2016). URL https://doi.org/10.1016/j.applthermaleng.2016.04.079

[40] FENG, Xiao ; PU, Jing ; YANG, Junkun ; HOONG CHU, Khim: *Energy Recovery in petrochemical complexes through heat integration retrofit analysis*. In: *Applied Energy* (2010). URL https://doi.org/10.1016/j.apenergy.2010.12.027

[41] BONHIVERS, Jean-Christophe ; KORBEL, Milan ; SORIN, Mikhail ; SAVULESCU, Luciana ; STUART, Paul R.: *Energy transfer diagram for improving integration of industrial systems*. In: *Applied Thermal Engineering* 63 (2014), Nr. 1, S. 468–479

[42] WALMSLEY, Timothy G. ; LAL, Nathan S. ; VARBANOV, Petar S. ; KLEMES, Jiri J.: *Automated retrofit targeting of heat exchanger networks*. In: *Frontiers of Chemical Science and Engineering* (2018). URL https://link.springer.com/article/10.1007%2Fs11705-018-1747-2

[43] KAMEL, Dina A. ; GADALLA, Mamdouh A. ; ABDELAZIZ, Omar Y. ; LABIB, Mennat A. ; ASHOUR, Fatma H.: *Temperature driving force (TDF) curves for heat exchanger network retrofit – A case study and implications*. In: *Energy* 123 (2017), S. 283–295

[44] NEMET, Andreja ; KLEMES, Jiri J. ; VARBANOV, Petar S. ; MANTELLI, Valter: *Heat Integration retrofit analysis—an oil refinery case studyby Retrofit Tracing Grid Diagram*. In: *Frontiers of Chemical Science and Engineering* (2015). URL https://link.springer.com/article/10.1007%2Fs11705-015-1520-8

[45] KLEMES, JIRI, JAROMIR ; VARBANOV, Petar Sabev ; WALMSLEY, Timothy G. ; JIA, Xuexiu: *New directions in the implementation of Pinch Methodology (PM)*. In: *Renewable and Sustainable Energy Reviews* 98 (2018), S. 439–468

[46] OLSEN, Donald ; LIEM, Peter ; ABDELOUADOUD, Yasmina ; WELLIG, Beat: *Thermal Energy Storage Integration Based on Pinch Analysis - Methodology and Application*. In: *Chemie Ingenieur Technik* 89 (2017), Nr. 5, S. 598–606

[47] JAMALUDDIN, Khairulnadzmi ; WAN ALWI, Sharifah Rafidah ; ABDUL MANAN, Zainuddin ; KLEMES, Jiri Jaromer: *Pinch Analysis Methodology for Trigeneration with Energy Storage*

System Design. In: *CHEMICAL ENGINEERING TRANSACTIONS* (2018). URL https://www.aidic.it/cet/18/70/315.pdf

[48] DEVOLD, Havard: *Oil and gas production handbook* : *An introduction to oil and gas production, transport, refining and petrochemical industry*. 3. Aufl. : ABB, 2013

[49] *Design characteristics for the gas development project*

[50] KENNETH, Arnold (Hrsg.); LAKE, Lary (Mitarb.): *Petroleum Engineering Handbook* : *Facilitites and construction engineering*. Chapter 5 : Society of petroleum engineers (3)

[51] ANSI B16.5 - STEEL PIPE FLANGES - PRESSURE AND TEMPERATURE RATINGS - GROUP 1.2. URL https://www.engineeringtoolbox.com/ansi-flanges-pressure-temperature-d_342.html

[52] KAREEM, Lateef A. ; IWALEWA, Tajudeen M. ; OMEKE, James E.: *Isobaric specific heat capacity of natural gas as a function of specific gravity, pressure and temperature*. In: *Journal of Natural Gas Science and Engineering* 19 (2014), S. 74–83

[53] FANCHI, John (Hrsg.); LAKE, Larry (Hrsg.): *Petroleum Engineereing Handbook, Volume 1: General Engineering*

[54] *Energy Insights by Mckinsey: Refinery Reference Desk* : *Specific Gravity*. URL https://www.mckinseyenergyinsights.com/resources/refinery-reference-desk/specific-gravity/

[55] ENGINEERS EDGE: *Overall Heat Transfer Coefficient Table Charts and Equation*. URL https://www.engineersedge.com/thermodynamics/overall_heat_transfer-table.htm – Überprüfungsdatum 2019-11-14

[56] DUTCH ASSOCIATION OF COST ENGINEERS: *DACE price booklet* : *Cost information for estimation and comparison*. Edition 32

9 APPENDIX A

9.1 Well fluid and product composition

Table 9-1: Well fluid composition (wet basis)

Components	Mole %			
	Overall	Vapour	Liquid	Aqueous
H_2S	0,0012	0,0014	0,0001	0,0000
CO_2	1,8029	2,1396	0,0364	0,0013
Nitrogen	4,5376	5,3371	0,0091	0,0001
Methane	65,0124	76,4502	0,4117	0,0000
Ethane	4,7326	5,5556	0,1827	0,0000
Propane	2,6110	3,0466	0,3945	0,0000
i-Butane	0,7880	0,9063	0,3273	0,0000
n-Butane	1,3430	1,5301	0,7898	0,0000
i-Pentane	0,7072	0,7636	1,0846	0,0000
n-Pentane	0,7012	0,7351	1,4247	0,0000
Mcyclopentan	0,1192	0,0981	0,6683	0,0000
n-Hexane	0,9953	0,8119	5,7006	0,0000
Benzene	0,0747	0,0621	0,4089	0,0000
Cyclohexane	0,1486	0,1144	0,9587	0,0000
n-Heptane	0,8746	0,4046	9,9126	0,0000
3-Mhexane	0,1554	0,0852	1,550	0,0000
Toluene	0,1376	0,0635	1,5620	0,0000
n-Octane	0,8618	0,1591	13,5729	0,0000
E-Benzene	0,0211	0,0039	0,3308	0,0000
p-Xylene	0,1219	0,0194	1,9686	0,0000
m-Xylene	0,0000	0,0000	0,0000	0,0000
o-Xylene	0,0458	0,0069	0,7452	0,0000
n-Nonane	0,6066	0,0378	10,7321	0,0000
124-MBenzene	0,0372	0,0015	0,6703	0,0000
n-Decane	0,5050	0,0101	9,2738	0,0000
n-C11	0,3605	0,0022	6,7015	0,0000

n-C12	0,1944	0,0004	3,6250	0,0000
n-C13	0,1644	0,0001	3,0695	0,0000
n-C14	0,1308	0,0000	2,4431	0,0000
n-C15	0,1196	0,0000	2,2340	0,0000
n-C16	0,0909	0,0000	1,6986	0,0000
n-C17	0,0708	0,0000	1,3221	0,0000
n-C18	0,0618	0,0000	1,1547	0,0000
n-C19	0,0511	0,0000	0,9539	0,0000
n-C20	0,0399	0,0000	0,7447	0,0000
n-C21	0,0327	0,0000	0,6108	0,0000
n-C22	0,0273	0,0000	0,5104	0,0000
n-C23	0,0224	0,0000	0,4184	0,0000
n-C24	0,0188	0,0000	0,3514	0,0000
n-C25	0,0157	0,0000	0,2929	0,0000
n-C26	0,0134	0,0000	0,2510	0,0000
n-C27	0,0112	0,0000	0,2092	0,0000
n-C28	0,0094	0,0000	0,1757	0,0000
n-C29	0,0085	0,0000	0,1590	0,0000
n-C30	0,0130	0,0000	0,2427	0,0000
n-DotriC32	0,0152	0,0000	0,2845	0,0000
C12plus	0,5080	0,0000	9,4763	0,0000
C36plus	0,0175	0,0000	0,3263	0,0000
H_2O	11,0430	1,6521	0,0285	99,9986

Table 9-2: Well fluid composition (dry basis)

Components	Mole %		
	Overall	Vapour	Liquid
H_2S	0,0013	0,0014	0,0001
CO_2	2,0470	2,1761	0,0371
Nitrogen	5,1009	5,4281	0,0092
Methane	73,0830	77,7527	0,4188
Ethane	5,3201	5,6500	0,1859

Propane	2,9352	3,0980	0,4013
i-Butane	0,8858	0,9214	0,3328
n-Butane	1,5097	1,5551	0,8031
i-Pentane	0,7950	0,7753	1,1016
n-pentane	0,7882	0,7460	1,4462
Mcyclopentan	0,1340	0,0992	0,6757
n-Hexane	1,1189	0,8204	5,7627
Benzene	0,0840	0,0628	0,4136
Cyclohexane	0,1670	0,1155	0,9685
n-Heptane	0,9831	0,4064	9,9582
3-Mhexane	0,1747	0,0857	1,5595
Toluene	0,1547	0,0637	1,5693
n-Octane	0,9688	0,1590	13,5689
E-Benzene	0,0237	0,0039	0,3307
p-Xylene	0,1370	0,0194	1,9672
m-Xylene	0,0000	0,0000	0,0000
o-Xylene	0,0514	0,0069	0,7446
n-Nonane	0,6819	0,0377	10,7060
124-MBenzene	0,0418	0,0015	0,6684
n-Decane	0,5677	0,0101	9,2445
n-C11	0,4053	0,0021	6,6787
n-C12	0,2185	0,0004	3,6125
n-C13	0,1848	0,0001	3,0587
n-C14	0,1470	0,0000	2,4345
n-C15	0,1344	0,0000	2,2262
n-C16	0,1022	0,0000	1,6926

Table 9-3: Quality specification of the products

Sales Gas Specification (1)	
Water Content	≤ 0.147 g/kg
Hydrocarbon Dew Point	≤ 0°C
H_2S	≤ 3.8 ppm

CO_2	≤ 3 mole %
Gross Calorific Value	≥ ≥ 35.4 MJ/m^3
Temperature	≤ 54°C (2)
Pressure	82.74 bar
Condensate Specification	
Salt	≤ 80 kg/m^3
Basic Sediment and Water	< 0.1 %
API Gravity	45.01 - 58
H_2S	< 5 g/m^3
Reid Vapour Pressure	7 psia

(1) At tie-in point with the Customer

(2) At GPF battery limit

9.2 Design characteristics of the process units

Table 9-4: Design data of the wellheads and flowlines

Reservoir Depth	R1 - 3581/ R2 - 3860
Wellhead Temperature	65°C - 100°C (1)
Wellhead Shut-in Temperature	65°C
Wellhead Shut-in Pressure at surface	227 barg
Minimum WTHP (upstream of choke)	26.6 barg
Maximum Pressure d/s of Choke	ANSI Rating 600# (Export Sales Gas Compressor will be required); or ANSI Rating 900# (Export Sales Gas Compressor will not be required)
Flow line size	0,254 m
Flow line length	0.6 to 6.5 km
Max. Well flow rates (Gas)	23543 to 30000 m^3/h
Soil Temerature (0.5 m below)	Min: 20°C Max: 40°C
Soil Thermal Conductivity	0.17 to 0.26 W/mK

Table 9-5: Design characteristics of the GSU

No. of trains	One
Feed	HP sour gas stream from inlet separator
Outlet	Sweetened gas to Gas Dehydration Unit CO_2 and H_2S to incinerator
Design flow rate of each train, MMSCFD	35 with 10% design margin
Inlet pressure, bar(g)	To be finalized during EPCC
Inlet Temperature, ℃	30-50 ℃ (in relation to inlet manifold condition)
Inlet Gas	H_2S: 35 mg/kg CO_2: 2-3.5 mole %
Outlet Gas specification	H_2S: ≤ 3.8 mg/kg CO_2: ≤ 3 mole %

Table 9-6: Design characteristics of the GDU

No. of trains	One
Feed	Sweetened gas from GSU
Outlet	Dried gas to Dew Point Control Unit
Design flow rate each train, MMSCFD	35 with 10% design margin
Inlet pressure, barg	To be finalized during EPCC
Inlet Temperature, ℃	To be finalized during EPCC
Inlet Gas water content	Saturated
Outlet specification	Water Content: ≤ 112 kg/m^3

Table 9-7: Design characteristics of the HCDPCU

No. of trains	One
Feed	Dried gas from Gas Dehydration Unit
Outlet	Sales Gas Meter

Design flow rate each train, MMSCFD	35 with 10% design margin
Inlet pressure, barg	To be finalized during EPCC
Inlet Temperature, ℃	To be finalized during EPCC
Hydrocarbon Dew Point	≤ 0℃
Gross Calorific Value	≥ 35.4 MJ/m^3
Outlet pressure, barg	83

Table 9-8: Design characteristics of the flash separator

No. of trains	One
Feed	HC Condensate from Inlet Separator
Outlet	Gas – to Fuel Gas System Condensate – to Condensate Stabilization Unit Water – to Produced Water Treatment and Disposal Facility
Design capacity:	
Gas	5886 m^3/h
Oil	15 733 kg/h
Water	6.62 m^3/h
Operating pressure, barg	To be finalized during EPCC
Design Margin	20%
Operating Temperature, ℃	To be finalized during EPCC

Table 9-9: Design characteristics of the CSU

No. of trains	1
Feed	Condensate from Flash Separator Liquid from HCDPU
Outlet	Stabilized Condensate – to storage Gas- to fuel gas system (stage 1)
Design Capacity each train, bpd	3300 and 10% design margin

Column operating pressure, Bar(g) (top)	To be finalized during EPCC
Column operating temperature, ℃ , (bottom)	To be finalized during EPCC
Outlet Specification	Reid vapor pressure: < 7 psia

10 APPENDIX B

10.1 Calculation of the specific heat capacity

Table 10-1: Average specific heat capacity for gases

Stream	γ_g	M $[kg/kmol]$	t (℃)	T (K)	a^*	b^*	c^*	d^*	$\bar{c}_{pm}$ $[kJ/kmol℃]$	$\bar{c}_p$ $[kJ/kg \cdot ℃]$
H1-in	0.689914	19.981	70.25	343.4	24.342	0.0798	$-6 \cdot 10^{-6}$	0	48.36	2.42
H1-out	0.690081	19.981	48.89	322	24.339	0.0798	$-6 \cdot 10^{-6}$	0	47.55	2.38
H3-in	1.944901	56.329	101.18	374.3	10.587	0.3498	$-1.73 \cdot 10^{-4}$	0	105.55	1.87
H3-out	1.944901	56.329	54	327.2	10.587	0.3498	$-1.73 \cdot 10^{-4}$	0	99.95	1.77
H4-in	1.158376	33.549	91.24	364.4	19.207	0.1806	$-6.8 \cdot 10^{-5}$	0	69.81	2.08
H4-out	1.158376	33.549	55	328.1	19.207	0.1806	-5	0	67.33	2.007
*- $a = a_1\gamma_g + a_2$; $b = b_1\gamma_g + b_2$; $c = c_1\gamma_g + c_2$; d= $d_1\gamma_g + d_2$										